

Information Report FF-X-66

January 1978

AIRPRO

AN AIR TANKER PRODUCTIVITY COMPUTER SIMULATION MODEL

THE EQUATIONS

(Documentation)

by

A. Simard and A. Young

Forest Fire Research Institute
Canadian Forestry Service
Department of Fisheries and the Environment
240 Bank Street
Ottawa, Ontario
K1G 3Z6

This report is one of a series describing AIRPRO. Other reports in this series are:

The Fortran Program (summary, documentation),
Information Report FF-X-64, August 1977.

ABSTRACT

This report discusses the development, assumptions, and behavior of the primary equations found in AIRPRO, an air tanker productivity computer simulation model. AIRPRO optimizes air tanker utilization by analyzing all reasonable combinations of resources and tactics and selecting the one which results in the lowest cost-plus-loss. The report begins by discussing the modeling process in general, and outlining the specifications used in developing the overall model. The remainder of the report is devoted to describing the five basic components of the model.

1. The administrative component links the model, the computer, and the user. It controls input and output functions, initializes the system, tabulates results, and controls the flow of the model.
2. The environmental component contains those processes which are external to the fire management system: distance calculation, sunrise and sunset, weather, and fuel.
3. The fire component generates fire occurrence with historical data, calculates rate of spread and intensity, and simulates fire growth with a four-segment elliptical point spread model.
4. The ground suppression component fights the fire; including determining a crew arrival schedule, calculating line construction rates, building line on each flank, and mopping-up. Suppression costs and losses are also determined with the use of regression equations.
5. The air tanker component first selects a resource and tactic combination for analysis. It then delivers retardant to the fire, drops the retardant, places the drop on one of the four flanks, and calculates air tanker costs.

RESUME

Ce rapport traite du développement, des hypothèses et du comportement des équations primaires contenues dans AIRPRO - un programme de simulation par ordinateur ayant trait au rendement des avions-citernes. AIRPRO optimise l'utilisation de l'avion-citerne en analysant toutes les combinaisons de ressources et de tactiques possibles et en choisissant celle qui permet de réduire au maximum les coûts et pertes. Les auteurs traitent d'abord du programme en général et soulignent les méthodes spécifiques utilisées dans le processus de développement du programme.

Le reste du rapport est consacré à la description du programme qui comprend cinq éléments de base:

1. "L'élément - administration" sert de lien entre le programme, l'ordinateur et l'utilisateur. Il contrôle les fonctions d'entrée et de sortie, initialise le système, classe les résultats et contrôle la marche du programme.
2. "L'élément - environnement" contient ces processus extérieurs au système de gestion du feu: soit le calcul des distances, l'heure du lever et du coucher du soleil, les conditions atmosphériques et les combustibles.
3. "L'élément - incendie" fournit des données sur la fréquence des incendies et l'historique du feu, calcule le taux de propagation et l'intensité du feu, dresse le modèle de progression du feu à l'aide d'un modèle de propagation elliptique, à quatre segments.
4. "L'élément - suppression au sol" combat l'incendie: il comprend la planification de l'intervention des équipes de lutte, le calcul des taux de construction des lignes d'arrêt, l'aménagement de lignes d'arrêt sur chaque flanc et l'opération de nettoyage. On détermine aussi, à l'aide d'équations de régression, les coûts d'extinction et les pertes.
5. "L'élément - avion-citerne" sélectionne d'abord une combinaison de ressources et de tactiques pour fin d'analyse. Il achemine ensuite les produits retardants vers le lieu de l'incendie, largue les retardants, effectue le largage sur un des quatre flancs et finalement calcule les coûts d'utilisation de l'avion-citerne.

TABLE OF CONTENTS

	<u>Page</u>
Introduction	1
1. Model Development	3
A - The Modeling Process	3
B - Goal Definition	6
C - Requirements	8
D - Model Description	14
E - Specifications for AIRPRO	23
2. General Simulation Functions	27
A - Elementary Processes	27
B - Time	29
3. The Environment	35
A - Distance	35
B - Sunrise and Sunset	38
C - Weather	40
D - Fuels	45
4. The Fire	49
A - Fire Occurrence	49
B - Fire Behavior	52
C - Fire Growth	61
5. Ground Suppression	83
A - Suppression	83
B - Mop-up	92
C - Economics	98
6. Air Tanker Utilization	116
A - Selecting Resources and Tactics	116
B - Retardant Delivery	123
C - Retardant Drop	131
D - Suppression	162
E - Costs	168
References	171
APPENDICES	
1. List of Variables	176
2. Derivation of Fire Growth Equations	185

LIST OF ILLUSTRATIONS

	<u>Page</u>
1. The Modeling Process	5
2. The Calibration Function	33
3. The Diurnal Cycle	42
4. Cumulative Probability Distribution for Expected and Simulated Fire Intensities	55
5. Fire Growth Multiplier as a Function of Relative Suppression Time	60
6. Relationship between the Length-to-Width Ratio of a Fire and Wind Speed	64
7. Rear and Flank Relative Rates of Spread as a Function of Wind Speed	67
8. Fire Area to Perimeter Relationship	70
9. Fire Growth Variables	74
10. Relationship between Arc Growth and Control Status .	76
11. Arc Growth Adjustment for the Start of Suppression .	78
12. A Typical Simulated Fire	80
13. Effect of Ground Crew Arrival Delay	86
14. Actual versus Calculated Time to Mop-up	97
15. Actual versus Calculated Suppression Cost	104
16. Actual versus Calculated Forest Damage	111
17. Percent of Original Intensity after a Long-term Retardant Drop	133
18. Total Retardant Depth for Sequential Releases	140
19. Typical Drop Pattern Profiles	152
20. Average Retardant Pattern Length under a Canopy	153
21. Maximum Useful Retardant Depth	154
22. Percent of Retardant Recovery under a Canopy	155
23. Relative Retardant Pattern Lengths under a Canopy ..	156

LIST OF TABLES

	<u>Page</u>
1. Size Classification for Simulation Models.....	16
2. Fuel Classifications.....	46
3. Relative Values of Icn.....	87
4. Statistics for Mop-up Regression Equations.....	96
5. Statistics for Cost Regression Equations.....	103
6. Summary of Damage.....	109
7. Statistics for Forest Damage Regression Equations..	110
8. Average Times for Selected Air Tanker Activities...	125
9. Data Used to Compute Relative Maneuverability.....	126
10. Optimum Release Interval versus Pattern Lengths for the CL-215, using Two Tanks.....	141
11. Air Tanker Drop Errors.....	148
12. Expected Total Error using a Binomial Distribution for Five Independent Errors.....	150
13. Relative Pattern Length Under a Canopy.....	157
14. Relative Retardant Transmission through a Canopy...	157
15. Relative Retardant Interception by a Canopy.....	158
16. Rainfall Retention in Forest Canopies.....	158
17. Relative Water/Thickened Retardant Pattern Lengths.	159

ACKNOWLEDGEMENTS

This report represents the efforts of many more persons than appear on the front cover. The authors wish to take this opportunity to thank those whose considerable efforts contributed in large measure to the success of this project.

Without initial financial support by the FIRESCOPE project of the U.S. Forest Service Fire Laboratory, Riverside, California, the project might never have been started. Without the continued support of our Director, Mr. D. E. Williams, over the past three years, the project certainly would not have been completed. Without the considerable efforts of the typists, Mrs. A. Laing and Mrs. S. Cybulski, the report could not have been printed. Finally, without the reviewers, R. Redmond and N. Eruce, the text would have been full of errors. To everyone mentioned above and those not mentioned specifically, thank you.

PREFACE

Those who read both the model description contained in this report and the program documentation contained in Information Report FF-X-64 will note that the variable nomenclature is not the same in the two reports. There are several reasons for the differences.

- Many names were associated with two or more variables in the program. This is both an acceptable and desirable practice, in that computer storage requirements are reduced. On the other hand, two or more definitions for a single variable is confusing in a mathematical discussion.
- Long variable names, as are commonly found in computer programs, tend to confuse the essence of an equation. When variable names are short and simple, the nature of the equation is more readily discernible.
- With three persons working on program development over a two and a half year span, a variety of nomenclature evolved. Closely related variables occasionally had unrelated names in the program.
- Equations written for a computer sometimes differ in form from standard mathematical nomenclature to increase computational efficiency.

In the light of the preceding, a new, better organized set of variable names is employed in this report. Hopefully, this will improve the comprehensibility of the model description while incurring only minimal difficulties with respect to interpreting the program.

The reader will note the absence of metric units. Model development took place over a four-year period, with metric conversion being instituted at the mid-point of the process. It was decided that the development process would be needlessly complicated by a conversion to metric units. Thus, the model as described in this report employs English units for input data, computations, and results. The model is being converted to metric units for future applications.

AIRPRO

AN AIR TANKER PRODUCTIVITY COMPUTER SIMULATION MODEL

THE EQUATIONS

(Documentation)

A.J. Simard and G.A. Young

Introduction

AIRPRO is a simulation model designed for computer implementation. Its purpose is to simulate the use of air tankers in wildland fire suppression operations. The model can be used to analyze a wide variety of questions with respect to air tanker systems including: dispatch, resource and tactic selection, productivity, effectiveness, fleet size and composition, and to a limited extent, allocation. In addition, because the model incorporates ground suppression and fire growth in some detail, it can also be used to analyze a variety of fire management problems.

This report contains a detailed discussion of the mathematics of AIRPRO. A computer program based on this model has been described previously (Simard et al. 1977). An air tanker system overview, in which the framework for the model was developed, will be discussed in a subsequent report. Validation and application of the model will also be considered in future reports.

In all, over 300 equations are described in this document. The discussion considers the development, inherent assumptions, and implications of the equations and tabular data used by the model, according to the relative significance of each.

The purpose of this report is to allow the air tanker system manager to satisfy himself that the internal workings of the model do, in fact, correspond to the way in which his system operates. It also provides the background needed to modify the model to fit specific user requirements or operating conditions.

Since a highly technical subject cannot be presented in a nontechnical manner, a nominal familiarity with elementary mathematics and statistics is required to fully understand the concepts presented in this report. For those who are uncomfortable in a mathematical environment, a comprehensive discussion is provided, allowing the reader to "read around" the equations, and still follow the general trend of the model.

This report contains six sections. The first describes the modeling process in general and develops a specific plan for the air tanker model. The second section briefly describes a few general simulation functions used in the model, including the processing of time. Each of the last four sections is devoted to one specific component of the model: the environment, fire growth, ground suppression, and air tanker use.

1. MODEL DEVELOPMENT

A. The Modeling Process

In many physical sciences, the modeling process has evolved over several decades. It is supported by fairly well developed theoretical foundations and data bases. In contrast, modeling in many nonphysical fields such as ecology and management is of much more recent origin, as are the sciences themselves. As a result, theory, data, and experience, the underpinnings of any modeling effort, are often severely lacking. While the use of modeling has been increasing significantly over the past decade, there has not been a commensurate increase in understanding the modeling process (Caswell et al. 1972). On one hand, there are volumes describing techniques of model construction: Naylor et al. (1966); Meier et al. (1969); Hamilton et al. (1969); McMillan and Gonzalez (1973); Forrester (1961); and Patten (1971, 1972). On the other hand, in a detailed survey of 132 projects, Shubik and Brewer (1972) found that, from virtually every point of view, management of the modeling process is poor to nonexistent. While there are a variety of reasons for this, lack of information is no doubt a primary cause. For example, information on fitting an appropriate model to a problem is scanty. Clymer and Bloedsoe (1969) discussed model scale, while Duncan (1973) discussed model size in relation to the eventual use to which the model will be put. While some light has been shed on the subject, a great deal more has to be learned.

At the other end of the process, Shubik and Brewer (1972) noted that: "The lack of cost information to construct, operate, improve, and evaluate models is poor to nonexistent. Thus, no criteria exist to measure the effectiveness of proposed efforts." It can be added that even if cost data were available, techniques of evaluation are equally nonexistent. For example, after visiting eleven interdisciplinary environmental modeling projects, Mar and Newell (1973) concluded: "Many modelers considered models validated when all variables they feel are important are included and none of the relationships between variables are incorrect by the modelers standards. One model is claimed to be better than another when it has more variables, it handles more nonlinearities, when it is more precise, etc. The premium appears to be on proof by exhaustion rather than a proof by finesse."

In light of the above, it would seem logical to examine the process of modeling from a systems point of view. A flow diagram of the modeling process is shown in Fig. 1. The system to be analyzed exists within an environment which is external to the modeling process. The system provides resources, in the form of money and manpower, to develop a model. Both the system and the environment provide information which is transformed into a model

by the modeling process. The process of modeling can be divided into four phases: planning, development, analysis, and implementation.

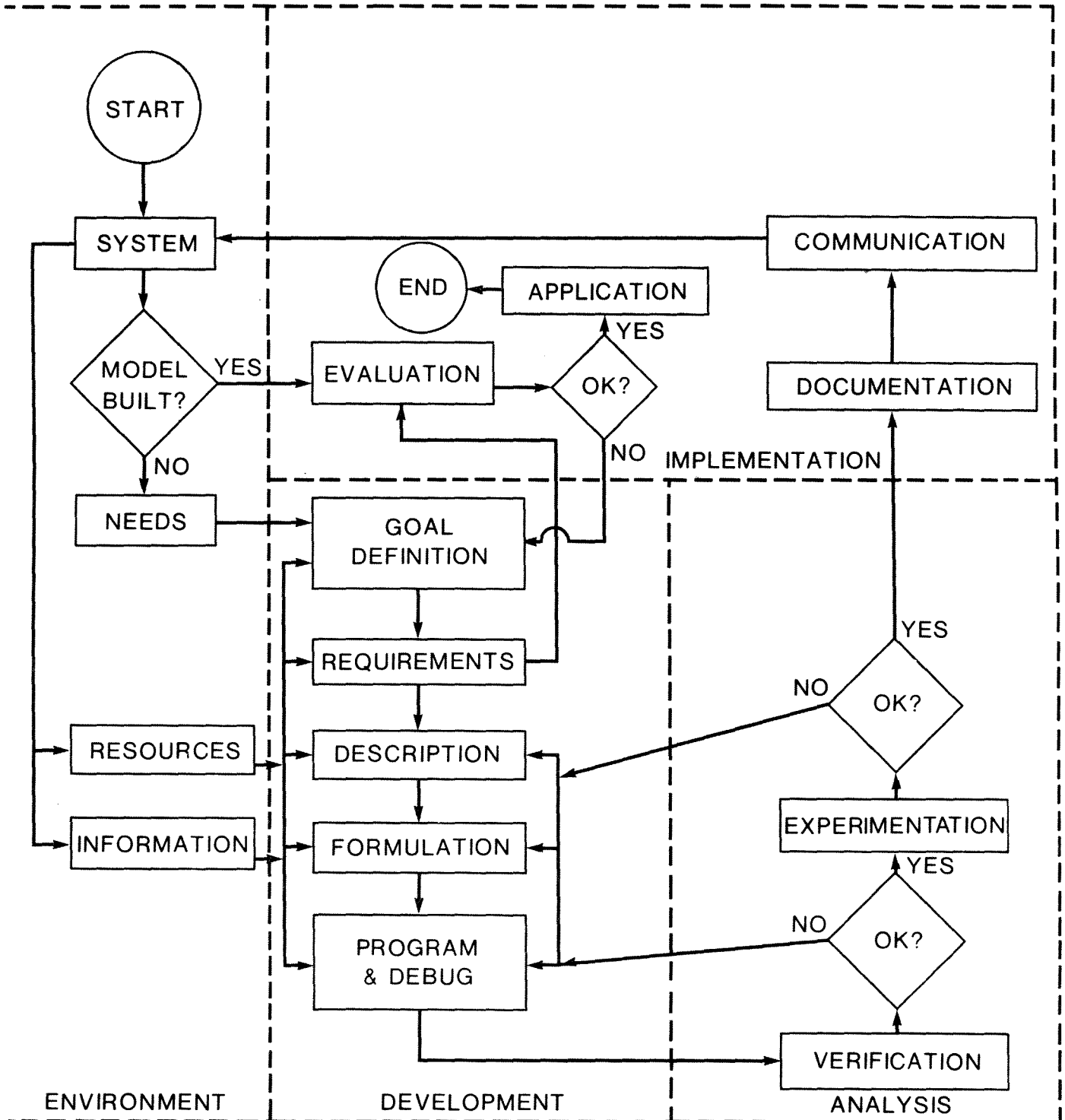
The process begins by relating the proposed model to the system in the planning phase. There are three steps to planning. First, the goals of the modeling process are related to the system. Then, the requirements which must be satisfied to meet the goals are determined. Finally, a description is prepared by specifying the characteristics which the model must have to fulfill the requirements. Planning requires managerial and modeling experience, combined with an understanding of the system being studied.

In the development phase, the emphasis is on model building. The variables and their interrelationships are defined in the formulation step. Then, the model is programmed and debugged. To this point, modeling is essentially a sequential flow-through process. During development, the primary activities involve systems analysis, mathematics, and computer programming techniques.

During analysis, emphasis shifts to studying the problem. This phase begins with model validation, wherein the quality of the model is determined. The analysis phase is a first order feedback process. As each component is developed, model characteristics are compared with corresponding requirements. If the comparisons are satisfactory, the process continues. If not, the process returns to the appropriate model development step to modify the model as necessary. After a satisfactory evaluation, the model is used to perform experiments related to the original problem. During analysis, classical scientific methods become paramount.

Finally, implementation is concerned with applying the results in the system. This phase involves the highest level of feedback. The modeling process interacts with its environment (the system which it is studying). First, model and experimental results are documented. These are communicated to the system and the results are then compared with the original needs of the system. If the comparison is satisfactory, the process moves to an overall evaluation step followed by application of the model in the system. If the comparison is unsatisfactory, the process returns to the planning phase, defines a new set of goals and requirements, and repeats the cycle.

Figure 1. The modeling Process



As suggested in Fig. 1, the modeling process does not take place in a vacuum. In addition to relating the model to the system, there are external information constraints which have to be considered. Many decisions required by the modeling process cannot be made strictly on the basis of the system or modeling techniques alone. There are four information constraints to consider: the data, knowledge, available techniques, and experience.

1) Data Availability

If data is lacking, the modeler is forced to use mental models or generate the necessary data. The latter is often a time consuming and expensive process. Similarly, the quality of the model will be limited to the quality of the available data, unless better data is generated. There is little sense in applying sophisticated models to limited sets of data. Conversely, large masses of data tend to require sophisticated models to analyze the information.

2) Knowledge

If the system is not well understood, the modeler will be limited to mental or correlative models unless experimental derivation of cause and effect relationships can be undertaken - again a costly and time consuming process.

3) Available Techniques

The degree to which the model represents the system will be limited by the degree to which available modeling techniques reflect system behavior. If the model is not representative of the system being analyzed, the results will be of limited value.

4) Experience

Generally, the best models will be constructed by persons who are thoroughly familiar with both the system and the modeling process.

In the remainder of this section, we will consider the planning process in greater detail. In addition, specifications for AIRPROC will be developed, based on the general discussion.

B. Goal Definition

Goal definition links the system with the model. It is the most critical aspect of the modeling process. If the linkage between the system and model is weak, modeling will tend to optimize internally. In practice, this function is often given little attention. The result, as noted by Hysmans (1970), is

that many models, perhaps even a majority, are not used for the purposes for which they were intended.

Goal definition can be thought of as an executive function, where policy guidelines for the remainder of the modeling process are determined. Decisions made at this point are primarily nontechnical in nature. They are based on the needs of the system. They should be arrived at by close consultation between a person who is familiar with the system and the modeler. Goal definition is a sequential process with each step based on previous steps. There are three steps: defining the problem, determining the use, and stating the objective.

1) Defining the Problem

This is the first step in virtually every published reference on model building. A problem arises when some aspect of a system deviates from the goals of the system. While problem definition would appear to be a fairly straight-forward undertaking, the fact that an analysis of wrong problems is a fairly common occurrence suggests that this step is often not performed adequately.

As with any scientific process, problem definition is more likely to be an evolutionary process rather than a one-time effort. As information about a system is acquired, progressive redefinition and refinement of the problem statement generally takes place throughout the course of the modeling process. These changes can take many forms, such as closer examination of more limited aspects of the problem, examination of problems that are discovered as a result of preliminary investigations, or simply a redefinition based on a deeper understanding of the nature of the system. It is possible, therefore, that initial and final problem statements may differ significantly.

2) Determining the Use

Use refers to what the system will do with the model. The final use affects the basic nature and structure of the model. Rather than defining general use categories (teaching, research, understanding, etc.) this statement should be specific to each modeling effort.

Also of interest is the experience of the person who will use the model. This not only affects the manner of communicating the results, but it could also influence the selection of a modeling technique. Sophisticated techniques will encounter more resistance in application than less complex ones to which the user can more readily relate. Similarly, increasing the level of aggregation will decrease the willingness of managers to accept the results. This in no way suggests that models must be simple.

If a sophisticated procedure is the best technique to solve a problem, it should be used. As the degree of sophistication increases, however, the manager and his values will have to become increasingly involved in the analysis. This will be particularly critical if the results contradict preconceived notions under which the decision maker has traditionally operated for years.

3) Stating the Objective

The goal statement specifies what the model will do. It is the focal point for subsequent decisions. It should reflect the problem and the use statements which have preceded it. Goal statements are generally brief and subjective. Precise definition of terms and criteria for measuring goal attainment will normally be specified in detail under requirements.

C. Requirements

Having summarized what is to be done, we now consider a more detailed list of model requirements. This is essentially a translation of the verbal problem, use, and goal statements into technical information to be used as a guide for formulating a model. Requirements can be divided into four categories: quality, analysis, implementation, and resources. It will be noted that each of the first three refer to one phase of the modeling process as defined in Fig. 1, while the fourth refers to the overall effort.

1) Quality

Quality is defined by Webster as "The degree of excellence." Quality measures how good the model is. This requirement applies to the formulation and programing components of model development. There are four quality characteristics that should be specified: errors, validity, scope, and resolution.

a) Errors

Clearly it is desirable to have no errors in a model. In practice, one strives to reduce errors to a reasonable minimum. There are three types of errors: Precision, correctness, and accuracy.

- Precision or measurement errors - normal practice is to measure variables with greater precision than needed to achieve the desired resolution.
- Correctness or programing errors - careful attention to detail and close examination of the results are needed, along with systematic programing and debugging procedures.

- Accuracy or errors of estimation - how well do the functional relationships represent the real world?

b) Validity

Is the model a true representation of reality? There are three concerns with respect to validity: assumptions, relationships, and system behavior.

- Assumptions - any assumptions which are significant to the system being analyzed should be closely examined.
- Relationships - the existence of a nonzero intercept, the sign and magnitude of coefficients, and the inclusion (or exclusion) of specific variables in regression equations should all be rationalized with respect to the phenomenon being simulated.
- System behavior - is the behavior of the system, as modeled, logical and consistent with what would be expected? Sensitivity of the model to ranges of input stimuli is a key test of model behavior.

c) Scope

How much of the system is being studied with the model? The scope of a model is related to four considerations: number of variables, number of interactions, system boundary, and data dependence.

- Variables - have all variables relevant to the system being analyzed been included?
- Interactions - have all interactions which are significant to the system being analyzed been included?
- System boundary - which variables and interactions are exogenous and endogenous?
- Data dependence - dependence of the model on the specific data set used for its derivation should be minimized.

d) Resolution

The smallest difference in the real system, which a model can distinguish, is called resolution. While it is possible to specify a desired degree of resolution for the model as a whole, it is not possible to specify the resolution required for each component in order to achieve the overall objective. If the overall effect of errors is compensating, one-half of the overall requirement might suffice for individual components. If, on the

other hand, the errors are additive, the resolution of individual components will have to be considerably better than the overall objective. There are a number of factors to consider.

- The maximum resolution that can reasonably be obtained.
- The minimum difference required for management to act.
- The level of resolution required for the problem being analyzed.
- The possibility of finer detail being required in the future, suggesting greater resolution than may currently be required.
- Are several problems being analyzed simultaneously? If so, resolution will have to be adequate to meet the most stringent requirements.

2) Analysis

There are two requirements for the analysis phase of the process; one for each of the two functions shown in Fig. 1 - validation and experimentation.

a) Validation

How will it be determined whether or not the desired quality attributes have been attained? Verification is normally done in two stages. The first stage relates to individual components and processes within the model. This stage is closely related to development, with a significant amount of reformulation and reprogramming taking place as discrepancies are detected. In fact, the boundary between development and verification is somewhat arbitrary. The latter is included in the analysis phase primarily because the interpretation of results is one of the key tools of verification. In addition, early runs often provide useful analytical results. By comparing the behavior of the model with invalid data or components to the behavior after corrections have been made, information is often obtained which would not have been acquired had only the "correct" version been run.

The points to consider in the first stage of verification have been discussed under model quality. They will not be repeated here. Application of a few common sense rules will allow the modeler to develop techniques appropriate to each model.

- Test as many combinations of data and system states as is reasonably possible. Something will inevitably go wrong with an untested combination.

- Verify every equation and component with hand calculation.
- Perform appropriate statistical tests to determine the significance of different results.
- Examine the smallest computational discrepancies in detail and identify the exact cause. A significant error might be nullified on the test case being examined.
- Do not rationalize unexpected behavior - verify it.

If one were to state a philosophy to follow in the first stage of verification, it might sound like "Assume nothing works - test everything."

In the second stage, we are concerned with validation of the overall model. The ultimate test is whether or not the model represents reality. A variety of evaluation techniques are available. Each is best suited to a specific type of model and modeling environment.

- Examine model output for reasonableness.
- Compare with historical data.
- Run the model parallel with the real system.
- Use output from the model as input for several iterations.
- Compare with results from other models.

No test can prove the validity of a model. Tests only validate the degree to which confirmation has been determined. Clearly, the greater the agreement between the model and various tests, the greater will be the confidence that can be placed in the assumption that the model is valid.

b) Experimentation

How will the model be used experimentally? What forms of output will it generate? How will the output be analyzed? With these questions we enter the realm of research techniques or operational procedures, depending on the use to which the model will be put. Suffice it to say that the requirements should include a brief statement on this topic. Further elaboration is beyond the scope of this discussion.

3) Implementation

The findings must be implemented in the system being studied. There should be a brief statement reflecting how each of the functions shown in Fig. 1 will be accomplished.

a) Documentation

As with any research effort, someone other than the modeler should be able to duplicate the results or apply the model to a new situation. This requires complete documentation, which discusses a number of topics.

- The mathematical model - equations, inherent assumptions, derivations, and references.
- The computer program - listings, flow charts, and variable lists.
- Verification - techniques and results.
- Input data - sources, processing required, and limitations.
- Results - listings, statistical analysis, and interpretation.

b) Communication

The results have to be transmitted to the system. While presenting the above documentation to system managers is one form of communication, it is a notoriously poor one. Such documentation is intended for researchers and programmers and is not likely to be well received by system managers. The following list mentions a few appropriate techniques.

- Written report - this should summarize the key findings and the modeler's estimate of his degree of confidence in them. It should be written in nontechnical language. Written reports should only be used to supplement other communication techniques.
- Informal presentation - discuss the results with system managers on a one-to-one basis.
- Formal presentation - an organized presentation to a group from within the system.
- Participation by system personnel - the most effective communicator is someone from within the system. There is considerable benefit to having someone who is trusted by system managers and who knows their language participate in

the modeling process so that he can understand and communicate the results.

c) Application

How will the model affect the system? Will it be used operationally? If so, the modeler should be prepared to aid in its implementation and to respond quickly when problems arise. If results are to be used, the modeler should aid in their interpretation. In either case, the modeler must be an active participant in the initial stages if application is to be successful.

d) Evaluation

How will the modeling effort be evaluated? Considering the unspectacular success of many efforts, it is understandable that this task is often omitted. There is little discussion of the evaluation of modeling in the literature. While to some extent, this reflects the recent and still ongoing evolution of the process, it will have to be dealt with if the "art" is to become a "science." Evaluation must go beyond a simple comparison of requirements versus achievements because, as will be noted subsequently, some requirements are mutually conflicting. The following is proposed as a simple yet comprehensive evaluation procedure.

- i) Assign relative weights to the four phases of the modeling process, as well as each function within the process (1.0 = average; 0.75 = 25% less important than average; 1.50 = 50% more important than average, etc.). The sum within each phase should equal 1.0. The sum of the four phases should equal 4.0.
- ii) Rate the relative achievement or nonachievement of each requirement where possible (50% more accuracy than required; 10% cost overrun; etc.).
- iii) Multiply the weights determined in i) (function x phase) by the corresponding relative achievements determined in ii).
- iv) Sum the results.

Assuming all requirements are rated, the break even point would be 4.0. A greater sum would indicate a good effort. The degree of goodness can be subjectively estimated by the difference between the sum and 4.0. Conversely, a sum of less than 4.0 would indicate that the effort has not lived up to its expectations. The relative shortcoming would also be a function of the difference between the sum and 4.0.

The use of loose, qualitative terms such as goodness is deliberate. It is not possible to objectively evaluate a model. The reader should not lose sight of the fact that the precise figures used in the calculation are, in themselves, subjective estimates. Thus, any inference suggesting more than a qualitative degree of precision is open to question.

4) Resources

A variety of resources are required to develop, run, and implement a model. On one hand, model quality, analysis, and implementation requirements generally determine the amount of resources that will be required. On the other hand, constraints imposed by the system may limit the amount of resources available. If the available resources are insufficient to fulfil the requirements, some form of compromise will be necessary. Either more resources will have to be made available or the requirements will have to be reduced, or both. There are four resource requirements which should be specified: time, cost, manpower, and equipment.

- Time - how long will it take to complete the modeling process?
- Cost - how much money will be required?
- Manpower - how many persons will have to be assigned to the project?
- Equipment - what type of computer facilities will be required?

The modeler will have to be able to tell system managers what resources will be required to achieve the desired quality objective. He will also have to be able to explain what can and cannot be achieved with fewer resources. He must avoid the natural tendency of promising too much too quickly. While preliminary attempts have been made to reduce the subjectivity inherent in estimating resource requirements (Duncan 1973) a great deal more needs to be done. Given the current state of the art, experience in a particular field of application appears to be the only route by which an individual can gain the necessary knowledge to accurately determine the amount of resources needed to develop a model.

D. Model Description

In this step, the characteristics of the model are specified. Whereas the requirements define what the model should do, the description centers around how it will be done. Once the characteristics of the model have been determined and the

modeling process is well along, few, if any, significant changes can be made without drastically reformulating and reprogramming the model. This process deserves no less consideration than is appropriate to its considerable impact on the overall effort. The skill with which the model is structured is a major factor in determining how well the requirements are met. There are four basic characteristics: general structure, design, technical characteristics, and modeling techniques.

1) General Structure

The general structure includes primarily qualitative characteristics which set the general tone for the design and technical characteristics which follow. They attempt to describe the general nature of the total model from different points of view. While the distinctions may be somewhat arbitrary, they are useful in that they provide an overview of the model and its structure, as well as the general philosophy used in the process. Further, since many of the terms have been used in the literature in a variety of ways, they should be assigned a place in the description process in the hope that a uniform standard might someday emerge. There are three general qualitative characteristics: level, size, and rigor.

a) Level

Level attempts to qualitatively describe several model characteristics using a single classification. For example, each level of a model normally has a level of effort and quality, as well as specific types of structures with which it is commonly associated. Three levels of models are defined: overview, framework, and operational.

- Overview - a small scale "quick and dirty" model, requiring a few days to a few weeks to develop. Overview models would be appropriate for uses such as project proposals, feasibility tests and training model builders. Although Duncan (1973) suggests a fairly wide range of uses for overview models, the information generated is so limited and gross that many of his suggested uses are hard to envisage.
- Framework - Bloedsoe and Jameson (1969) stated: "This type of model provides a framework for bringing together the parts of the system which are too complex to recognize and comprehend, otherwise." This is an intermediate level model whose main purpose is to provide preliminary information about a system to both the modeler and user. The framework model attempts to include all variables which may effect the system and then, with sensitivity analysis, determines which variables are significant and which can be aggregated or dropped. The primary purpose is to include the full range of variance of

each variable and the full range of its effects rather than to elegantly model specific processes. A framework model is more concerned with significance levels than with precision and validity.

- Operational - there are two categories of operational models - management and research. The differentiation is based on the direction of change from the framework model level. Management models will normally tend towards efficiency, dropping all considerations not significant to the question at hand. Thus, management models will, in all likelihood, become smaller than the framework model. Research models, on the other hand, will likely tend to grow from the framework stage as the search for information is enhanced by quality rather than efficiency. Whatever the use, however, operational models imply a thorough "verification." Management models will tend to be based primarily on data and knowledge which is available at the time the project is undertaken. They will often tend to be of the correlative type. Research models may be based on data and knowledge which has to be artificially generated. Alternatively, they might well tend to be based on laboratory data.

b) Size

A size classification should convey the physical dimensions of the model. The sum of the number of variables plus interactions would be useful to describe model size. The number of variables alone would not be sufficient, as a highly interactive model would be far larger than a sequential model with the same number of variables. To make the classification significant, it was arbitrarily decided that each class should be about an order of magnitude larger than the one below it. Appropriate class boundaries and midpoints for the various size classes are listed in Table 1.

Table 1. Size classification for simulation models

Sum of variables plus interactions	
Small:	50 (10 to 100)
Medium:	500 (100 to 1,000)
Large:	5,000 (1,000 to 10,000)

Since size is strictly a qualitative description, more detail than is given would be of limited value.

c) Rigor

This describes the degree to which the functional relationships are based on theory. De Neufville and Stafford

(1971) describe three classes of rigor: mental, correlative, and mechanistic. These three classes should suffice for our purposes. While most models will contain combinations of two or all three classes of rigor, one type will normally predominate.

- Mental (observational) models - these are normally the first type of model developed relative to a specific problem. They are primarily based on experience, intuition, and limited data. They tend to be qualitative in nature, but do provide preliminary insight into a problem. These models normally imply the lowest level of understanding of the system.
- Correlative (empirical) models - these involve the correlation of dependent variables with a set of significant independent variables, based on a set of empirical data. These models tend to be specific to a particular set or type of data. They are used primarily in situations where the modeler is interested in output from a system but not the mechanism whereby the output is generated.
- Mechanistic (theoretical) models - these models employ mechanistic functions where the relationships can be substantiated on theoretical grounds. They normally result from a great deal of experimentation and verification. They require the highest level of understanding of the system. These models are considered the most rigorous. All things being equal, this level of model is preferred over other levels.

2) Design Characteristics

Design characteristics differ from the general structure in that they describe the manner in which components of the model fit together. There are three characteristics of interest: organization, aggregation, and scale.

a) Organization

There are two basic organization formats: unified and modular.

- In the unified model, all components are in a single large program. This format is best suited to small models. While this procedure avoids interfacing problems, it becomes excessively cumbersome for large models.
- In the modular model, major parts are grouped into blocks which, in theory, can be developed independently from the remainder of the model and readily inserted or removed. In practice, while there are numerous interfacing problems

(Clymer and Bloedsoe 1969) the modular approach is virtually mandatory, if large systems are to be modeled successfully.

b) Aggregation

There are three schools of thought concerning the aggregation of variables: integrated, disassociated, and intermediate.

- The integrated model - the basic philosophy is that a system can be modeled in its entirety with a few variables which aggregate many smaller parts of the system. Its major advantage is ease of model development. Its major disadvantage is the difficulty of analyzing complex systems on the level of the whole. Such models generally only consider the gross overall behavior of a system.
- The disassociated model - the basic philosophy might be called the classical approach in that small, well understood parts of the system are joined in an attempt to model the entire system. The major advantage is that it is possible to understand and verify the function of the individual parts. On the other hand, a basic premise of systems theory is that the whole is greater than the sum of its parts. Simply putting the parts together is not necessarily sufficient for understanding the functioning of the overall system.
- The intermediate model - this, as the name implies, is between the two extremes. The basic approach is to develop large parts of the system as complete units and then join the parts into a coherent whole. It is a compromise between the advantages and disadvantages of the two extremes.

c) Scale

Scale is a three dimensional descriptive property of a model. The three dimensions are time, space, and system level. Clymer and Bloedsoe (1969) suggest that two dimensions are adequate to define scale: time (minutes, hours, days, months, years, etc.) and system level (consumers, plants, soil organisms, soil, etc.). A third dimension is needed, however, to specify the physical size of the variables in the model. For an ecosystem model, such as described by Clymer and Bloedsoe (1969), unit area would be an appropriate measure. Appropriate order of magnitude changes in area would be m^2 , $100m^2$, km^2 , etc. The units could just as well be hectares or whatever unit (slope, watershed, etc.) was appropriate to the problem at hand.

3) Technical Characteristics

These describe the mechanisms whereby variables and flows within the model are processed. The selection of technical

characteristics is based on the requirements of the model and the nature of the system. There are four technical characteristics: time, flow, certainty, and analytical technique.

a) Time

There are three methods of modeling time: static, even increment, and uneven increment.

- Static - as the name implies, static models do not consider time as a variable. Rather, they analyze the system at a specific point in time. Such a procedure is well suited to many real-world problems such as the optimization of resource allocation, job shop scheduling, and network flows. Static models are obviously poorly suited to systems which change significantly over time.
- Even increment - these models are well suited to systems which tend to be fairly regular. This can arise in two different ways. In the business world, it is generally desirable to perform a variety of audit functions at regular intervals. The impact of individual transactions or events (sales, production of one unit, etc.) is small relative to the overall business. Thus, it is logical that a model of such a process would simply accumulate totals for one time interval, determine the state of the system at the end of the interval, and advance to the next period. A second type of system which is well suited to even time increment modeling is a continuous flow system. In such a system, there are no "events" as such. Many physical and biological processes such as the accumulation of moisture in forest litter or plant growth can be modeled as continuous processes. Thus, it is logical that time be advanced by regular intervals and the state of the system monitored at the end of each interval.
- Uneven increment - these models are well suited to systems which are strongly "event" oriented, with little activity between events. Emergency service dispatch (police, fire, ambulance) fits this pattern. The system responds significantly to an individual event, while little happens between events. Thus, system state is determined at the completion of one event, after which, time is advanced to the next event.

b) Flow

There are two methods of modeling flow: discrete and continuous.

- Discrete flow - event-oriented systems can be classified as having a discrete flow. In other words, stimuli tend to be in the form of individual pulses. As the impact of an individual pulse increases, the arguments in favour of discrete flow modeling also increase.
- Continuous - systems in which individual events or pulses cannot be identified are best modeled as continuous flow processes. In addition, the work of Forrester (1961) indicates that event-oriented systems can also be modeled as continuous flow processes, if the impact of individual events is small relative to the level of aggregation being considered.

c) Certainty

Certainty can be modeled in three ways: deterministic, stochastic, and mixed.

- Deterministic - if the occurrence of an event or the behavior of a system is predictable with certainty or near certainty, a deterministic model is appropriate. Deterministic models imply a reasonably high degree of understanding of the mechanistic processes involved in a system. They also assume that all of the significant independent variables needed to predict the behavior of the dependent variables have been included in the model. Obviously, deterministic models require considerable theoretical justification and support.
- Stochastic - when only the probability of the occurrence of an event or the behavior of the system is determinable, stochastic modeling is appropriate. The occurrence of forest fires or calls on a telephone network are examples of stochastic processes. Stochastic models normally involve random samples drawn from generated probability distributions. When events are not mutually independent, joint probability distributions are required, which often necessitates fairly complex modeling. Stochastic models require less understanding of the mechanistic behavior of the system than deterministic models.
- Mixed - some processes are neither predictable with relative certainty nor mutually independent. To use either stochastic or deterministic techniques in isolation would be incorrect. Thus, some form of mixture of the two techniques is employed, such as calculating an average deterministically, and then generating random variation about that average.

4) Modeling Techniques

Contrary to the opinion of some, a model should be selected to fit a particular problem. The problem should not be adjusted to fit a convenient model format. Failure to proceed in the first manner will invariably limit the usefulness of the results. Further, any modeling procedure is less than a perfect representation of the real world, and as such contains some error. It is not uncommon that the magnitude of the error in the modeling process is greater than differences between successive runs of an analysis. This also applies to differences between simple and sophisticated analytical procedures. There is no clear answer to the question: Is it better to optimize an abstract formulation of the problem, or to find a good solution to a more realistic formulation?

We will now consider a selection of modeling techniques. It should be noted that in most situations, there is no single technique that is appropriate for every component of a large model. Thus, the modeler will be concerned with selecting a set of techniques rather than a single one.

a) Examine the real world

In a sense, this is not a modeling technique. The real world itself is being used as a model. One simply observes what happens, and tries to draw conclusions about the processes involved.

b) Examine observations

This generally refers to the conduct of experiments where all but a few factors are held constant. This has the disadvantages of high costs relative to the quantity of information provided and long time periods are often required. The chief advantage is that only a minimal understanding of the internal mechanisms of the system being analyzed need be known. This technique is only practical for relatively simple situations where only two or three factors are involved.

c) Empirical models

In general, this refers to the use of regression techniques to develop predictive models based on observations of real world or experimental data. Such models indicate a relationship between factors, but not the mechanisms whereby the relationship occurs. These have the advantage of being able to include more factors than was the case above. They also have the advantage of only modest cost and time requirements. Empirical models are particularly useful for components which are not critical to the

system under consideration, particularly where the achievement of reasonable predictive accuracy is sufficient.

d) Gaming models

These involve the use of experienced persons playing a hypothetical game which is designed to simulate a particular situation of interest. The output of the procedure is the action of the players. The basic concept is that it may be possible to discern trends in the actions of several players, and thereby gain an increased understanding of the basic mechanisms involved. The ability of such procedures to disclose useful, quantitative information is open to question, however.

e) Simulation models

These models generate activities or processes which simulate the behavior of a real system. Simulation models are often used when the individual parts of a system are reasonably well understood, but the dynamic behavior of the overall system is not known. Simulation is also used when a system is too complex to model with other procedure. An additional benefit is that simulation models are relatively easy for persons other than the modeler to understand. Simulation has the disadvantage of being costly and generally requires a considerable amount of time to program. Further, simulation is poorly suited to finding optimal solutions. To some, simulation is the method of last resort. More properly, the procedure should be given equal consideration in the initial stage of the model selection process.

f) Mathematical programming models

These have several important advantages. They find optimal solutions; they are very powerful and efficient; and their cost and time requirements are low. It is not surprising, therefore, that a great deal of effort is often expended to make a problem fit the required mathematical programming framework. They have disadvantages, however. Their framework is rigid and the real world often simply does not fit; they generally require considerable abstraction; the analyst must understand the functioning of the entire system; they are static; they are sophisticated, and, thus, often not comprehensible to the average reader.

g) Mathematical models

This generally involves the highest level of abstraction and sophistication. It also requires the greatest knowledge of the system. Mathematical models have the advantages of being relatively inexpensive and require relatively little time to develop. Mathematical modeling is the most efficient way of

deriving an optimal solution. On the other hand, only relatively simple processes (in the sense that they must be smooth, continuous, and not have too many variables) can be modeled mathematically.

We will now apply the preceding concepts to the development of a set of specifications for an air tanker productivity computer simulation model.

E. Specifications for AIRPRO

1) Goal Definition

- a) The problem - There is no procedure currently available to quantitatively determine air tanker productivity or effectiveness and hence, the appropriate role of air tankers in wildland fire management systems.
- b) Use of the model - The model will be used by researchers, to provide data to aid fire management agencies with air tanker system presuppression planning.
- c) Goals - The model should be able to:
 - i) quantitatively measure air tanker productivity and effectiveness;
 - ii) determine the optimum combination of resources and tactics to employ in specific fire suppression operations; and
 - iii) summarize the above for an agency over one or more fire seasons.

2) Requirements

a) Quality

- i) Errors - The cumulative effect of all errors should be insignificant relative to the results, when summarized over a large set of data. The cumulative effect of errors should not exceed 10% when results are summarized over small sets of data (30 fires).
- ii) Validity - All assumptions and relationships which perturb the overall system by more than 5% will be verified.

- iii) Scope - The model should be applicable to all fire suppression environments in North America where air tankers are used.
- iv) Resolution - The model should be able to detect statistically significant system responses on the order of 10%.

b) Analysis

i) Validation

- Simulation output generated by the environmental, fire and ground suppression components will be statistically compared with historical data.
- Output generated by the air tanker component will be examined for reasonableness and compared with previous air tanker research, to the extent possible. A sensitivity analysis will also be undertaken.

ii) Experimentation

- The model will test all reasonable combinations of air tanker resources and tactics on a set of 3,000 historical fires which occurred in the province of New Brunswick.
- The results will be analyzed and inferences will be made, if warranted.

c) Implementation

- i) Documentation - The model and computer program will be fully documented. There will also be a report on the analysis of the data, the results, and their interpretation.
- ii) Communication - The findings will be summarized and written reports presented to system managers. In addition, formal and informal verbal presentations will also be made.
- iii) Application - This is the prerogative of system managers. The authors will provide whatever assistance is necessary.
- iv) Evaluation - The overall effort will be evaluated using previously outlined procedures.¹

¹ See Part 1., Section C., 3), d), of this report.

d) Resources

- i) Time - Three months will be needed for planning, two years for model development, six months for analysis, and one year for implementation.
- ii) Cost - \$30,000 will be needed for model development and analysis, and \$10,000 for data analysis and preparation (excluding salaries).
- iii) Manpower - Three persons will be required; one project supervisor and two programming assistants.
- iv) Equipment - A large computer with remote access, time sharing, and interactive debugging will be needed.

3) Model Description

a) General

- i) Class - operational model - to provide research data.
- ii) Size - medium.
- iii) Rigor - as appropriate to the specific component.
 - Mental models (tactic selection, suppression, etc.).
 - Correlative models (mop-up, growth, etc.).
 - Mechanistic models (distances, sunset time, etc.).

b) Design

- i) Organization - modular - In general, one subroutine for each major component and function.
- ii) Aggregation - mixed - The air tanker component will be disassociated while the remaining components will tend toward intergration.
- iii) Scale
 - There are three scales of time measurement: 0.1 to 1.0 hours for individual fires; zero to several days between fires; and one to several years for overall totals.

- Space is measured in acres, with 0.1 acres or 10% of the area (whichever is greater) considered the minimum significant difference.
- Three system levels are considered: fire suppression, air tanker utilization, and some air tanker utilization subsystems.

c) Technical characteristics

- i) Time simulation - Uneven increment is used between events, with even increment being used for fire growth and ground suppression.
- ii) Flow
 - Continuous flow is used for fire growth and ground suppression.
 - Discrete flow is used for events (crew arrival, change of hour, sunrise, sunset, and air tanker drops).
- iii) Certainty - deterministic - A large sample size is used to simulate the effect of stochastic elements.

d) Modeling Technique

The primary technique will be simulation, with real-world observations, empirical data, regression analysis, and mathematical models being used as appropriate.

2. GENERAL SIMULATION FUNCTIONS

In this section, a variety of elementary processes found throughout the model will be discussed. We will also consider the manner in which time is incremented, a process external to the air tanker system and its environment. The four technical components of the model (the environment, fire, ground suppression, and air tankers) will be considered in subsequent sections.

A. Elementary Processes

Processing a mathematical model with a computer generally requires an extensive body of supportive computations. The current model is no exception, in that over half of the program can be classed as supportive rather than technical. In addition, a significant amount of elementary calculations are also performed within the technical subroutines. Due to the simplicity and standardized nature of these calculations, a single description of the general form suffices for all variants found throughout the model. Three processes will be considered: initialization and storage, accumulation, and rounding off.

1) Initialization and Storage

In all simulation models, the initial state of the system must be specified. In addition, as in the present case, it is often necessary to reinitialize the system for analyzing alternative strategies and to reset the system to a noninitial state for analyzing subsets of strategies. Initialization can be done in two ways - logically and mathematically. Logical techniques employing programming statements such as READ, DATA, COMMON, EQUIVALENCE, etc., are described in the program documentation (Simard et al. 1977) and will not be considered here.

The simplest form of mathematical initialization is:

$$(1) \quad V = c$$

where: V = the variable to be initialized and
 c = a constant (typically, but not necessarily zero).

When the initial value is not a constant, a variable is substituted for c :

$$(2) \quad V = V_s$$

where: V_s = a storage variable that has been assigned the initial value.

In any model where reinitialization or resetting is required, the initial or appropriate value of the system descriptors must be stored, because the values are altered during simulation. As with initialization, this can be done either logically or mathematically. The mathematical expression is the same as for initialization with the terms reversed:

$$(3) \quad V_s = V.$$

2) Accumulation

Simulation models are often used to process a set of independent events (such as fires). In these cases, it is useful to determine the cumulative total of the results of each event (i.e. total retardant dropped). It is also often necessary to determine the number of occurrences of subevents (i.e. air tanker fires). The standard recursive equation for accumulating occurrence frequency is:

$$(4) \quad N' = N + 1$$

where: N, N' = number of observations before and after accumulation respectively.²

When a result is involved, the equation becomes:

$$(5) \quad R_t' = R_t + R$$

where: R_t, R_t' = total before and after accumulation, respectively and
 R = outcome for the current event.

3) Rounding Off

Processing integers is considerably more efficient than decimal numbers. Further, integers require less core storage as well as less space on input and output files. Finally, a program often requires integer approximations of decimal numbers (array subscripts for example).

² N and N' are the same variable. The prime is used because mathematically, $N = N + 1$ is not correct, whereas in the computer this instruction means add one to the quantity stored at the address associated with N .

The simplest procedure is to truncate:

$$(6) \quad V_i = V_r$$

where: V_i = integer portion of a decimal number
(to the left of the decimal point) and
 V_r = a decimal number.

A more accurate procedure is to round off:

$$(7) \quad \begin{aligned} V_i &= V_r + c & ; & \quad V_r \geq 0 \\ V_i &= V_r - c & ; & \quad V_r < 0 \end{aligned}$$

where: $c = 0.5$ for simple rounding off and
 $c = 1$ for $V_r \geq 0$, when an array subscript is required.

In the interest of programming efficiency, the equation for $V_r < 0$ was not included in the model, as negative values were only possible for dollar savings, and such values were of only marginal interest.

B. Time

AIRPRO simulates the behavior of a system over time. As is the case with all nonstatic simulation models, procedures are required for incrementing time and moving the simulation forward. Since time is not part of the technical relationships of the system under consideration, it is appropriate that it be described separately. The system contains both event-oriented and continuous processes. Therefore, the model incorporates two mechanisms for processing time: an event calendar, and an even-increment fire suppression and fire growth loop.

1) The Event Calendar

There are several aspects of the system being modeled which are strongly event oriented. That is, their occurrence is in the form of a pulse which perturbs the system, with little or no activity taking place between occurrences. There are four events which clearly fall into this category: the arrival of a crew, an air tanker drop, sunrise, and sunset. In addition, the diurnal weather cycle has been modeled as an event, with an even time increment between occurrences (1 hour). There are three reasons for modeling the effect of this continuous process as an event.

- The complexity of a continuous model would exceed its significance relative to the system.
- Changes from one hour to the next are not great (0%-20%).

- The event processing mechanism was already in existence.

In effect, the model incorporates 24 point observations of the continuous effect of the diurnal weather cycle.

The event calendar is a simple five-element array. Each element indicates the time of the next occurrence of the corresponding event. All times are elapsed from the time of detection, which is defined as $T = 0$. There are three steps to processing an event calendar: initialization, selecting the next event, and calculating the time of the next occurrence of an event.

a) Initialization

At the start of a fire, the first occurrence of each event is determined and inserted in the array. The elapsed time to the arrival of the first crew (E_{i_1}) is independent of the detection time. The first arrival is, therefore, equated directly to the sum of the dispatch and travel times which are found in the input data.

The elapsed time to the initial hourly update, sunrise, and sunset, on the other hand, are related to the time of detection. To determine the event time, it is first necessary to convert the time of detection from hours and minutes to hours and fractions of an hour. The necessary variables are calculated by using the following sequence of equations:

$$(8) \quad Hr = \frac{T_{dm}}{100},$$

$$(9) \quad p = \frac{T_{dm} - (100Hr)}{60}, \text{ and}$$

$$(10) \quad T_d = Hr + p$$

where: T_{dm} = detection time (hours and minutes, i.e. 1145),
 Hr = hour in which fire was detected (minutes are truncated i.e. 11),
 p = decimal equivalent of minutes (i.e. 45 min. = .75), and
 T_d = detection time (hours and fractions of an hour, i.e. 11.75).

The initial occurrence of a weather update (E_{i_2}) is, therefore:

$$(11) \quad E_{i_2} = 1 - p.$$

The initial time of sunrise (E_{i_3}) is given by:

$$(12) \quad \begin{aligned} E_{i_3} &= T_{sr} - T_d + 24 & ; & \quad T_{sr} \leq T_d \\ E_{i_3} &= T_{sr} - T_d & ; & \quad T_{sr} > T_d \end{aligned}$$

where: T_{sr} = time of sunrise.

Similarly, the initial sunset time (E_{i_4}) is obtained by:

$$(13) \quad \begin{aligned} E_{i_4} &= T_{ss} - T_d & ; & \quad T_{ss} \geq T_d \\ E_{i_4} &= T_{ss} - T_d + 24 & ; & \quad T_{ss} < T_d \end{aligned}$$

where: T_{ss} = time of sunset.

The method of calculating T_{sr} and T_{ss} will be described in the section on the environment. The time of the first air tanker drop (E_{i_5}) involves a series of technical calculations which will be discussed under the air tanker component.

b) Selecting the next event

The model begins the simulation by setting the start of the event interval (T_s) to 0 and selecting the next event (n), such that:

$$(14) \quad E_n = \min (E).$$

The end of the event interval (T_f) is then equated with E_n . Subsequent iterations begin by setting $T_s = T_f$ and then follow the procedure for the initial selection.

Subsequent crew arrivals (E_1) and air tanker drops (E_5) will be discussed under the corresponding technical section. Subsequent weather updates (E_2) occur each hour:

$$(15) \quad E'_2 = E_2 + 1.$$

Subsequent occurrences of sunrise (E_3) and sunset (E_4) are simply 24 hours apart:

$$(16) \quad E'_n = E_n + 24$$

where: n = sunrise (3), sunset (4).

2) Fire Suppression and Fire Growth

Fire suppression and fire growth are continuous dynamic processes. In a theoretically correct model, their impact on the system would be simultaneously integrated over time. Given the nature of the remainder of the model, however, such an approach would be relatively complex. In the interest of expediency, it was decided that each process would be integrated separately. This approach introduces bias into the results, in that processing fire growth before suppression increases area burned, while processing suppression first reduces area burned. The amount and direction of bias is adjustable. For example, as the interval between subsequent calls approaches zero, the difference between simultaneous and independent processing also approaches zero. Unfortunately, operating costs increase as the interval decreases. Another procedure to reduce bias would be to alternate the order of calling the two processes on subsequent iterations.

The model is programmed in such a way as to allow modification of the time interval between calls as well the order of calling. In this way, it is possible to balance the amount of bias against operating efficiency. This feature also provides a convenient mechanism for calibrating the model against observed results. That is, the cumulative effect of all errors in the growth and suppression components can be nullified by a simple adjustment of the calling sequence.

The process is as follows:

$$(17) \quad Dte = Tf - Ts - .001,$$

$$(18) \quad Dtn = 1 + \frac{Dte}{Dtx}, \text{ and}$$

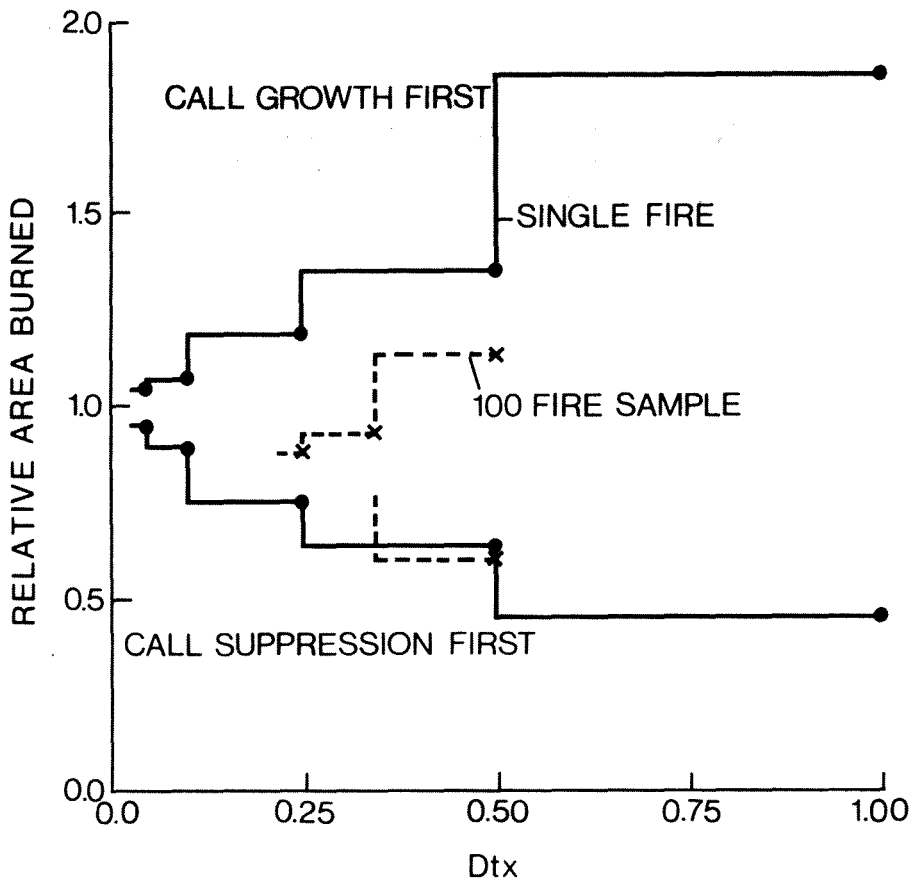
$$(19) \quad Dt = \frac{Dte}{Dtn}$$

where: Dte = time interval between events,
 Dtx = maximum allowable time between calls to growth and suppression,
 Dtn = number of intervals Dtx occurring during interval Dte , and
 Dt = time interval between calls to growth and suppression.

In essence, Eqs. 17-19 determine the number of calls to fire growth and suppression (D_{tn}) that will be made between events, such that the interval between calls does not exceed the maximum allowable interval. The subtraction of 0.001 in Eq. 17 prevents the accumulation of D_t over D_{tn} intervals from exceeding D_{te} , due to computer rounding. The user modifies the sequence by changing the value of D_{tx} in the input data.

The relationship between the "calibration function" and D_{tx} is shown in Fig. 2. Data for both a single fire and a sample of 100 fires are shown.

Figure 2. The calibration function



The following points are apparent from Fig. 2.

- The function is essentially discrete in that most of the changes will only occur at intervals which are integer divisions of one hour (i.e. 1/2, 1/3, 1/4, etc.).
- The 100-fire sample has a narrower range of sensitivity to changes in D_{tx} than the single fire sample.
- The overall model is slightly biased, in that the mid-point for the 100-fire sample (at $D_{tx} = 0$) is not equal to 1.

Finally, time is advanced in the growth and suppression sequence with the equation:

$$(20) \quad T_f = T_s + D_t.$$

This completes the discussion of the nontechnical aspects of time simulation. In the previous section, we considered a variety of supportive elementary computations. With this background, we now proceed to the four major components of the model, starting with the environment.

3. THE ENVIRONMENT

The environmental component of the model consists of those processes that affect the system, but are external to it. Four such processes will be discussed in this section: measurement of distance; calculation of sunrise and sunset time; diurnal weather variation; and fuels. Topography is not included in the current version of the model as there is no topographical information of value in the original fire report data from the test area.

A. Distance

There are two distances required by the model: fire-to-base and fire-to-lake. A different routine is used to calculate each distance. We will start with the fire-to-lake distance, as it is the simpler of the two.

1) Fire-to-Lake Distance

For water-based operations, flying time between drops (hence costs and effectiveness) is a function of air tanker speed and the fire-to-lake distance. Compounding the problem, each air tanker requires a different length of lake for safe water pickup. To code the distance to the nearest usable lake for each air tanker on every fire would be a considerable undertaking. For this reason, some simplifications were made. First, the actual distance from each fire to the nearest lake, 1.5 miles or more in length, was coded. Second, average fire-to-lake distances for seven different lake lengths were calculated for each region, based on a 10% sample of actual fires.³

These data were used to obtain the expected fire-to-lake distance for a specific air tanker model and fire, using the equations:

$$(21) \quad \ell = 2 + \frac{L_m}{2500} \text{ and}$$

$$(22) \quad D_{rf} = D_l \frac{D\ell a_{r,\ell}}{D\ell a_{r,4}} ; \quad \ell \leq 7.$$

where: ℓ = lake length class (rounded off to the nearest 1/2 mile),
 L_m = lake length required for pickup (ft.),
for air tanker model m,
 D_{rf} = fire-to-retardant distance (mi),
 D_l = actual fire-to-lake distance for the
nearest 1.5 mile long lake (mi.),

³ Data on file at the Forest Fire Research Institute.

D_{la} = average fire-to-lake distance, and
r = region.

Equation 21 determines the lake length class required for the specific air tanker model. Recalling that integer fractions are always truncated, a required length of less than 2,500 feet will fall into class 2 (0.5 miles). Class 1 (0.0 miles) is for helicopters only. Equation 22 modifies the actual distance from the fire to the nearest 1.5 mile long lake. It increases or decreases the distance, depending on whether the required length is greater or less than 1.5 miles. The change is a function of the ratio of the average distances in the region for the required length and a length of 1.5 miles.

2) Fire-to-Base Distance

For all operations, fire-to-base flying time must be calculated. As in the previous case, this is a function of air tanker speed and the fire-to-base distance. Unlike the previous case, however, actual distances are used, because the location of every fire and base are coded. The following sequence of equations is used to obtain the distances between pairs of points on the earth's surface, given the latitude and longitude of each point. These formulae are from Peterson (1973), who adapted the work of Clark (1880) and Bomford (1962). Since this process is external to the system, only the output is of interest. The equations are, therefore, presented here without comment. Only those formulae necessary for calculating distance between points are listed. The original work includes formulae for the inverse operation as well as calculating azimuth.

The following symbols are used for Eqs. 23-37.

La₁, La₂ = latitude of point 1 and 2
Lo₁, Lo₂ = longitude of point 1 and 2
Az = azimuth
D = distance (m)
a = major axes of spheroid (6,378,206.4 m)
b = minor axes of spheroid (6,356,583.8 m)
e = eccentricity of spheroid

$$(23) \quad e^2 = \frac{a^2 - b^2}{a^2}$$

$$(24) \quad x_1 = a(1 - e^2 \sin^2 La_1)^{-\frac{1}{2}}$$

$$(25) \quad x_2 = a(1 - e^2 \sin^2 La_2)^{-\frac{1}{2}}$$

$$(26) \quad DLo = Lo_1 - Lo_2$$

$$(27) \quad y = \cos La_2 \sin DLo$$

$$(28) \quad z = \frac{b^2}{a^2} \cos La_1 \sin La_2 - \cos La_2 \sin La_1 \cos DLo \\ + \frac{x_1}{x_2} e^2 \cos La_1 \sin La_2$$

$$(29) \quad \cos Az_{1,2} = \frac{z}{(y^2+z^2)^{\frac{1}{2}}}$$

$$(30) \quad f = \frac{e}{(1-e^2)^{\frac{1}{2}}} \sin La_1$$

$$(31) \quad h = \frac{e}{(1-e^2)^{\frac{1}{2}}} \cos La_1 \cos Az_{1,2}$$

$$(32) \quad F = \frac{fh}{1+h^2}$$

$$(33) \quad H = \frac{f^2 - h^2}{1+h^2}$$

$$(34) \quad \frac{k}{x_1} = \left[\left(\frac{x_2}{x_1} \cos La_2 \cos DLo - \cos La_1 \right)^2 + \left(\frac{x_2}{x_1} \cos La_2 \sin DLo \right)^2 \right. \\ \left. + \left(\frac{x_2}{x_1} \frac{b^2}{a^2} \sin La_2 - \frac{b^2}{a^2} \sin La_1 \right)^2 \right]^{\frac{1}{2}}$$

$$(35) \quad \frac{k}{r} = \frac{k}{x_1} \left[1 + \left(\frac{e^2}{1-e^2} \right) \cos La_1 \cos Az_{1,2} \right]$$

$$(36) \quad k = \frac{k}{x_1} x_1$$

$$(37) \quad Di = k \left[1 + \frac{1}{24} \left(\frac{k}{r} \right)^2 - \frac{1}{8} F \left(\frac{k}{r} \right)^3 + \left(\frac{3}{640} + \frac{3}{80} H + \frac{1}{4} F^2 \right) \left(\frac{k}{r} \right)^4 \right. \\ \left. - \left(\frac{3}{16} FH + \frac{5}{12} F^3 \right) \left(\frac{k}{r} \right)^5 \right]$$

In a comparison of results obtained with Eqs. 23-37 vs. officially published distances, the average difference was 0.03 km for distances up to 500 km (Valenzuela 1971). This error is much smaller than the error inherent in the fire location data, which is coded to the nearest minute, implying an average error of 0.5 to 1 km, depending on latitude.

B. Sunrise and Sunset

The time of sunrise and sunset are significant factors in a fire control operation. They set limits for air tanker activity and denote the time of changeover from daytime to nighttime productivity for ground forces. The following sequence of equations is used to calculate the times of sunrise and sunset. The equations and constants were derived by A. Muir* from data presented by List (1950).

The following symbols are used for the sunrise and sunset equations.

Lac = latitude coefficient = $La \times .01745$
da = day of month
dm = monthly sun declination parameter
dn = daily sun declination parameter
ds = sun's declination
Tsr = time of sunrise
Tss = time of sunset
Tn = median passage of sun
La = latitude
Lo = longitude
Loc = longitude at the center of the time zone.

The sunrise-sunset sequence begins by calculating two intermediate variables:

$$(38) \quad X = dm + (da \, dn) \text{ and}$$

$$(39) \quad Y = X + 0.03348 \sin (X - 4.9177).$$

The time of the median passage of the sun (Tn) is given by:

$$(40) \quad h = \arctan \left(\frac{0.91744 \sin Y}{\cos Y} \right) \text{ and}$$

$$(41) \quad Tn = 12 - \frac{57.296 (X - h)}{15}.$$

* Work on file at the Fire Research Institute.

The sun's declination (ds) is calculated with:

$$(42) \quad ds = \arcsin (0.39786 \sin Y).$$

If $Lac \geq 0$ and

$$(43) \quad | ds + 0.01484 | < 1.5708 - Lac ,$$

the sun will rise and set in the northern hemisphere. Alternatively, if $Lac < 0$ and

$$(44) \quad | ds - 0.01484 | < 1.5708 + Lac ,$$

the sun will rise and set in the southern hemisphere. Having passed the appropriate test, we calculate a set of intermediate variables:

$$(45) \quad x = \frac{-0.1483 - \sin Lac \sin ds}{\cos Lac \cos ds} ,$$

$$(46) \quad \begin{aligned} h &= \arccos x && ; \quad x \geq 0 , \\ h &= 3.1416 - \arccos (-x) && ; \quad x < 0 , \text{ and} \end{aligned}$$

$$(47) \quad H = \frac{57.295 h}{15} .$$

Sunrise at the center of the time zone (Trz) is given by:

$$(48) \quad Trz = Tn - H.$$

Finally, sunrise at the point of interest (Tsr) is calculated with:

$$(49) \quad Tsr = Trz + \left(\frac{Lo - Loc}{15} \right) .$$

The program advances time by one-half day and repeats the above sequence through Eq. 46, with the exception of the median

passage of the sun. The time of sunset at the center of the time zone (T_{sz}) is given by:

$$(50) \quad T_{sz} = T_n + H$$

which is entered into Eq. 49 to obtain T_{ss} .

A test of Eqs. 38-50 indicated that errors were in the range of 0-2 minutes, for all possible locations of interest in North America. This is certainly well within the range of accuracy of the available fire suppression data (0.1 hr.).

C. Weather

Of the three environmental factors governing fire behavior (weather, fuels, and topography), weather is by far the most important. Two levels of the meteorological environment are incorporated in the model: hourly variation and daily change. In this section we will consider the manner in which these two factors affect the two primary fire behavior controlling variables, the Initial Spread Index (ISI) and the Fire Weather Index (FWI). We begin with hourly variation.

1) Hourly Variation

Meteorological conditions vary during a 24-hour period according to a predictable cycle. In New Brunswick, fire behavior at minimum conditions is as low as one-seventh as severe as that at maximum conditions. It follows that the effectiveness of an air tanker drop at one time of the day would be significantly different from the same drop on the same fire at a different time. Two aspects of hourly variation will be discussed: the diurnal cycle and modifying average data to reflect initial conditions.

a) The diurnal cycle

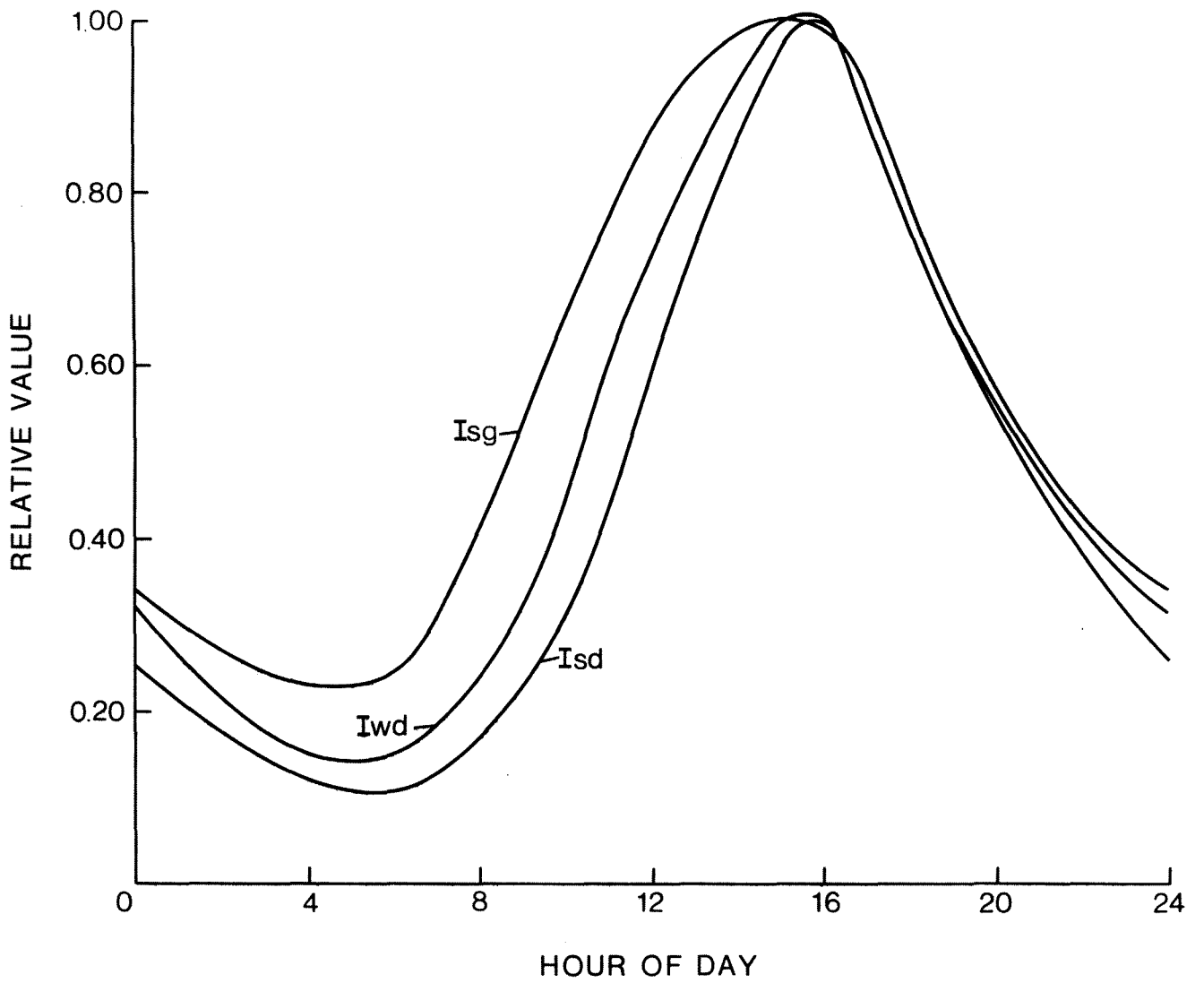
The value of the Initial Spread Index for any hour (I_{sh}) is given by:

$$(51) \quad I_{sh} = I_s I_{sd}_h I_{ss}_h$$

Similarly, the hourly value of the Fire Weather Index (I_{wh}) is calculated with:

$$(52) \quad I_{wh} = I_w I_{wd}_h I_{ws}_h$$

Figure 3. The diurnal cycle



The adjustment procedure is relatively simple. First, the expected length of the interval (T_i) is estimated. Procedures for this will be discussed under fire behavior. The numerator for the spread adjustment ratio is calculated by multiplying T_i by the initial value of I_{sd} . The denominator is calculated by summing values of I_{sd} for each hour of interval T_i . Thus, the ratio:

$$(53) \quad a_i = \frac{I_{sd}_h T_i}{T_i + h \sum_{i=h} I_{sd}_i}$$

where: h = initial hour for interval T_i ,

yields the adjustment required to convert the observed average to an initial value (a_i).

Between the hours of 0600 and 1600, the initial value will generally be less than the average, as the diurnal cycle will generate increasing spread rates as the fire progresses. Conversely, between 1600 and 0600 hours, the initial value will generally be greater than the average, as the diurnal cycle will be reducing the spread during the interval. Exceptions to both of the preceding will occur when one of the two crossover points (0600 and 1600 hours) lies within the interval of interest, as the effect of the diurnal cycle will be generating both higher and lower spread rates.

2) Daily Change

Afternoon meteorological conditions describe one day in relation to another. Thus, the day-to-day change in weather must be superimposed on the diurnal cycle. In other words, when a fire burns beyond midnight, the model must adjust the diurnal cycle to reflect conditions on the following day. Two steps are required: determining afternoon values and calculating a daily change adjustment factor.

a) Afternoon values

There are four procedures for determining afternoon values. The choice is based on the number of days since detection of the fire.

- i) For the day of detection, afternoon weather conditions form part of the data set pertaining to each fire. Two types of information are available: the six codes and indices of the Canadian Forest Fire Weather Index (FFMC,

DMC, DC, ISI, ADMC, and FWI) (Canadian Forestry Service 1970); and the four weather variables from which the indices are derived (wind speed, temperature, relative humidity, and rainfall).

- ii) The afternoon FWI for the second day (Iw_2) is available directly from the input data. The afternoon ISI for the second day (Is_2) is determined with the ratio Iw_2/Iw . If $Iw = 0$, Is_2 is equated with Is .
- iii) For the third through fifth days, Iwn and Isn are equated to 90% of the previous day's value. This process is intended to reflect the increasing probability of rain with time since ignition. An adjustment of 90% was chosen because it gave reasonably good results when compared with observational data.
- iv) On the sixth and subsequent days, Iwn and Isn are set to zero, to prevent a fire from getting away in the model. In other words, all fires eventually stop growing (but are not extinguished) in response to rain. Six days were chosen because an average of five days elapsed between recorded precipitation during the summer in New Brunswick.

The meteorological modeling is relatively crude after the second day. This is not considered critical for the following reasons.

- Most of the air tanker activity will take place within the first two days.
- Most fires that escape do so during the initial stages of the control operation.
- The emphasis of the model is on the initial attack phase of fire suppression.

The remainder of the activity is included primarily for the sake of completeness with respect to seasonal totals.

b) Daily change adjustment

Having determined the afternoon values of the two index variables, it remains to gradually incorporate the change from one day to the next. In addition to not reflecting reality, it was found that a drastic discontinuity at midnight generated unrealistic fire behavior. The current procedure modifies the previous hours value by $1/16$ of the difference between the two afternoon values once each hour until 1600.

The equations are:

$$(54) \quad I_{wh} = I_{w_{h-1}} - [0.0625(I_{w_n} - I_{w_{n+1}})] \text{ and}$$

$$(55) \quad I_{sh} = I_{s_{h-1}} - [0.0625(I_{s_n} - I_{s_{n+1}})].$$

The effect of the daily change must be incorporated into the procedure for converting average data to initial conditions. This is done in two steps. First, the hourly component of the daily difference (Dh) is calculated:

$$(56) \quad Dh = 0.0625 (I_{w_n} - I_{w_{n+1}}) \quad ; \quad I_{w_n} \geq 1.$$

Then, the adjusted hourly percentage (Isa) is determined:

$$(57) \quad I_{sah} = I_{sdh} \left(\frac{1-Dh \ Nh}{I_{w_n}} \right) \quad ; \quad I_{w_n} \geq 1 \\ \quad \quad \quad \quad \quad \quad \quad \quad \quad \quad ; \quad Nh \leq 16$$

where: Nh = total number of hours since the start of the interval.

The daily change is incorporated by replacing Isd in Eq. 53 with Isa. The limit $I_{w_n} \geq 1$ is incorporated in Eq. 56 for compatibility with Eq. 57, where it is required. The limit $Nh \leq 16$ is incorporated in Eq. 57, as the daily change adjustment is terminated at 1600 hours.

D. Fuels

No attempt was made to model the causal relationship between various fuel configurations and fire behavior, or ground suppression, or air tanker use. To do so would have been a hopelessly complex task. Rather, the available fuel information was used to stratify fires so that the response of various system variables was relatively uniform within each sample. There are three fuel classifications: the input data, the standard set, and a specific set for New Brunswick. Codes and descriptions for all three fuel classifications are given in Table 2.

Table 2 Fuel classifications

A. Input Data

Surface Fuels	
0	Unknown
1	Litter
2	Duff
3	Grass
4	Brush
5	Slash
6	Snag
7	Windfall
8	Lichen or Moss
9	Miscellaneous Known
Principal Overstory Species	
0	Unknown
1	Nonforest
2	Swamp or Bog
3	Grass or range
4	More than 75% pure softwood
5	50-75% pure softwood
6	Mixtures with hardwood species common
7	Pure softwood and pure hardwood types mixed
8	Intermixed softwood and hardwood species
9	Mixtures with softwood and hardwood species
10	50-75% pure hardwood
Size Class of Overstory	
0	Unknown
1	Slash
2	Cutover - no slash
3	Reproduction
4	Young growth
5	Pulpwood, poletimber
6	Sawtimber
7	Merchantible and cutover
8	Merchantible and young growth
9	Cutover and young growth

Input Data Equivalents

B. Standard Fuel Types

	<u>NFU*</u>	<u>NSP</u>
1	Conifers	
2	Mixedwood	4, 5
3	Hardwoods	6, 7, 8
4	Spruce	9, 10
5	Red pine	
6	Yellow pine	
7	Jack pine	
8	White pine	
9	Douglas fir	
10	Cedar, hemlock (western)	
11	True firs, larch, hemlock (eastern)	
12	Poplar	
13	Maple	
14	Birch	
15	Grass, moss	3
16	Slash	5, 7
17	Brush (eastern)	4
18	Brush (western)	
19	Miscellaneous, unknown	0
20	Nonforest	1, 2

* Note that when one of the four fuel type codes was encountered, it overrode the species code.

C. Fuel Types for Agency Specific Regression Analysis (New Brunswick)

	<u>Input Data Equivalents</u>	
	<u>NFU</u>	<u>NSP</u>
0	Unknown	0
1	Litter	1
2	Duff	2
3	Grass	3
4	Brush	4
5	Softwood slash	5
6	Snag	6, 7
7	Windfall	-
8	Lichen and moss	8
9	Miscellaneous known	9
10	Mixedwood slash	5
11	Hardwood slash	5
12	Nonforest	1
13	Overall (all fuels together)	6, 7, 8, 9, 10

1) Input Data

The input data contains three fuel descriptors: principal overstory species (Fsp), size class of overstory (Fz), and surface fuel description (Fu).

2) Standard Set

The species and fuel type codes were equated with a standard set (Fg), which includes most of the principle cover types found in Canada. Model parameters were developed for each of the standard fuel types. The purpose of this two-step procedure is to increase the ease with which the model can be run in different regions. The user has only to equate fuel descriptors in any region with the standard set. No changes have to be made to the model itself to reflect different fuel types.

3) New Brunswick Set

There are three model components for which generally applicable equations cannot be developed. They are: ground suppression cost, damage, and mop-up time. To a significant extent, these functions are a reflection of management policies, operational efficiency, and accounting practices of a specific agency. For this reason, each run of the model in a new region will require the development of agency specific equations for these three components. Since there is no requirement for a standard set of fuel types for these components, it was decided to select an agency specific set of fuel types (Fnb), such that predictive accuracy would be maximized, constrained by a minimum number of observations per fuel type.

At this point, the discussion of the environmental component of the model is complete. We now proceed to the first of the three central components of the system being analyzed - the fire.

4. THE FIRE

Most computerized fire management studies have three processes in common: the simulation of fire occurrence, behavior, and growth. These processes, in a sense, represent the demand for the particular fire management activity being analyzed. By modifying the level and nature of the activity, the impact of the fire processes (such as area burned) is also modified, normally in an inverse relationship. The latter represents system output. By comparing system output with system input, superior or optimum strategies and tactics may be selected. In this section, we will discuss each of the three fire processes to which the fire management system must respond.

A. Fire Occurrence

1) The Occurrence Distribution

Most fire management studies process a sample of fires. There are two basic procedures used to generate the sample: simulation and collecting historical data from actual fires. Simulation is the more general procedure in that it can be used to consider occurrence patterns that are possible but did not occur historically. Simulation can also be used to consider much longer time periods than is practical for historical data. Further, it can be used to analyze prevention effectiveness, where causes of fire occurrence are of paramount interest. Finally, it can significantly reduce the cost of data acquisition.

Since occurrence distributions are normally generated from historical data, it is also reasonable to argue against adding unnecessary abstraction, as well as an extra step in the experimental process. If the historical sample is reasonably representative of most occurrence distributions, and if a rare occurrence pattern is not a significant part of the analysis (such as the flood control planner's desire to consider the 100 and 1,000 year flood), and if occurrence itself is not the primary topic of interest, the use of historical data is preferred.

Thus, AIRPRO uses actual fire data to generate the occurrence distribution. Individual forest fire report data (obtained from the agency) is combined with weather data (obtained from the Atmospheric Environment Service, D.O.E.) and spatial information (obtained from maps) to provide a sample of fires for the model to process. The procedures used to acquire, code, and process the information are covered in detail elsewhere (Simard et al. 1972, 1973).

2) Data Editing and Calibration

Although the use of historical input data is closer to the real world than simulation, it poses certain problems. There may be anomalies in the data which require some form of adjustment. In addition, the data may not be relevant to current conditions if significant time has elapsed since its acquisition. Procedures for solving these problems are incorporated in the model.

First, minimum values are required for rates of growth to prevent illogical results and computational difficulties. Thus, rate of free-burning perimeter growth (Pgf) and perimeter growth during suppression (Pgs) are set to a minimum of 5 ft./hr. Similarly, minimum rates are required for the rate of line construction ($Lc \geq 30$ ft./hr.) and rate of mop-up ($10.0 \geq \mu \geq 0.01$ ac./hr.). Even when extrapolated over 24 hours, the preceding minimums did not generally alter the outcome of individual fires by significant amounts.

Second, the model uses both a free-burning and suppression growth rate observation. This is necessary because the model cannot simulate reality with acceptable accuracy when there are discrepancies between the two observations, if only one is used. The use of both growth rates proved adequate in most cases. In cases where the discrepancies are particularly large, however, an adjustment to the data is necessary to permit the model to generate acceptably accurate results. The simultaneous occurrence of three conditions require an adjustment to the data.

The conditions are:

- $Lc/Pgs \geq 3.0$,
- $Pgs/Pgf \geq 5.0$ or $Lc/Pgs \leq 1.1$, and
- observed fire area ≤ 30 acres.

When all of the preceding applied to a particular fire, it indicated that the observed Pgs was too large, relative to both Pgf and Lc, resulting in excessive simulated area burned. This could be the result of an erroneous time or fire size estimate at the start of suppression. In such cases, Pgs was equated with $Pgf/2$. In addition, if $Pgs < 25$ and $Lc > 5,000$, Lc was set to 500, in order to prevent difficulties arising from the first adjustment. These adjustments affected about one percent of all fires in the sample.

Third, the fire growth model requires free-burning rate of growth. During the control interval, however, a gradually increasing percentage of the perimeter is being controlled, and

thus no longer expanding. Therefore, the observed perimeter growth rate will decrease as control progresses. Barring changes in environmental conditions, however, free-burning growth rate does not change.

From the preceding argument, it is clear that P_{gs} must be modified to render it conceptually equivalent to P_{gf} . If it is assumed that control proceeds at a uniform rate and that every portion of the perimeter is spreading at the same rate, the observed average P_{gs} will equal $P_{gf}/2$. The reasoning is as follows: at the start of suppression, $P_{gs} = P_{gf}$; and when the fire is controlled, $P_{gs} = 0$. Therefore, $P_{gs} = P_{gf}/2$. While the first assumption is reasonable, the second is somewhat simplistic. Clearly, the majority of spread comes from the head and that is the portion of the fire attacked first. In the model, however, P_{gs} is converted to separate spread rates for the head, flanks, and rear of the fire, thereby accounting for the nonuniformity of spread along the perimeter. In the present context, therefore:

$$(58) \quad P_{gs}' = 2 P_{gs}$$

is a reasonable procedure to conceptually equate P_{gs} with P_{gf} .

Finally, in order to make the observed data applicable to a uniform time period, an array of six calibration coefficients (Ca) is included in the model: 1) travel and dispatch time, 2) fire perimeter at detection, 3) rate of line construction, 4) rate of mop-up, 5) ground costs and losses, and 6) air tanker costs. Differences between averages obtained from the input data and averages obtained from current information can be reconciled by using the ratio of the two as the calibration coefficient. This procedure also applies to differences within the data itself (i.e., 1960's fire data and 1970's air tanker cost data). The model multiplies each variable by the appropriate calibration coefficient. For example:

$$(59) \quad P' = ca_2 P.$$

Equipment loss (De) and nonforest damage (Dn), are multiplied by the ratio Ca_2/Ca_3 (perimeter adjustment/line construction adjustment). The reasoning is as follows. As will be explained subsequently, relative changes to De and Dn are related to relative changes in fire size. Since a smaller size at detection as well as an increased rate of line construction both result in a smaller final fire size, both calibration coefficients have to

be considered to adjust historical values of I_e and D_n to current conditions.

B. Fire Behavior

Once data for a fire has been acquired, the potential behavior of the fire must be determined. While there are several descriptors of fire behavior, only two are required in the model: rate of spread and intensity. In this section, we will discuss the manner in which various aspects of spread and intensity are modeled.

1) Theoretical Forward Rate of Spread

The primary role of the theoretical forward rate of spread (F_{st}) is to relate the diurnal weather cycle to observed rates of spread. F_{st} incorporates the nonlinearity between relative hourly changes to index values and spread rates. The basic equation for calculating F_{st} was given by Van Wagner (1973):

$$(60) \quad F_{st} = c_2 c_3 I_s \left(\frac{I_a}{40}\right)^{c_4}$$

where: c = fuel type constant and
 I_a = ADMC.

Van Wagner listed values of c for seven fuel categories for which data were available. Values for all 20 standard fuel types ($F_{p2,3,4}$) were obtained by subjective extrapolation of Van Wagner's data.

When Eq. 60 was combined with the diurnal cycle, the simulated daily variation became far larger than what was noted in the data. In an effort to balance the two processes, a linear form of Van Wagner's equation was developed to reduce the effect of diurnal changes to I_s :

$$(61) \quad F_{st} = F_{p1} F_{p2} I_s.$$

When combined, Eqs. 51 and 61 produce a diurnal spread effect which matches observed data reasonably well. It was found that F_{st} , as calculated in Eq. 61, required calibration to bring the average value into line with the average observed forward rate of spread. Whether or not this resulted from the use of Eq. 61 rather than Eq. 60 was not determined. Since the model responds to relative, rather than absolute values of F_{st} , a detailed analysis of this point was not considered necessary.

The calibration procedure simply multiplies F_{st} by an adjustment coefficient (C_s). The value 8.75 minimizes the difference between the observed and theoretical means for all fuel types other than grass, where a value of 2.5 is used. In addition, for grass fuels where $I_s \leq 5$, a variant of Eq. 60, when combined with the diurnal cycle, was found to yield results that matched observational data reasonably well:

$$(62) \quad F_{st} = 1.6 \text{ cs } I_s^2.$$

2) Theoretical Intensity

As with F_{st} , the theoretical fire intensity (I_t) is used to relate diurnal index variation to changes in fire behavior. In addition, since there are no observational data on fire intensity, the theoretical value is also used to modify ground and air tanker suppression effectiveness. The following sequence is used to calculate theoretical fire intensity:

$$(63) \quad \begin{aligned} x &= \ln (I_w)^{1.546} & ; & \quad I_w > 1, \\ x &= I_w & ; & \quad I_w \leq 1, \text{ and} \end{aligned}$$

$$(64) \quad I_t = 2.686 e^x.$$

Equations 63 and 64 represent basic relationships found in the Canadian Forest Fire Weather Index (Van Wagner 1974). These equations estimate fire intensity, based on weather variables alone. Clearly, this is an oversimplification. Intensity is also related to the available quantity and spatial arrangement of the fuel being consumed. Thus, an effort has been made to incorporate fuels into the intensity calculation. It was reasoned that as fire intensity increases, the difficulty of control also increases. All things being equal, as difficulty of control increases, area burned increases correspondingly. Therefore, relative area burned for each fuel type should be related to relative fire intensity for each type.

To obtain relative area burned by fuel type, data for 45,000 fires from across Canada were processed.⁵ Large fires (over 25,000 acres) were removed from the sample, as they biased the results in two ways.

- Most large fires were classified as mixedwood, as they burned over many fuel types.

⁵ Unpublished work on file at the Forest Fire Research Institute.

- Many species do not cover extensive areas.

Average area burned by fuel type within each province was converted to a relative value to render the data comparable between provinces. A weighted average of the provincial relative values was obtained for all of Canada. The average relative areas burned were used as the fuel type intensity coefficient (Fp_1). These were multiplied by I_t , obtained from Eq. 64.

In addition to relative differences between fuel types, intensity must also be related to the quantity of fuel available for consumption. Regardless of the degree of drought (hence, potential intensity), grass or hardwood litter cannot generate the same intensity as logging slash or a fully developed crown fire in a stand of sawtimber.

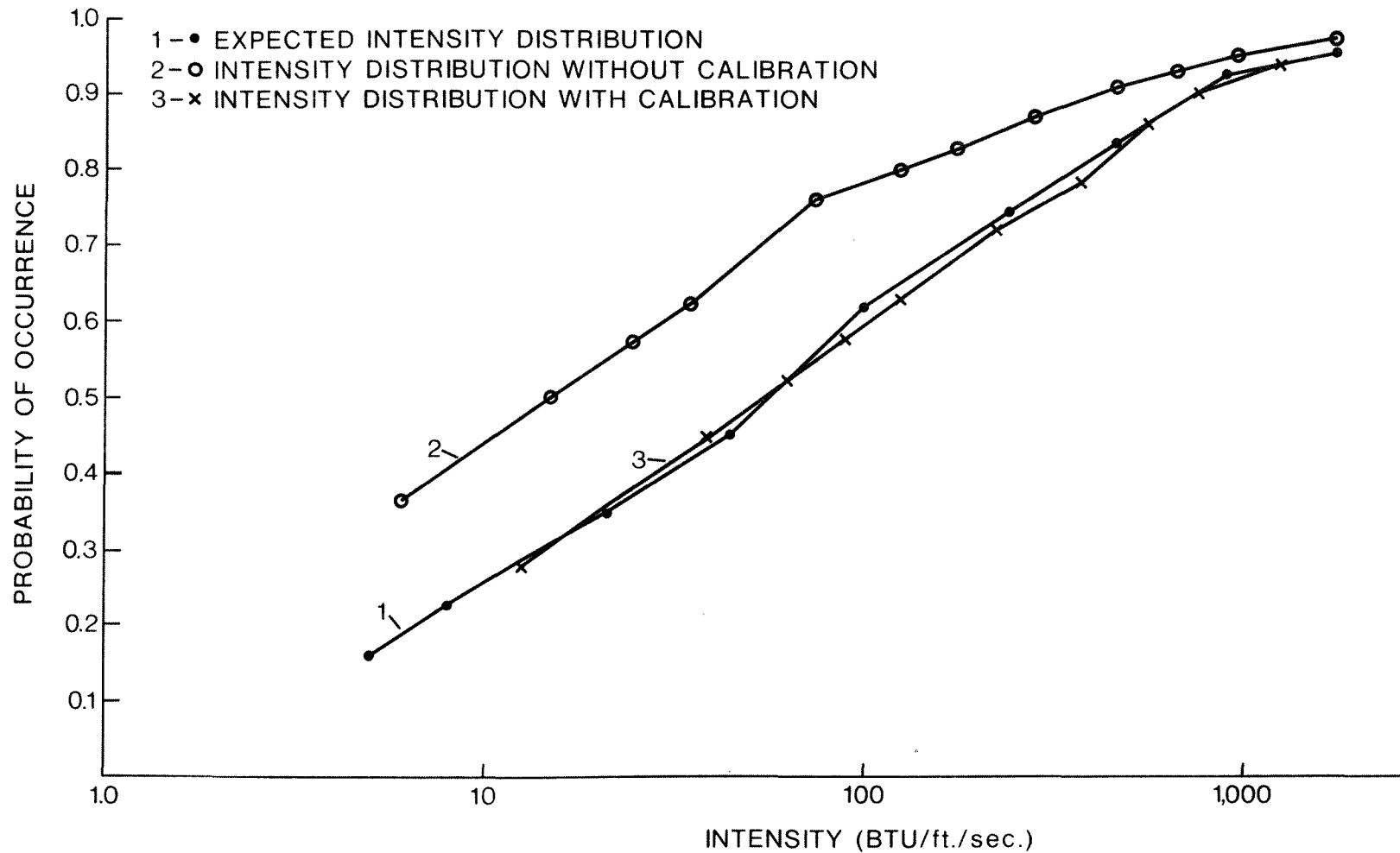
Using data presented by Swanson and Helvig (1973) as a starting point, subjective limits on the maximum possible intensity were derived for each fuel type. In general, softwood timber stands and logging slash were set to 50,000 BTU/ft./sec., with other types (grass, brush, hardwoods, etc.) set to lower values. Immature stands were treated as brush. Grass and hardwood stands were adjusted upwards for spring conditions. The resulting values were used as the fuel type intensity limit parameter (Fp_6) such that $I_t \leq Fp_6$.

As a final check of the preceding calculations, as well as the calibration to be discussed under fire growth, the distribution of simulated head fire intensities was compared with the expected distribution of fire intensities (for fire days only) in New Brunswick. The results are shown in Fig. 4. As can be seen, there is a significant bias when the uncalibrated distribution is compared with the expected (Curves 1 and 2). To correct the bias, the equation:

$$(65) \quad ci = 2.5 - 0.03 \sqrt{I_t}$$

is used to calculate an adjustment factor (ci). When ci is multiplied by I_t , the resulting distribution (Curve 3) closely matches the expected distribution.

Figure 4. Cumulative probability distribution for expected and simulated fire intensities



3) Converting Averages to Initial Values

Twice during a fire's history, the observed average rate of spread is converted to an initial value. The first conversion occurs at the start of the fire. The expected duration of free-burning growth (T_i) is obtained by:

$$(66) \quad T_i = T_{ds} + T_t + T_a$$

where: T_{ds} = dispatch time,
 T_t = travel time, and
 T_a = attack time.

If $T_i \geq 2$, the required adjustment (a_i) is obtained from Eq. 53, by using the value of T_i , obtained from Eq. 66. The observed average is multiplied by a_i to obtain the initial value:

$$(67) \quad P_{gf}_i = a_i P_{gf}$$

No adjustment is made for free-burning intervals of less than two hours.

The same procedure is used when a crew arrives. The observed suppression growth rate (P_{gs}) is substituted for P_{gf} . Estimating the expected time to control is somewhat more involved than was the case for the free-burning period. In cases where $P_{gs}/2 < L_c$ (most fires) the approximation:

$$(68) \quad T_{ce} = \frac{P_s}{L_c - \left(\frac{P_{gs}}{2}\right)}$$

where: T_{ce} = estimated time to control and
 P_s = perimeter at the start of suppression,

yields a reasonable estimate of the expected control time.

Essentially, Eq. 68 uses the difference between the growth and suppression rates to calculate effective suppression rate, and hence the estimated time to control (T_{ce}). Note that, as mentioned previously, the observed P_{gs} has been doubled, hence the use of $P_{gs}/2$ to represent effective rather than free-burning growth. When $P_{gs}/2 > L_c$, T_{ce} would be negative, while at $P_{gs}/2 = L_c$, T_{ce} would be undefined. Thus, a different form of equation is required. The relationship:

$$(69) \quad T_{ce} = \frac{5.0 P_s}{L_c}$$

was found to yield an estimated time to control which matched observed results reasonably well. Finally, if the observed fire area exceeded 40 acres, the equation:

$$(70) \quad T_{ce} = \frac{P_{co}}{L_c}$$

where: P_{co} = observed fire perimeter at control,

was used to estimate T_{ce} .

It was found that in the case of large fires, the observed final perimeter was required to obtain a reasonable estimate of T_{ce} . Note, however, that T_{ce} is only used to determine the average-to-initial adjustment for rate of spread. Since the maximum length of time considered in the adjustment is 24 hours, and since most large fires burn over longer periods, estimates of T_{ce} are not critical to the overall process. Therefore, the decision was made to adopt the simplest estimation procedure possible.

A final adjustment for nighttime conditions was included when fires less than 40 acres were involved. If suppression started during the day but extended past sunset, the equation:

$$(71) \quad H_n = \min(T_{ce} - E_4, E_3 - E_4)$$

was used to estimate hours of nighttime suppression (H_n). If suppression began in the dark, the relationship:

$$(72) \quad H_n = \min(T_{ce}, E_3 - E_1)$$

was used. Since the model assumes a nighttime suppression rate of one-half the daytime rate, H_n was simply added to T_{ce} to account for the increased suppression time required, resulting from the reduced nighttime suppression rate. Whenever $T_{ce} \geq 1.5$, a value for a_i was calculated, using Eq. 53, and applied to the perimeter growth rate, using Eq. 67.

4) Hourly Adjustments

The procedure for making hourly adjustments is relatively simple. Old-to-new spread and intensity ratios (R_o) are calculated. Spread and intensity for each flank during the previous hour are then divided by R_o to obtain values for the current hour:

$$(73) \quad R_{o1} = \frac{F_{st_{h-1}}}{F_{st_h}}$$

$$(74) \quad Ro_2 = \frac{It_{h-1}}{It_h},$$

$$(75) \quad Ag_{f,h} = \frac{Ag_{f,h-1}}{Ro_1},$$

$$(76) \quad I_{f,h} = \frac{I_{f,h-1}}{Ro_2},$$

where: Ag = rate of spread,
 I = fire intensity,
 f = flank, and
 h = hour.

In addition, the current-to-initial forward rate of spread ratio (Ri) is also determined:

$$(77) \quad Ri = \frac{Fst_h}{Fst_i}.$$

5) Large Fire Growth Rate Pulse

A final adjustment was found to be required at the start of those fires where the observed final area burned exceeded 40 acres and $Lc/Pgs \leq 1.1$. Without the adjustment, the simulated area burned was consistently low. The reason for this is readily understandable. Many large fires spread very quickly for a few hours and then settle down to more moderate growth rates. During the initial phase, the actual fire is not controlled by initial attack forces, resulting in a subsequent influx of additional men and equipment. If average rates of growth and suppression are applied at the start of suppression in such situations, the model controls the fire much more effectively than was the case in real life. Thus, the simulation must consider growth as a dynamic rather than a static process (in addition to the diurnal cycle). If, in fact, actual growth and suppression rates for each hour were available, this dynamic behavior (i.e., escaped fires) would probably be handled quite well by the model. Modifications are required primarily because only average data are available.

Fire growth for large fires was modified with a pulse. The philosophy is much the same as for the conversion of average-to-

initial values. The initial growth rate is increased significantly and then gradually decreased so that the total simulated growth over the life of the fire is approximately equal to the observed total growth. In order that the simulated area at the start of suppression be related to the observed area at the same time, the pulse is only applied when the first ground forces arrive at the fire. The strength of the pulse is determined with the following equations:

$$(78) \quad P_i = 4.0 \left(1.25 - \frac{L_c}{P_{gs}} \right) \quad ; \quad \frac{L_c}{P_{gs}} \leq 1.1$$

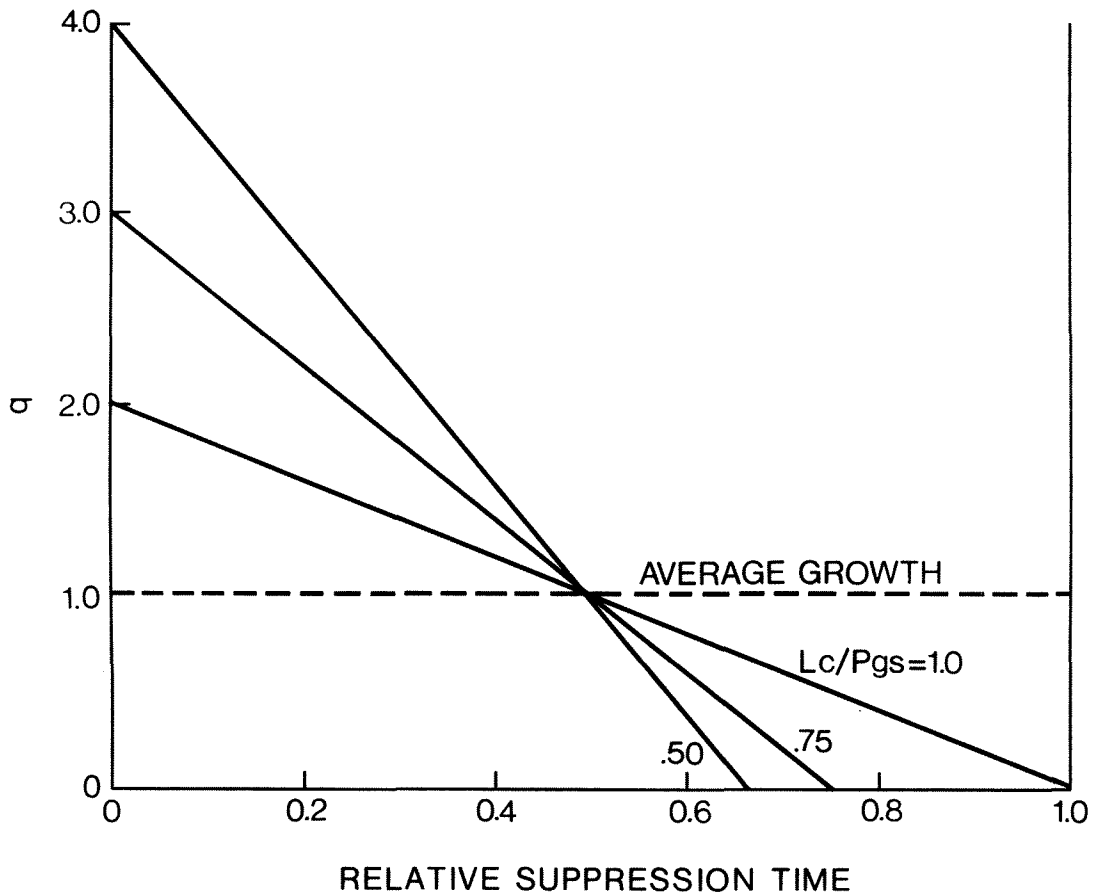
$$(79) \quad q = (1 + P_i) - 2.0 P_i \left(\frac{E_n - T_{sc}}{T_{ce}} \right) \quad ; \quad q \geq 0$$

where: P_i = relative pulse increment,
 q = current multiplying factor for growth rate,
 E_n = time of next event, and
 T_{sc} = time suppression started.

Note that Eq. 79 contains two basic terms. The first accounts for the magnitude of the pulse required. The second reduces the value of q on the basis of the total pulse previously applied. The behavior of q for various L_c/P_{gs} ratios is illustrated in Fig. 5. Ratios of L_c/P_{gs} less than 0.5 were not encountered in the data. (Recall again that P_{gs}' is twice P_{gs} to make it compatible with P_{gf} .) Thus, P_{gs} never exceeded L_c , a necessary condition for control to be achieved in the model.

As L_c decreases relative to P_{gs} , the strength of the pulse required to prevent the model from controlling the fire too soon increases. Note that for ratios of L_c/P_{gs} less than 1.0, the integrated value of q exceeds the area bounded by the average growth rate over the suppression interval. It was found, however, that the relationships in Eqs. 78 and 79, when combined with an initial suppression delay, matched the observed data fairly well.

Figure 5. Fire growth multiplier as a function of relative suppression time



6) Average Intensity

It has been pointed out that observed free-burning and suppression growth rates (P_{gf} and P_{gs} , respectively) are both used in the model. As will be discussed, these variables are used to relate I_t to I at the time of detection and the time of the start of suppression. There are often significant discrepancies between P_{gf} and P_{gs} . There is no information on which to base a conclusion that either observation is more accurate than the other. It was, therefore, decided that a weighted average of the free-burning and suppression intensities would be superior to either one alone. The procedure for obtaining the weighted average intensity is as follows.

First, the proportion of the total elapsed time between detection and control during which free-burning growth took place (p) is calculated:

$$(80) \quad p = \frac{T_{so}}{T_{so} + T_{co}}$$

where: Tso = elapsed time to the start of
suppression and
Tco = elapsed control time.

Then, the weighted average theoretical-to-observed spread ratio (Ra) is calculated:

$$(81) \quad R_a = p R_f + (1-p) R_s$$

where: Rf = free-burning theoretical-to-observed
spread ratio and
Rs = suppression theoretical-to-observed
spread ratio.

The calculation of Rf and Rs will be discussed subsequently.*

This is followed by the ratio of the average to the original ratio (Rx):

$$(82) \quad R_x = \frac{R_a}{R_f}$$

Finally, average flank intensity (Ix) is calculated by multiplying the initial flank intensity by Rx:

$$(83) \quad I_{ax} = R_x I_f \quad ; \quad I_{ax} \leq I_m$$

Average intensity is used for determining air tanker drop effectiveness.

To this point, we have a fire as well as the two basic behavior parameters of interest: spread and intensity. It remains only to put these variables into a fire growth model - the heart of the fire component.

C. FIRE GROWTH

Given the relative importance of the fire process, it is not surprising that there are numerous fire growth models currently in existence. They are generally of two basic types. One type considers the entire perimeter as a unit. The advantages of this type are processing efficiency and nominal site-specific data requirements. The disadvantage is an assumption of constant conditions over the entire fire area. These models are, therefore, subject to significant error when highly variable site conditions are encountered.

* See Eq. 100.

A variety of fire shapes have been used in unified models: triangular (Newburger 1966), elliptical (Van Wagner 1969), double elliptical (Anderson 1973, in Albini 1976), and lemniscate (Stade 1966). Only Newburger's model considers the head of the fire separately from the remainder of the perimeter. Anderson's and Stade's models vary the length-to-width ratio of the fire in response to wind speed.

The second type of model can be classed as segmented. This type has the advantage of relatively good accuracy on individual fires even with highly variable site conditions. The segmented model can have the disadvantage of requiring considerable computation time as well as large amounts of site specific information. The ultimate segmented model is the cell growth type developed by Kourtz and O'Regan (1971). Every cell (unit area) encountered by the fire is processed individually, necessitating site specific data for every cell. Such a model has the greatest potential accuracy.

Recently, attempts have been made to reduce the considerable logistic and computational difficulties associated with a cell growth model by considering only a sample of points along the perimeter (Sanderlin and Sunderson 1975). The point spread approach represents a compromise between the simple unitized models and the cell growth type. The number of points processed can vary, with between 8 and 32 commonly employed for small fires, with more points as fire size increases.

The limited data available (individual fire reports) and a required capability of processing thousands of fires many times each, dictated that a simple fire growth model be used. If the model were to be applied to individual fires as part of the dispatching process, the development of a more accurate site-specific model would be justifiable.

The fire growth model has three basic characteristics.

- The fire has an elliptical shape for simplicity, combined with a reasonable representation of empirical observations.
- The length-to-width ratio varies with wind speed. This is a significant factor in that although rate of spread increases with wind speed, the relative effectiveness of controlling only the head increases proportionally. In addition, the head-to-perimeter ratio decreases with increasing wind speed. If topographic information were available, its effect on rate of spread and fire shape could be easily incorporated into the model.

- The fire perimeter is divided into four components (head, two flanks, and rear) each of which is processed separately. This was considered essential as the highly flexible nature of air tanker operations requires that the model permit attacking individual flanks separately, as is done in the field. In a sense, the model used here represents the most basic point growth approach (four points), combined with a parabolic connection between points.

In this section we will discuss four aspects of fire growth: the shape of the fire, the initial size and growth rate, fire growth, and final fire size.

1) Fire Shape

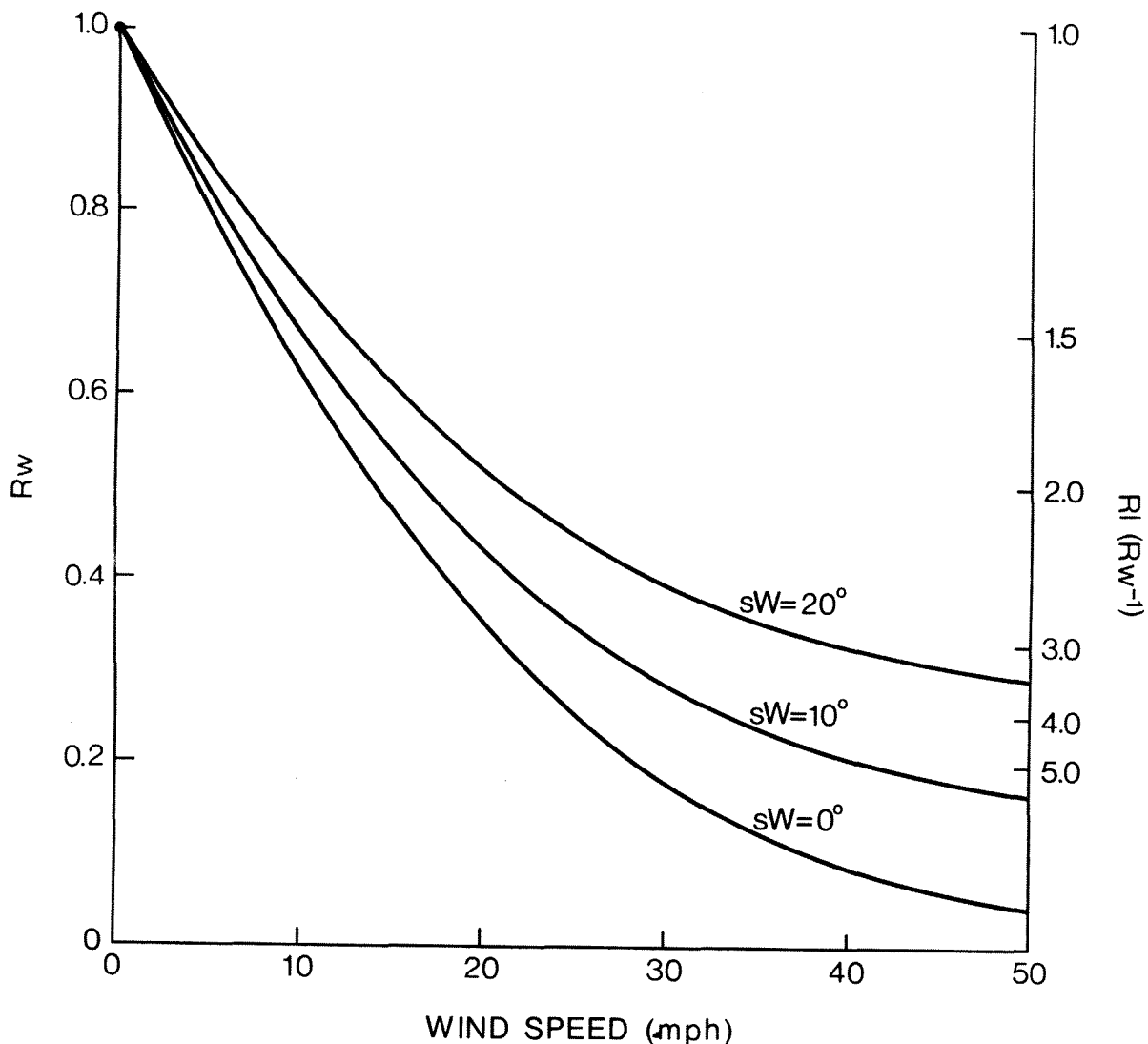
The basic shape assumed by the model is an ellipse with the length-to-width ratio related to wind speed. Using previously published data (Simard 1969), an empirical function relating the width-to-length ratio (R_w) to the wind speed (W) for an elliptical shape was derived:

$$(84) \quad R_w = e^{(-0.0287 W^{1.2})} + 0.000312sW.$$

The above general function includes a term for wind direction variability, which is estimated by the standard deviation of the wind direction (sW). Lacking individual data on this term, a value of 10° was used for all fires. Fig. 6 shows R_w and its inverse (R_l).

The next step involves determining the slope of the tangent at the point of intersection of the head and flank (s). For this, it is necessary to define the point of intersection. Three possible definitions were examined. Two had a tangent at the point of intersection with a fixed angle relative to the horizontal axis (45° and 60°), while the third was defined such that $s = R_l$.

Figure 6. Relationship between the length-to-width ratio of a fire and wind speed



With an intersection of 45° , the head would constitute 25% of the perimeter at a wind speed of zero. Since the shape is a simple circle in the absence of wind, and since all four flanks are equal, each flank should constitute 25% of the perimeter when $R_l = 1$. Unfortunately, at wind speeds greater than zero, the intersection defined by $s=1$ reduced the percentage of head much more quickly than appeared reasonable. The head was only 10% of the perimeter at $R_l = 2$. While the 60° point of intersection ($s = \sqrt{3}$) had 19% of the fire classed as head at $R_l = 2$, it had 33% head at $R_l = 1$, clearly an illogical result. When the point of intersection was defined such that $s = R_l$, it had the desirable property of 25% head at $R_l = 1$ as well as an acceptable head of 20% at $R_l = 2$. Thus, $s = R_l$ was chosen as the point of intersection of the head and flank.

The following sequence of equations is used to determine the relative length of the head and flank for a standard ellipse. Their derivation is given in Appendix 2, along with illustrations.

The x and y coordinates of the intersection point for a fire with a semi-major axis of 1 (the standard ellipse) are calculated with:

$$(85) \quad Z = \sqrt{R\ell^2 + s^2},$$

$$(86) \quad ix = \frac{s}{R\ell Z}, \text{ and}$$

$$(87) \quad iy = \frac{R\ell}{Z}.$$

The relative length of head (Ah) is given by:

$$(88) \quad f = \frac{1 - iy}{ix^2},$$

$$(89) \quad g = \sqrt{1 + 4f^2 ix^2}, \text{ and}$$

$$(90) \quad Ah = ix g + \frac{1}{2f} \ln(2f ix + g).$$

The relative length of one flank (Af) is determined by:

$$(91) \quad f = \frac{\frac{1}{R\ell} - iy}{iy^2},$$

$$(92) \quad g = \sqrt{1 + 4f^2 iy^2}, \text{ and}$$

$$(93) \quad Af = iy g + \frac{1}{2f} \ln(2f iy + g).$$

Finally, the total perimeter (Px) for the standard ellipse is:

$$(94) \quad P_x = 2(A_h + A_f).$$

Two additional variables are necessary to complete the standard ellipse. They relate rear and flank spread to the forward rate of spread. Using the wind function found in the ISI (Van Wagner 1974), the ratio of the no wind spread to spread with wind was plotted as a function of wind speed in Fig. 7. Since the no wind spread is equivalent to the rear rate of spread, curve R_r shown in Fig. 7 denotes the rear/forward spread ratio as a function of wind speed. If $s_w = 0^\circ$, flank spread would equal the rear spread. Since an average of $s_w = 10^\circ$ is used in the model, the flank spread ratio (R_{fl}) is slightly greater than R_r . The following two equations were derived from the data plotted in Fig. 7:

$$(95) \quad R_r = e^{(-0.075W)} \text{ and}$$

$$(96) \quad R_{fl} = R_r + 0.000167(W s_w).$$

If slope and its direction were available, as well as the direction of the wind, it would be possible to incorporate topography into the various spread ratios with relatively little difficulty.

2) Initial Size and Growth Rates

At this point, we have a standard ellipse, given the observed wind speed. The model now relates the standard ellipse to the fire and calculates initial size and growth rates for the fire and for each flank.

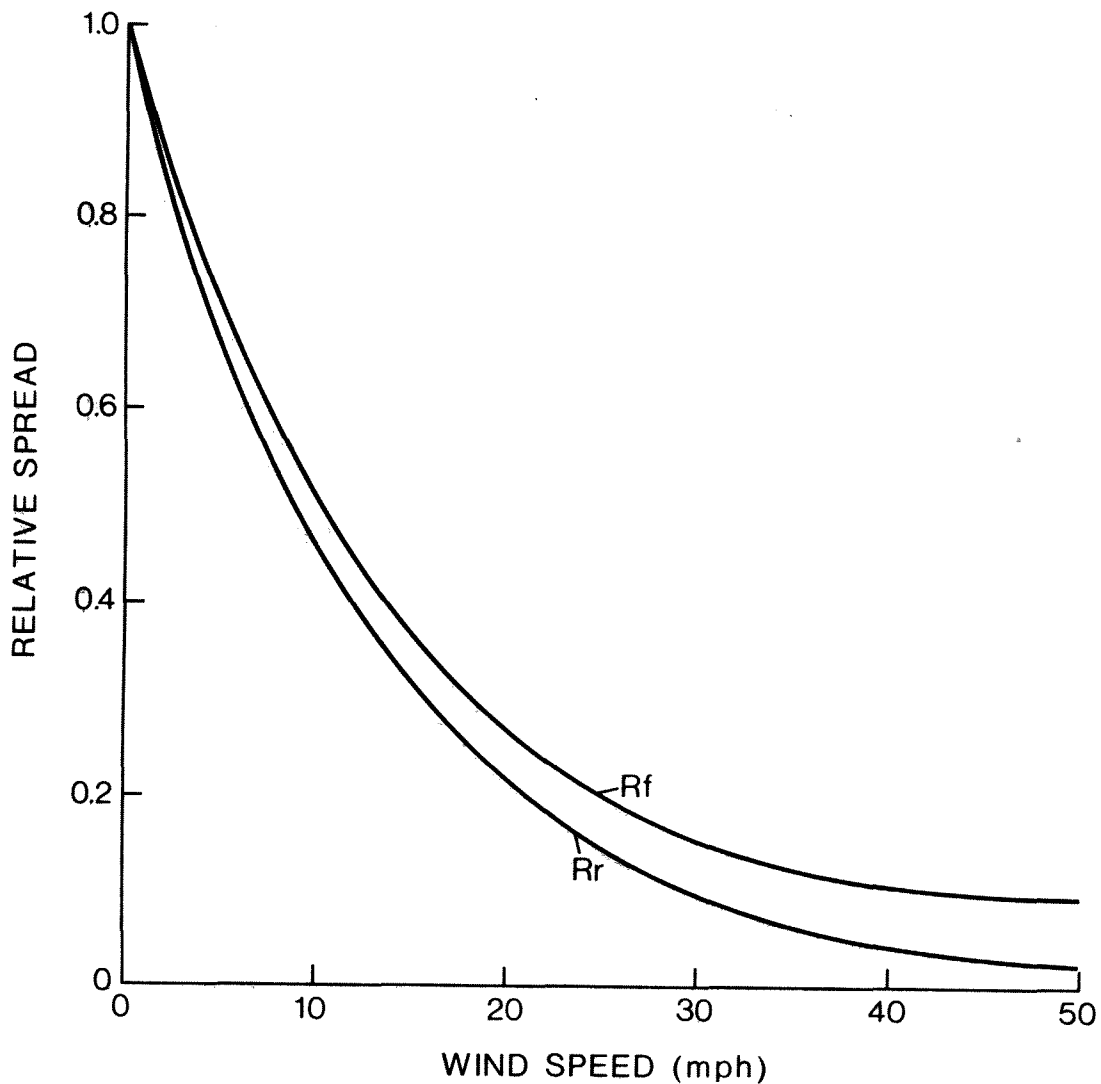
a) The fire

First, the model calculates the perimeter growth-to-forward rate of spread ratio (R_p):

$$(97) \quad R_p = P_x \left(\frac{1 + R_r}{2} \right).$$

The derivation of Eq. 97 is given in Appendix 2.

Figure 7. Rear and flank relative rates of spread as a function of wind speed



The model can now determine either forward rate of spread (Fs) given rate of perimeter growth (Pgs) or Pgf given Fs, depending on which observation is available:

(98) $S_f = \frac{P_{gf}}{R_p}$ and

(99) $P_{gf} = \frac{S_f \cdot R_p}{R_p}$

At this point, the theoretical spread (Fst) is linked to the observed value through a spread ratio (Rf):

$$(100) \quad Rf = \frac{Sf}{Fst}.$$

Whenever Fst changes, a corresponding change is applied to Fs by using Rf. In addition, an observed head fire intensity is estimated by multiplying the theoretical intensity by Rf on the premise that spread and intensity are directly proportional:

$$(101) \quad I_1 = I_t Rf c_i.$$

At the start of suppression, Pgs is substituted for Pgf in Eqs. 98 and 99. A suppression spread ratio (Rs) is then calculated and substituted for Rf in subsequent computations.

The rear and flank rates of spread are determined next:

$$(102) \quad Sr = Sf Rr \text{ and}$$

$$(103) \quad Sl = Sf Rfl.$$

Two additional variables will be needed to determine growth rates for the various flanks: the rate of growth of the semi-major axis for the fire (Gm), and the rate of forward movement of the center of the ellipse (Fc):

$$(104) \quad Gm = \frac{Sf + Sr}{2} \text{ and}$$

$$(105) \quad Fc = \frac{Sf - Sr}{2}.$$

Finally, the area and perimeter of the fire have to be related (only one need be supplied - the model calculates whichever is missing). An empirical relationship between the area and perimeter of an ellipse was developed, based on data presented by Simard (1969):

$$(106) \quad \begin{aligned} ap &= 620.3 + 96.11 Rl & ; & \quad Rl > 1.5 \text{ and} \\ ap &= 694.2 + 45.65 Rl & ; & \quad Rl \leq 1.5. \end{aligned}$$

The relationship between a_p and R_l can be seen in Fig. 8.

Area and perimeter can now be related:

$$(107) \quad P = a_p \sqrt{A} \quad \text{or}$$

$$(108) \quad A = \left(\frac{P}{a_p}\right)^2$$

where: P = fire perimeter (ft.) and
 A = fire area (acres).

The rate of area growth (G_a) is given by:

$$(109) \quad G_a = \frac{P g f P}{a_p^2}$$

b) The flanks

The model now has sufficient information to calculate the length and growth rate for each flank. It begins with flank intensity, which is related to intensity at the head through the relative spread ratio:

$$(110) \quad I_f = I_1 R_{fl}$$

To calculate intensity at the rear, R_{fl} in Eq. 110 is replaced with R_r .

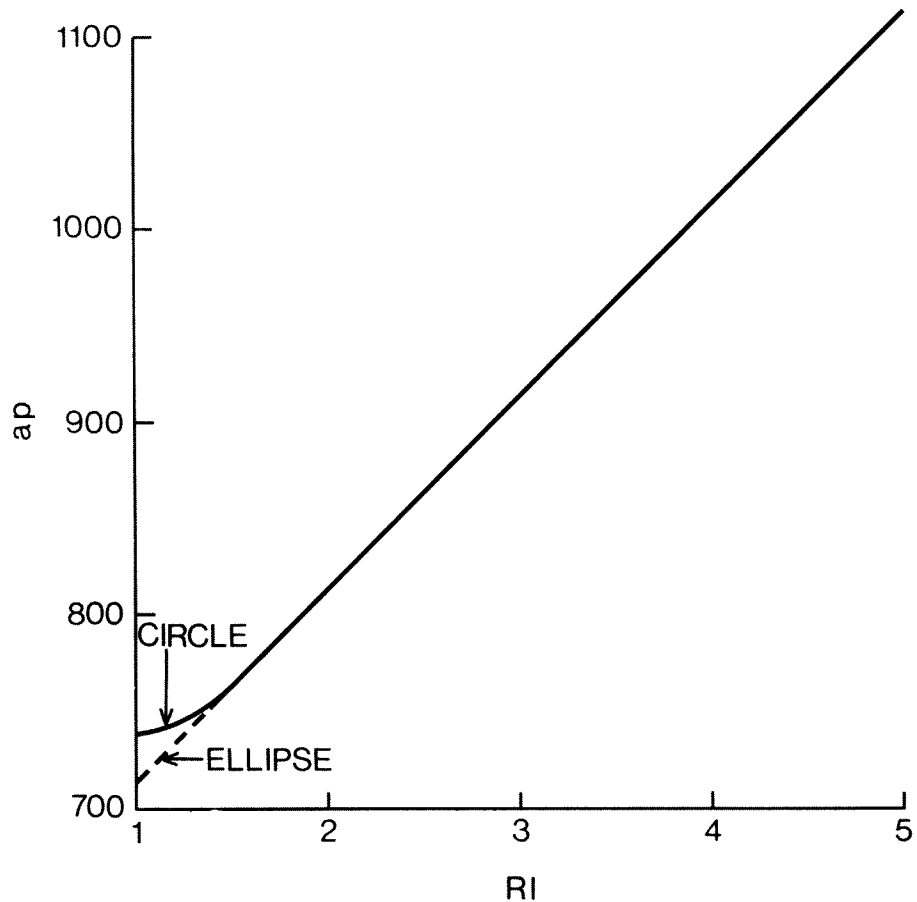
Four variables are calculated for each arc of the ellipse (fire flank): arc length, arc-to-chord ratio, initial arc growth rate, and chord growth rate. The model begins by calculating the ratio (R_e) between the perimeter of the fire and the perimeter of the standard ellipse:

$$(111) \quad R_e = \frac{P}{P_x}$$

The length of the head (A_{l_1}) is given by:

$$(112) \quad A_{l_1} = A_h R_e$$

Figure 8. Fire area to perimeter relationship



Similarly, the flank (A_{l_2}) is given by:

$$(113) \quad A_{l_2} = A_f R_e.$$

The rear (A_{l_4}) is equated to the head (A_{l_1}), and A_{l_3} is equated to A_{l_2} . The head arc-to-chord ratio (R_{c_1}) is calculated with:

$$(114) \quad R_{c_1} = \frac{A_h}{2ix}.$$

Similarly, the flank arc-to-chord ratio (R_{c_2}) is given by:

$$(115) \quad R_{c_2} = \frac{Af}{2iy}$$

As was the case for arc length, R_{c_4} is equated to R_{c_1} , and R_{c_3} is equated to R_{c_2} .

The model also calculates growth rates for each chord. These rates are simple combinations of forward, flank, and rear rates of spread. The ends of the head and rear chords expand laterally, at the same rate, in opposite directions. A separate growth rate is determined for each end of each chord. Recall that, for the standard ellipse, ix is the distance from the center axis to the ends of the head and rear chord, and that lengths in the standard ellipse are proportional to rates of growth in the fire ellipse. Thus, the lateral rates of growth of the head and rear chords (G_l) are given by:

$$(116) \quad G_l = ix G_m.$$

The ends of the flank chords expand in a forward and rearward direction at different rates. The distance from the center axis to the ends of the flank chord is given by iy , while the forward movement of the center axis is defined by F_c . Thus, the forward rate of growth of the flank chord (G_f) is given by:

$$(117) \quad G_f = (iy G_m) + F_c.$$

The rearward rate of growth of the flank chord (G_r) is given by:

$$(118) \quad G_r = (iy G_m) - F_c.$$

In the case of Eq. 118, when iy is unusually small and F_c approaches G_m in magnitude, it is possible the G_r could be negative, implying that the forward movement of the center of the ellipse is greater than the rearward growth of the chord. Since negative or very small growth rates caused computational difficulties in subsequent calculations, Eqs. 117 and 118 were replaced when $G_r < 0.1$ by:

$$(119) \quad z = 2iy G_m,$$

$$(120) \quad G_f = .867 z, \text{ and}$$

$$(121) \quad Gr = .133 z.$$

Essentially Eqs. 119-121 simply allocate the growth of the major axis on the basis of 87% to the head and 13% to the rear. These equations were only required in a few instances.

Finally, the initial rate of growth of the arc (Agi) is required in subsequent calculations. Arc growth is proportional to the chord growth rate and the arc-to-chord ratio. Thus, for the head and rear arcs, the initial growth rate is:

$$(122) \quad Agi_1 = 2 Gl Rc_1,$$

while for the flanks it is:

$$(123) \quad Agi_2 = Rc_2(Gf + Gr).$$

The fire is now initialized. We have calculated the overall size and growth rate. In addition, we have calculated the length and growth rate for each flank of the fire. We now proceed to fire growth.

3) Fire Growth

a) Free-burning growth

In the first step, the length of free-burning arc (Ab) is calculated by subtracting the length which has been controlled from the total arc length:

$$(124) \quad Ab_f = Al_f - \max(Pca_{f,j}, Pcg_{f,j}) - \max(Pca_{f,k}, Pcg_{f,k})$$

where: Pca = perimeter controlled by air tankers,
Pcg = perimeter controlled by ground forces,
f = flank, and
j,k = direction of attack and opposite
direction (interchangeable in Eq. 124).

If $Ab < 0.1$, the arc is considered controlled and the next arc is processed. If $Ab \geq 0.1$, the arc is allowed to grow:

$$(125) \quad Al'_f = Al_f + Ag_f \left(\frac{Ab_f}{Al_f} \right) Ti q.$$

Thus, the growth of an arc during any period is proportional to: the arc growth rate (A_g); the ratio of the free-burning-to-total-arc length (which is always 1 during free-burning growth); the length of the time interval (T_i); and the growth pulse (q). Note that for all small fires, $q = 1$.

Recalling Eqs. 122 and 123, note that A_g is not dependent on either T_i or A_l . The value is updated hourly in response to the diurnal cycle (see Eq. 75). Equations 124 and 125 constitute the free-burning growth sequence. In anticipation of the start of suppression, one additional equation is required to keep track of the current chord length for each arc. A simple proportion is all that is required:

$$(126) \quad Cl_f = \frac{Al_f}{Rc_f}$$

b) The start of suppression

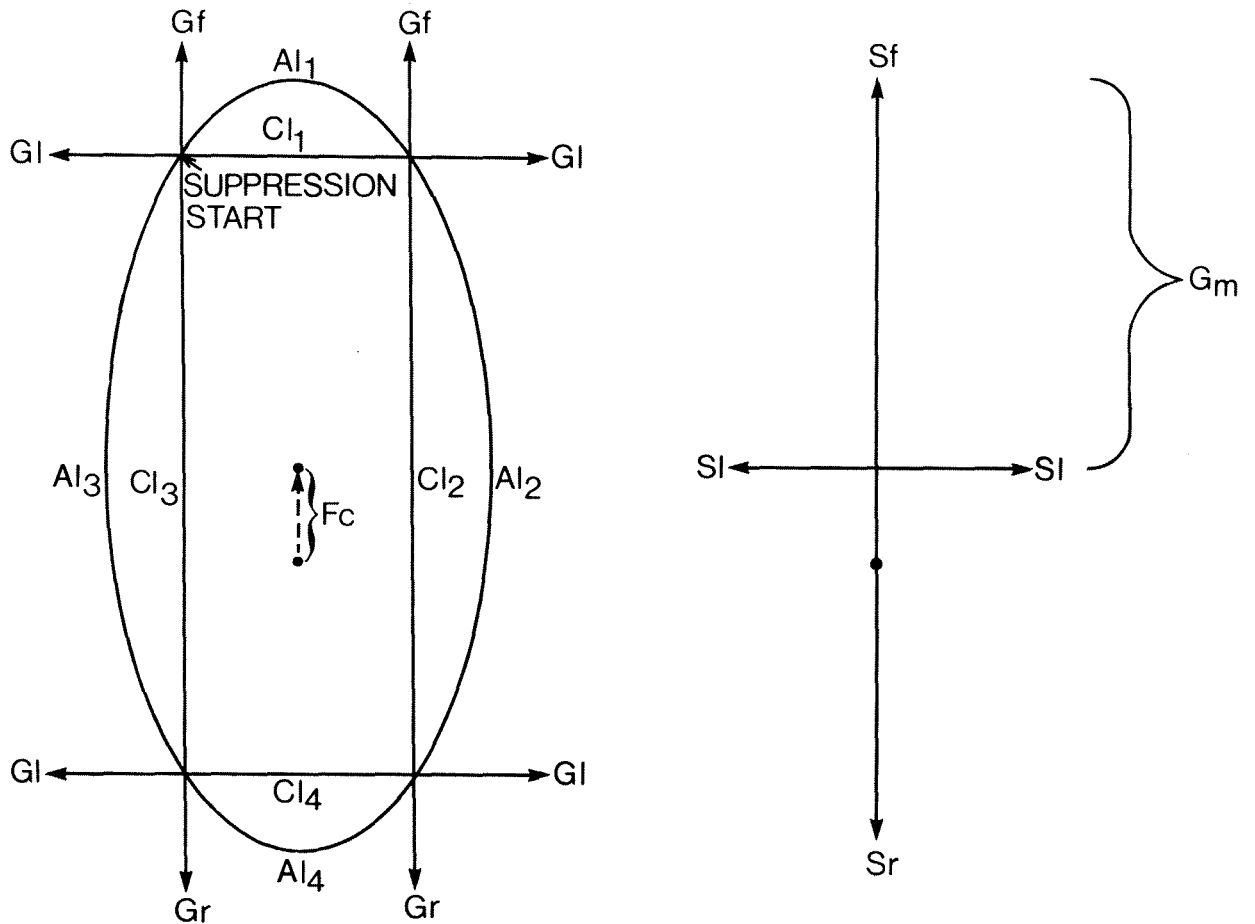
When the fire growth sequence receives an indication that either ground or air suppression is starting, some adjustments are made. In the model, suppression is always assumed to start at one of the four intersections between arcs. Since the current model does not consider fires burning around the end of a line, growth is assumed to stop at the point of intersection where suppression begins. Thus, assuming a start at a head/flank intersection, G_f and G_l associated with that point are set to zero. Further, a different form of growth model will now be employed, in which the chord length is the primary variable. Thus, the horizontal components of each chord (Ch) are initialized by equating them with the current chord length (Cl). At this time the vertical chord components (Cv) are set to zero.

Referring to Fig. 9, assume that suppression starts at the intersection between arc₁ and arc₃. G_l associated with the left side of arc₁ and G_f associated with arc₃ are both set to zero. Ch_1 is equated to Cl_1 and Ch_3 is equated to Cl_3 .

Finally, the growth rate for the arc must be modified. When one or both ends of an arc are controlled, Rc no longer remains constant. For example, arc lengths at $t+1$ under conditions B and C (ends controlled) in Fig. 10 are both longer than A (free-burning growth). In addition, the chords at $t+1$ for B and C are both shorter than the chord in A. Thus, under the assumptions of the model, arc growth rates change when an end is controlled. The logic of this behavior can be verified with the following explanation. In Fig. 10B, the right-hand side of the arc is seen to be the same as the right-hand side under free-burning conditions (A). This is as it should be, because the right-hand side is burning freely. The left-hand side of the arc in B is

stretched out, since it must reach from the point of control to the point where the free-burning arc would be. Note also that although the arc is longer in B than in A, the area burned is less in B than A. The argument obviously also applies to C (both ends controlled).

Figure 9. Fire growth variables



Clearly, in the real world, one cannot think in terms of holding only one end of a flank and allowing the remainder to burn freely. If, however, we think in terms of a suppression operation proceeding from left to right in Fig. 10B, coupled with very short time increments, we have, in effect, many points of control. The overall effect of a suppression operation over time will thus be very much as shown in Figs. 10B and 10C. The one real-world exception is the case where the arc adjacent to the one being controlled burns around the start of the control line. In the ground suppression component of the model, this problem is solved by splitting the suppression crew and having the two components work in both directions from the starting point. This problem is not addressed with respect to the air tanker component in the current version of the model, primarily due to the complexity involved. A solution may be added prior to subsequent applications.

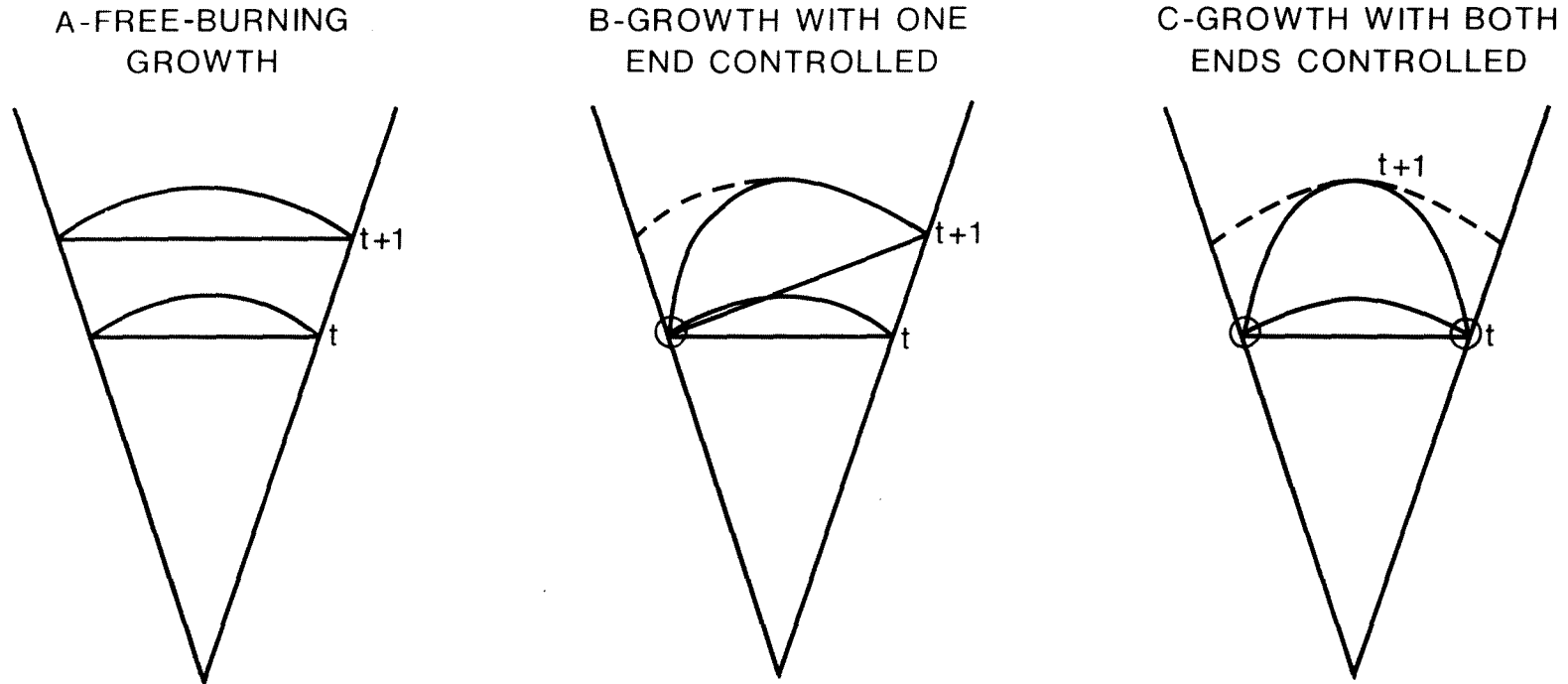
The equation for modifying the arc growth rate (Ag) at the start of suppression is:

$$(127) \quad Ag'_f = Ag_f + Ri (Gc_{a,d} - Gc_{f,o}) R_{c_f} \left(\frac{Al_f}{Ab_f} \right)$$

where: Gc = chord growth rate,
 f = flank of attack,
 a = adjacent arc,
 d = direction of attack, and
 o = opposite direction.

Prior to executing Eq. 127, the model equates Gc with Gf , $G1$, or Gr , as appropriate. In essence, Eq. 127 subtracts the growth rate for the chord of the arc of attack in the opposite direction to which suppression is taking place and adds the growth rate for the chord for the adjacent arc in the same direction as suppression. In the example shown in Fig. 11, $G1$ is subtracted from Gf and the difference added to Ag . The reasoning is that at all times there is both a horizontal and vertical component to the fire growth vector at any point on the perimeter. During free-burning growth, only the horizontal component need be considered for each arc, as the vertical component is accounted for by the growth of the adjacent arcs. When the horizontal component of the arc adjacent to the arc being attacked is set to zero, that growth component must be added to the arc being considered. All of the remaining terms in Eq. 127 are for the purpose of making chord growth rates proportional to current conditions on the arc.

Figure 10. Relationship between arc growth and control status



- The current-to-initial spread ratio (Ri) adjusts initial values of Gc to current conditions. With the use of Ri, only one variable has to be updated each hour rather than eight, as would be the case if Gc were updated directly.
- Rc relates linear chord growth to the arc growth rate.
- The ratio Al/Ab is the inverse of the ratio found in Eq. 125 and is inserted here for compatibility.

At the start of suppression, the growth rate for the arc adjacent to the one under consideration must also be adjusted. A modification of Eq. 127 is used:

$$(128) \quad Ag'_a = Ag_a + Ri (Gc_{f,o} - Gc_{a,d}) Rc_a.$$

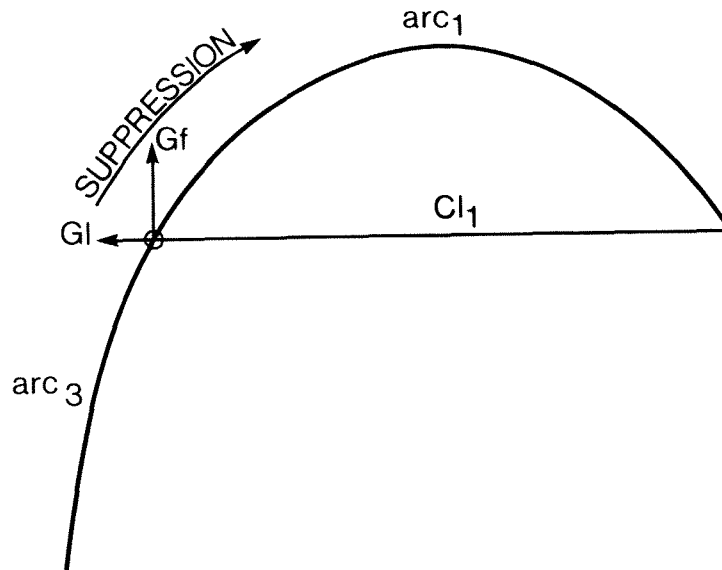
In this case, the growth rate for the adjacent chord in the same direction as suppression is subtracted from the growth rate for the chord in the opposite direction to suppression, and the difference added to the adjacent arc growth rate. In Fig. 11, for arc₃ at the start of suppression, G_f is subtracted from G_l. Note that in this case, Ag₃ will be reduced. Finally, the term Al/Ab is not necessary in Eq. 128 since, at the start of suppression, the ratio always equals 1.

Clearly, the adjustments calculated in Eqs. 127 and 128 are correct only at the time when suppression starts on an arc. As the crews move along the perimeter, the relative difference between the two growth variables at various points will change. It was found, however, that the single adjustment for each arc resulted in a quite acceptable and reasonable progression of fire growth rates during the course of suppression. It was, therefore, decided that the further complication of a dynamic adjustment was not warranted.

c) Growth during suppression

As might be inferred from the preceding discussion, there are two arc growth sequences during suppression, one for one end controlled, and one for both ends controlled. In both cases, the growth of the arc is calculated with Eq. 125, where growth is proportional to previous growth and the relative amount of free-burning perimeter. The only change from the free-burning condition is that $Ab/Al < 1$.

Figure 11. Arc growth adjustment for the start of suppression



Suppression growth is only concerned with calculating chord length and the arc-to-chord ratio. In the case of both ends controlled, only R_c need be calculated, since the chord length is fixed:

$$(129) \quad R_{c_f} = \frac{A l_f}{C l_f}$$

The case of one end controlled is somewhat more involved. First, the horizontal and vertical components of chord growth at the free end must be calculated:

$$(130) \quad Ch'_f = Ch_f + Ti Ri Gc_{f,d} q \text{ and}$$

$$(131) \quad Cv'_f = Cv_f + Ti Ri Gc_{a,o} q$$

The vertical component calculated in Eq. 131 is obtained from the chord growth component from the arc adjacent to the free end and opposite to the direction of suppression. Chord length (Cl) is then calculated:

$$(132) \quad Cl_f = \sqrt{Ch_f^2 + Cv_f^2}.$$

Finally, the arc-to-chord ratio is calculated, using Eq. 129.

d) Final fire size

Throughout the growth process, the model has increased the size of each arc independently of the remainder of the perimeter. When control of the fire is achieved, the four flanks must be reunited to form a complete fire. Total perimeter is simply the sum of the four arc lengths:

$$(133) \quad P = \sum_{f=1}^4 Al_f.$$

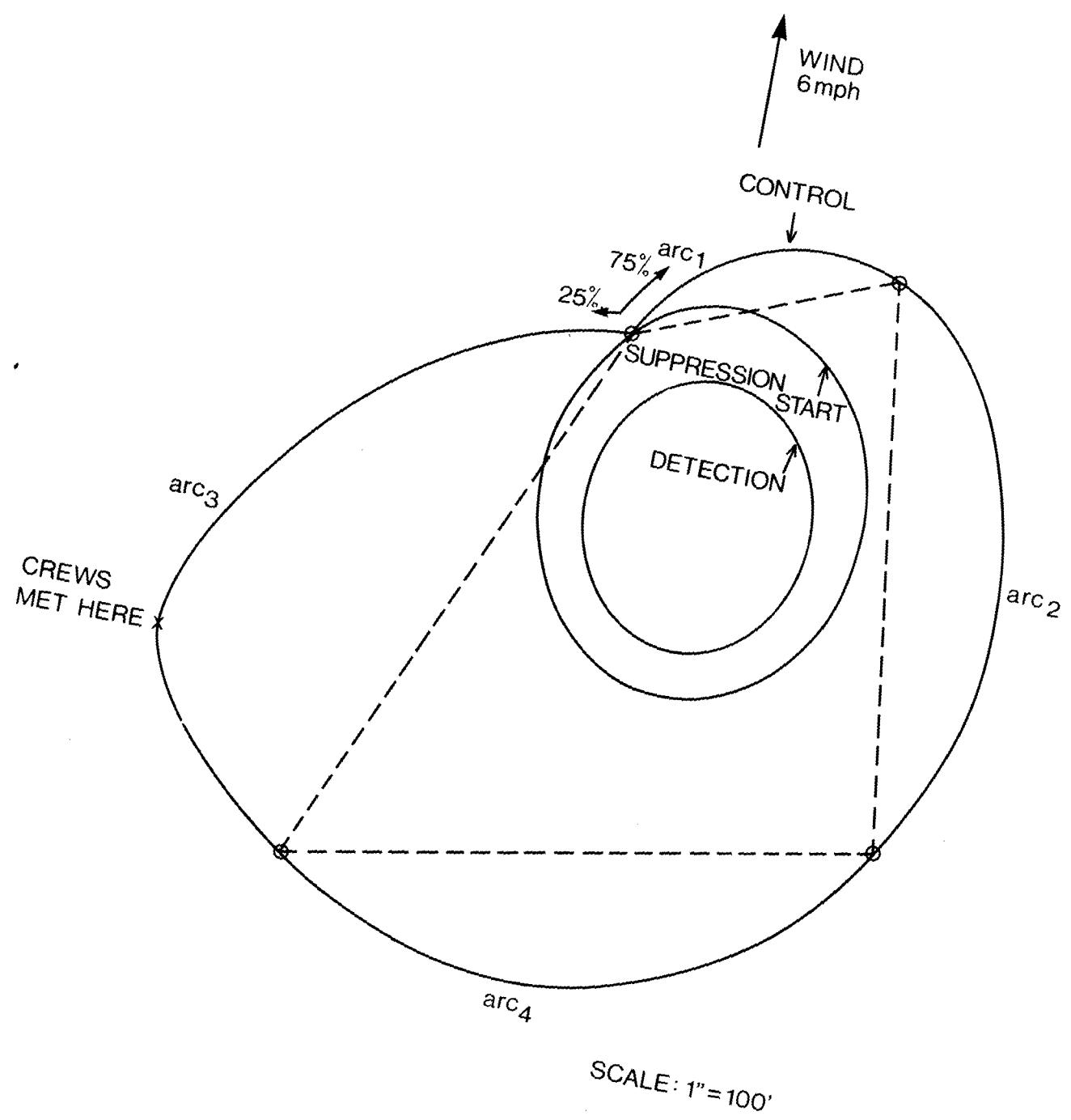
While calculating the final area is also relatively simple, the equation involves an assumption which warrants discussion. When the four arcs are rejoined to form a complete fire, the resulting shape is not at all similar to the simple ellipse from whence it originated. This can be seen in Fig. 12, which is a plot of a typical simulated fire.

To obtain Fig. 12, the preceding fire equations and subsequent ground suppression equations were programed and run for a typical fire with the following data:

- wind speed = 6 mph. (R1 = 1.25),
- forward rate of spread = 160 ft./hr.,
- detection size = 0.5 ac.,
- suppression start size = 1.15 ac., and
- rate of line construction = 400 ft./hr.
(75% on head, 25% on flank).

The perimeter of the fire was plotted at half hour intervals during the course of suppression. For simplicity, only the detection, suppression start, and final perimeters are shown in Fig. 12. The simulated time to control was 3.6 hours and the simulated area (obtained graphically from Fig. 12) was 4.74 acres.

Figure 12. A typical simulated fire



The primary purpose of the exercise was to test various procedures for estimating the area of the fire given the available data. Two techniques were considered. The first was relatively simple.

- i) An elliptical shape was assumed.
- ii) The four chords were averaged and R1 was calculated.
- iii) The area was obtained using Eqs. 106 and 108.

The preceding calculations yielded R1 = 1.4 and area = 4.92 acres, a surprisingly close estimation (+ 3.8%), considering the simplicity of the process and the assumptions required.

The second technique was expected to be more precise.

- i) A parabolic shape was assumed for each arc.
- ii) The height of each arc was calculated.
- iii) The area between each arc and chord was calculated.
- iv) The distance between opposite arc intersections was calculated.
- v) The areas of the two triangles formed by pairs of adjacent chords and a line connecting opposite arc intersections were calculated.
- vi) All areas were summed.

The latter procedure yielded an area of 4.57 acres, which is 3.5% too low. As a result of this exercise, it appeared that there was no justification for employing the more complex procedure, and it was not pursued further. Thus, the model calculates R1 with the equation:

$$(134) \quad Rl = \sqrt{s \left(\frac{Cl_2 + Cl_3}{Cl_1 + Cl_4} \right)}$$

The derivation of Eq. 134 is given in Appendix 2. The sum $Cl_2 + Cl_3$ is proportional to the average flank chord length (y), while $Cl_1 + Cl_4$ is proportional to the average head chord length (x). Finally, the area of the fire is calculated with Eqs. 106 and 108.

The description of the fire growth model is now complete. The reader may well ask whether a model involving 50 equations can be classed as relatively simple. While it is considerably

less involved than the Kourtz-O'Regan model, it is certainly more complex than the models of Van Wagner and Anderson. While the model is beyond what could be considered practical for hand calculation, and it would likely strain the average programable hand calculator, it is inconsequential for even a small computer. This is conclusively demonstrated by the fact that a computer was able to completely process a fire (including ground and air suppression and tabulation as well as fire growth) in an average of 0.03 seconds.

Many equations are required because the model keeps track of many things. Yet, the equations are simple in themselves. There is no calculus involved in the actual computation, and it is only required for a small part of the derivation. Every equation is readily understandable by a person with a reasonable knowledge of algebra. The variables are in terms of readily identifiable phenomena such as wind speed, forward rate of spread, length-to-width ratio, length of flank, etc. In conclusion, it could be said that the fire growth model combines reasonable comprehensibility with the minimum complexity required to accomplish the specific task.

5. GROUND SUPPRESSION

In warfare, victory can ultimately only be gained by the foot soldier. Air power can, of course, play a decisive role in determining the final outcome - that is in supporting the infantry. In this sense, as in many others, fire control is similar to military operations. While air tankers can drop vast quantities of water and chemicals, they generally do not put a fire out. Air tankers may "hold" a fire until ground forces arrive, or they may reduce the intensity so that ground forces can work more effectively, but complete extinguishment is an exceptional accomplishment. Even when air tankers extinguish a fire, their success must be verified by ground observation.

It is clear, therefore, that air tanker utilization cannot be analyzed in isolation. It must be examined in the context of the ground suppression system which it supports, if results are to be meaningful. To incorporate this concept, the model examines fire suppression using unaided ground forces and compares the results with those obtained by using ground forces supported by air tankers. Thus, ground suppression is a major component of the air tanker productivity model. In this section we will consider three aspects of ground suppression that are contained in the model: suppression, mop-up, and economics.

A. Suppression

1) Crew Arrival

When a fire is detected (data read in), the arrival schedule for suppression crews is established. The arrival time of the first crew (T_1) is obtained directly from the data by using Eq. 66, which simply sums the observed travel, dispatch, and attack delay times. It was found that for all fires with an observed final size less than 30 acres (96% of all fires), no further calculations were necessary to generate an acceptably accurate simulation.

For fires larger than 30 acres, a procedure similar to that used for the growth of fires was required for ground suppression, to ensure that ground forces did not catch the fire too quickly in the model. This is not surprising, considering the nature of the data being used. The overall average line construction rate is not generated by the initial attack crew, but rather by the cumulative effectiveness of several crews which arrive at various times after suppression has begun. Thus, a simulated delay schedule for crew arrivals was established from the observed data.

The first step involves estimating the expected control time, beginning with the perimeter control rate (Pr):

$$(135) \quad Pr = Lc - \frac{Pgs}{2} \cdot$$

This is followed by the estimated perimeter at the start of control:

$$(136) \quad Pc = Pd + T_1 \frac{Pgs}{ai}$$

where: Pe = estimated perimeter at the start of suppression,
 Pd = observed perimeter at detection, and
 T_1 = time of arrival of initial attack crew.

Essentially, Eq. 136 simply adds the expected growth to the detection perimeter. The observed perimeter growth rate (Pgs) is divided by ai to render it compatible with the growth that will be obtained by using Eq. 67. Finally, the estimated control time (Te) is determined:

$$(137) \quad Te = \frac{Pe}{Pr} \quad ; \quad Pr > 0,$$

$$Te = \frac{5 Pe}{Lc} \quad ; \quad Pr \leq 0.$$

The delay schedule is established with the following sequence. First, a simulated number of crew arrivals (Nc) is determined:

$$(138) \quad Nc = 1 + \frac{Lc}{500} \quad ; \quad 2 \leq Nc \leq 4.$$

Nc is directly related to the observed average rate of line construction. For every 500 feet per hour of line construction rate, an additional crew is assumed to be on the fire. The number of crews is limited to between 2 and 4, to keep the delay schedule within reasonable bounds. The rate of line construction per crew (Lcc) is simply the average rate divided by Nc :

$$(139) \quad Lcc = \frac{Lc}{Nc} \cdot$$

The time interval between crew arrivals (Tic) is given by:

$$(140) \quad Tic = \frac{Te}{2 Nc - 1} \quad ; \quad Tic \leq 4.$$

Note the use of $2 N_c$. This is required because the delay schedule must incorporate two arrival times for each crew. This can be better understood by examining Fig. 13, which portrays the effect of various crew arrival sequences. Each time a crew arrives, its contribution (L_{cc}) to overall suppression is added to the previous total, yielding the rate of line construction for the number of crews currently at the fire site (L_{cn}). By associating only part of the observed L_c to the initial attack crew, a deficit in the simulated total amount of line built is created. The deficit is shown graphically in Fig. 13 as the area below the line $L_c = 1.0$ and above L_{cn} during the early stages of suppression. To render the simulated and observed totals compatible, that deficit must be made up by having a period of line construction with an excess rate equal to the deficit and lasting for the same length of time.

It is reasonable to assume that in the field, additional forces can arrive at the fire site within four hours of the initial attack crew, and at comparable intervals thereafter. Hence, a limit of four hours was imposed on T_{ic} . When $T_{ic} \leq 4$, L_{cn} will increase in a stepwise fashion until it reaches a peak, at about the same time that the fire is controlled. When T_{ic} would have been greater than 4 (before being limited), L_c will increase as for the previous case, but starting four hours after the last crew arrives, the observed average L_c will be used for the remainder of the suppression interval.

The delay schedule is established with the iterative sequence:

$$(141) \quad T_n = T_{n-1} + T_{ic} \quad ; \quad n \leq 8$$

where: T = cumulative delay time until crew arrives and
 n = crew number.

The end of the crew arrival delay sequence is indicated by $T = 0$.

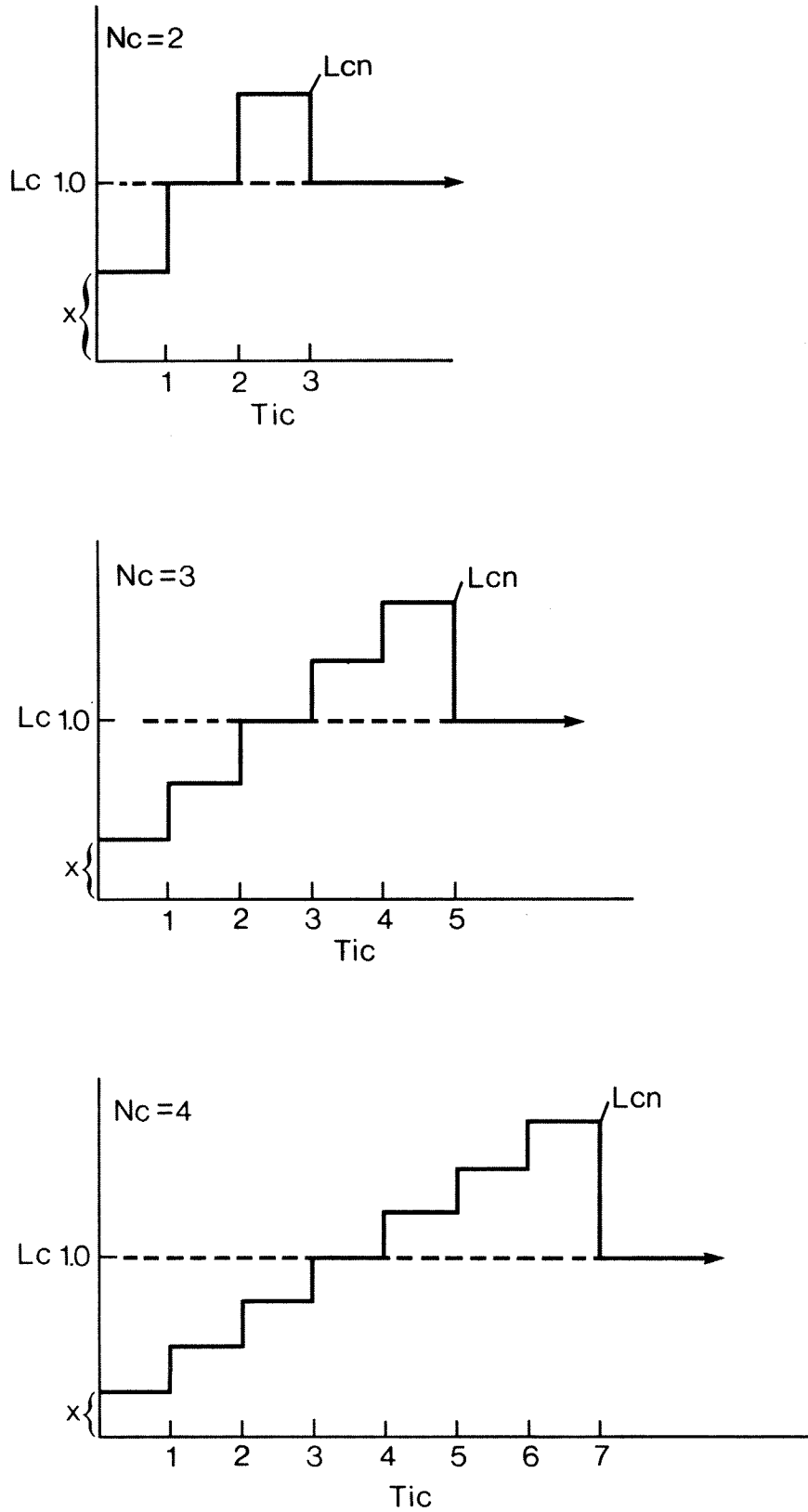
2) Rate of Line Construction

In the early stages of model development, current rate of line construction (L_{cn}) was calculated with an equation which yielded the response shown in Fig. 13:

$$(142) \quad L_{cn} = L_c + (N_f - N_c) \frac{L_c}{N_c}$$

where: N_f = number of crews currently at the fire.

Figure 13. Effect of ground crew arrival delay



It was determined in early runs that Eq. 142 did not produce a sufficient delay to achieve the desired objective (allowing more area burned in the simulated fires, thereby better matching observational data). The delay function was, therefore, strengthened:

$$(143) \quad L_{cn} = n L_{cc} + (N_f - N_c) \frac{L_{cc}}{N_c}$$

The output of Eqs. 142 and 143 is listed in Table 3. As can be seen, while the averages for both equations are the same, Eq. 143 has a lower initial L_{cn} compared with a matching higher compensation in latter stages of the fire. When $T = 0$, indicating that no more crews are scheduled to arrive, L_{cn} is equated with L_c .

As mentioned in the discussion on fire growth, the rate of line construction on each flank of the fire is related to the relative intensity on the flank. This is calculated by first determining the average intensity on the fire (I_f):

Table 3 Relative values of L_{cn}

Equation		<u>$N_c = 2$</u>		<u>$N_c = 3$</u>		<u>$N_c = 4$</u>	
		142	143	142	143	142	143
Nf	1	0.50	0.25	0.33	0.11	0.25	0.07
	2	1.00	1.00	0.67	0.55	0.50	0.38
	3	1.50	1.75	1.00	1.00	0.75	0.69
	4	1.00	1.00	1.33	1.45	1.00	1.00
	5			1.67	1.89	1.25	1.31
	6			1.00	1.00	1.50	1.62
	7					1.75	1.93
	8					1.00	1.00

$$(144) \quad I_f = \frac{\sum_{f=1}^4 I_f}{4}$$

where: f = flank of attack.

This is followed by the relative line construction rate (Lcr):

$$(145) \quad Lcr_f = \sqrt{\frac{I_f}{\bar{I}_f}}$$

Essentially, Lcr is related to the square root of the ratio of the average intensity to the intensity on the flank. In other words, as flank intensity increases, Lcr decreases.

Finally, the rate of line construction on each flank (Lcf) is given by:

$$(146) \quad Lcf = Lcn Lcr_f$$

During suppression, the rate of line construction applicable to the specific combination of crews and conditions on the flank must be determined. When the crews are not split, the percentage of the total rate for the number of crews currently on the fire (Lcn) allocated to the crew on the flank in question (Lcp) is equal to 1.0. If the crews are split, a percentage of the total rate is allocated to the crew being processed. The percentages are determined by the user. The current model simply allocates 50% of the total to each crew. The specific rates of line construction are given by:

$$(147) \quad Lcs = Lcf Lcp \text{ and}$$

$$(148) \quad Lcx = 2 Lcf Lcp$$

where: Lcs = standard rate of line construction,
 Lcx = augmented rate of line construction in
an air tanker drop, and
 $Lc4$ = rate of line construction on the rear.

The augmented rate in an air tanker drop is simply twice the rate on the rear flank. Finally, if it is dark at the time, both rates are reduced by 50%.

3) Fighting the Fire

The suppression sequence begins by calculating the duration of the period under consideration:

$$(149) \quad Dt = Tf - Ts.$$

The time left in the period (Tl) is equated with Dt at this time. The model then processes each flank separately.

The length of uncontrolled perimeter on a flank (Fl) is calculated with the equation:

$$(150) \quad Fl = Al - Pcg_{f,d} - Pcg_{f,o}$$

where: f = flank of attack,
 d = direction of attack, and
 c = opposite direction.

The model then calculates the amount of work time remaining until the rate of line construction will change (Tw). One of four equations is used, depending on the particular combination of circumstances prevailing at the time. If the crew is not in an air tanker drop and there is no drop between the crew and the flank boundary, the standard rate of line construction is used until the flank boundary is reached:

$$(151) \quad Tw = \frac{Al_f}{Lcs}$$

If the crew is not in a drop, but is approaching a drop from the opposite direction, the standard rate is used to the edge of the drop pattern:

$$(152) \quad Tw = \frac{Al_f - Pcg_{f,d} - Pca_{f,o}}{Lcs}$$

In the case of Eqs. 151 and 152, the rate of line construction to be used (Lcu) is equated with Lcs.

If the crew is in an air tanker drop coming from the opposite direction, the augmented rate will be used to the end of the arc:

$$(153) \quad T_w = \frac{A\ell_f}{L_{cx}}$$

Finally, if the crew is in an air tanker drop coming from the same direction, the augmented rate is used to the edge of the drop pattern or the flank boundary, whichever comes first:

$$(154) \quad T_w = \frac{P_{ca_{f,d}} - P_{cg_{f,d}}}{L_{cx}}$$

In the case of Eqs. 153 and 154, (L_{cu}) is equated with L_{cx} .

If $T_l < T_w$, line is built until the end of the period:

$$(155) \quad P_{cg_{f,d}'} = P_{cg_{f,d}} + (T_l L_{cu}) \text{ and}$$

$$(156) \quad P_c' = P_c + (T_l L_{cu})$$

where: P_c = total perimeter controlled by ground forces.

T_l is set to zero and the model checks for a second crew on the flank (working from the opposite direction). If a second crew is indicated, the suppression sequence is repeated on the same flank. If there is no second crew (which will be the case on all but the last flank) the next flank is processed.

If $T_l > T_w$, line is built until the rate of construction changes, by substituting T_w for T_l in Eqs. 155 and 156. In this case, however, there is time remaining at the end of the period:

$$(157) \quad T_l' = T_l - T_w.$$

If there is some uncontrolled perimeter remaining on the flank, the sequence repeats, starting with Eq. 150. If there is no uncontrolled perimeter left on the flank being processed, the next flank for the crew is determined, and the process repeats, starting with Eq. 147 (except that T_l is not reinitialized). Note that the next flank for the crew is not necessarily the same as the next flank being processed by the sequential search

pattern in the model. For example, each flank is examined with respect to ground activity in the order 1, 2, 3, and 4. A crew which starts at the intersection of arcs 1 and 3 and proceeds in a clockwise direction, will control the flanks in the order 1, 2, 4, and 3. In a counter clockwise direction, the order will be 3, 4, 2, and 1. If a different starting point is used, the order will change correspondingly.

When a flank with ground crew activity is identified, the crew on that flank continues fighting the fire until T_l equals zero, or the other crew is met. Inquiries concerning the status of ground activity on any flank during sequential flank processing reflect activity previously accounted for during the current time interval. For example, assume that flank 1 is completed in a clockwise direction and $T_l > 0$. The crew then moves on and builds line on flank 2 until $T_l = 0$ before returning to the sequential search pattern. When the status of flank 2 is examined, a work-done indicator in a clockwise direction will cause the sequential search to skip flank 2 and move on to flank 3.

The preceding procedure is followed until all four flanks are controlled. The end of the control operation is indicated when the next flank of attack for a crew has already been controlled. At this time, the time at which the fire was controlled is determined:

$$(158) \quad T_f' = T_f - \frac{T_l}{N_{cd}}$$

where: N_{cd} = number of crew divisions (1 or 2).

Equation 158 is necessary because control will generally occur sometime during the interval between events. The division by N_{cd} accounts for the fact that the control activity of each subcrew is processed sequentially. For example, assume that 15 minutes are required for the first subcrew to reach the other in the simulation. Since the two crews are working towards one another, only 7.5 minutes would have actually elapsed before they met.

Equation 158 applies when there is only one crew, or the second of two crews finishes the line. When the crews are split and the first crew completes the control operation, Eq. 158 must be modified:

$$(159) \quad T_f' = T_f - \left(\frac{T_{li} + T_l}{2} \right)$$

where: T_{li} = initial value of T_l .

The addition of $T_{li}/2$ is required because the time during which the second crew would have worked is not accounted for in the model when the first crew controls the fire. Finally, the total time required to control the fire (T_c) is given by:

$$(160) \quad T_c = T_f - T_{sc}.$$

In essence, the mathematics of controlling the fire with ground forces are relatively simple. Most of the effort centers around identifying previous, current, and subsequent ground activity and taking appropriate action, depending on the status of the fire and air activity.

B. Mop-up

Controlling the fire is not the end of the suppression operation. The fire must be mopped-up and patrolled for some time after control is achieved to ensure complete extinguishment. While air tankers are not normally employed in the mop-up phase, their use affects it. By reducing the area burned by a fire, the effort required to mop it up is reduced proportionally. An analysis of the data from the province of New Brunswick indicated that mop-up and patrol accounted for about 25% of the total cost of fire suppression. It was, therefore, decided to include a mop-up component in the air tanker productivity model.

The first question to consider was the form of output required from the mop-up component. Ultimately, we will be interested in the total cost of suppression. It was found that the most significant mop-up variable with respect to overall suppression cost was the time required for mop-up. It was further decided that an empirical relationship for mop-up time would be satisfactory for the present purpose. Therefore, a series of equations for calculating mop-up time were determined by regression analysis.

Within a specific fuel type, (F_{nb}) the time required for mop-up (T_m) is related to two basic variables.

- The size of the area involved (area, perimeter, and indirectly, the time required for control, and rate of growth).
- The rate at which mop-up takes place. This can be observed or estimated directly, or estimated by combining two secondary variables. They are the amount of work required per unit area (related to fire intensity, which, in turn, can be related to the fire weather index variables) and the

strength of the ground forces (which can be indirectly estimated from control time and rate of line construction).

From a preliminary list of variables and variable combinations, the following ten variables were selected as being the most promising for the regression procedure, based on correlation with time of mop-up (T_m).

- Ia = adjusted duff moisture code (build-up index)
- Ma = average rate of mop-up for the ground station nearest the fire (ac./hr.)
- Tam = average time required for mop-up for the ground station nearest the fire (hr.)
- Id = drought code (DC)
- A = fire area (ac.)
- Pc = perimeter of the time of control (ft.)
- Ga = average free-burning rate of area growth (ac./hr.)
- Lc = rate of line construction (ft./hr.)
- M = rate of mop-up (ac./hr.)
- Tc = time to control (hr.)

Using a standard multivariable stepwise regression procedure,⁷ the following equations were developed.

$$F_{nk} = 0$$

$$(161) \quad T_m = 18.45 - 0.0869 \frac{A}{Ma} + 0.6624 Tam + 0.0166 Pc - 60.49 M + 302.5 \frac{A}{Lc} + 0.0841 \frac{A}{M} + 2.157 Ga + 0.5155 Ia - 0.1312 Id - 5.688 \sqrt{Tc}$$

$$F_{nk} = 1$$

$$(162) \quad T_m = - 10.80 - 6.918 Tc - 0.6995 M - 0.6032 Ia + 0.1034 Id + 37.41 \sqrt{Tc}$$

$$F_{nk} = 2$$

$$(163) \quad T_m = - 6.232 - 0.2951 \frac{A}{M} + 0.2681 \frac{A}{Ma} + 10.19 \sqrt{Tc} + 0.2571 Tam - 3.079 Ga + 0.0072 Pc$$

$$F_{nk} = 3$$

$$(164) \quad T_m = - 17.25 + 5.471 \sqrt{Tc} + 0.0937 \frac{A}{M} + 0.1963 Ma + 51.58 \frac{A}{Lc} + 0.0101 Pc - 0.4723 A + 0.0582 Id - 0.6436 Ga + 0.0588 \frac{A}{Ma}$$

⁷ DSTEP - Information on file at the Forest Fire Research Institute, Ottawa, Ontario.

Fnb = 4

$$(165) \quad T_m = - 4.497 - 9.111 \sqrt{T_c} + 10.32 \text{ Ga} - 11.35 \text{ M} + 3.438 \frac{\text{A}}{\text{Ma}} \\ + 0.3043 \text{ Tam} + 0.2053 \text{ Ia}$$

Fnb = 5

$$(166) \quad T_m = - 57.96 + 1.412 \text{ Tam} + 0.1639 \text{ Id} + 0.0483 \text{ Pc} \\ - 1.774 \text{ A} - 2.437 \text{ Ga} - 22.33 \text{ M}$$

Fnb = 6

$$(167) \quad T_m = - 12.24 + 0.543 \text{ Pc} - 52.52 \text{ M} - 0.8774 \frac{\text{A}}{\text{M}} + 0.1321 \text{ Id}$$

Fnb = 7, 8

$$(168) \quad T_m = 11.42 + 31.68 \sqrt{T_c} - 0.1102 \text{ Id} + 7.755 \text{ A} - 10.79 \text{ M} - 4864. \frac{\text{A}}{\text{Lc}}$$

Fnb = 9

$$(169) \quad T_m = 81.60 + 698.5 \frac{\text{A}}{\text{Lc}} + 0.5466 \text{ Pc} - 2.387 \text{ A} - 64.14 \text{ M} - 0.6607 \text{ Tc} \\ - 0.3972 \text{ Ia} - 15.61 \sqrt{T_c} - 1.824 \text{ Ga} - 0.1223 \text{ Id}$$

Fnb = 10

$$(170) \quad T_m = - 31.00 + 0.0126 \text{ Pc} + 0.0523 \text{ Id} + 0.5393 \text{ Tam} + 9.906 \sqrt{T_c} \\ + 0.084 \frac{\text{A}}{\text{Ma}} - 0.2199 \text{ A} + 0.2625 \text{ Ia}$$

Fnb = 11

$$(171) \quad T_m = - 25.36 + 0.5756 \frac{\text{A}}{\text{Ma}} + 10.73 \sqrt{T_c} + 0.2554 \text{ Tam} - 0.1931 \frac{\text{A}}{\text{M}} \\ + 0.4101 \text{ Ia} - 2.451 \text{ A} + 0.0132 \text{ Pc} + 643.1 \frac{\text{A}}{\text{Lc}}$$

Fnb = 12

$$(172) \quad T_m = 6.302 + 1627. \frac{\text{A}}{\text{Lc}} + 8.986 \text{ Tc} - 1.788 \text{ M} + 0.9433 \frac{\text{A}}{\text{Ma}}$$

All fuel types

$$(173) \quad T_m = - 25.98 + 0.0155 P_c + 0.0813 I_d + 0.3908 T_{am} + 8.910 \sqrt{T_c} \\ - 4.278 M - 0.2982 A + 0.0375 \frac{A}{M} + 0.0644 \frac{A}{M_a}$$

Statistics associated with Eqs. 161-173 are listed in Table 4. The use of equations for individual fuel types resulted in a 25% reduction in the standard error of the estimate relative to the use of a simple overall equation. On the basis of this justification, the individual fuel type equations were used in the model.

A plot of observed versus calculated values of T_m is shown in Figure 14. Due to an error in the standard plot routine used, only a sample of points are shown in the lower left-hand corner. Since the points plotted are correct, the sample was felt to be an adequate graphical representation of the behavior of the mop-up equations.

Considering the amount of scatter evident in Fig. 14, a statistical analysis of the slope and intercept was not warranted. Some points are apparent, however, based on a simple visual examination.

- An assumption of a y intercept of zero appears reasonable.
- Individual points are relatively widely scattered about the 45° line.
- With the exception of one point, the amount of scatter does not appear to increase with increasing values of T_m .
- The regression equation appears to have a downward bias at high values of T_m (i.e., the slope of a line through the points would be less than 1).

In general, the accuracy of Eqs. 161-172 is less than desired. An average error for T_m of ±100% is clearly inadequate for predicting individual events. There are some mitigating circumstances with respect to the current application, however.

- Mop-up only constitutes an average of 25% of the total suppression cost. An error of 100% in T_m would, therefore, generate a cost that would be in error by only 25%, on the average. In addition, T_m is not considered in the damage equations, further reducing its impact on the order of 50%.

Table 4 Statistics for mop-up regression equations

<u>Fnb</u>	<u>Sample size</u>	<u>\bar{T}_m</u>	<u>R^2</u>	<u>STD. ERR.</u>	<u>$\frac{SE}{\bar{T}_m}$</u>
1	114	28.9	.76	31.2	1.08
2	23	16.9	.40	16.0	.95
3	45	21.8	.90	14.1	.65
4	139	17.4	.77	18.2	1.05
5	30	19.2	.84	15.6	.81
6	86	29.4	.46	58.4	1.98
7,8	43	33.3	.52	47.6	1.43
9	16	17.4	.61	20.4	1.17
10	106	32.2	.73	40.4	1.26
11	99	33.8	.77	33.6	.99
12	77	26.5	.73	24.5	.93
13	73	17.6	.84	15.2	.86
Weighted average	71	25.8	.72	30.0	1.13
Overall	851	25.8	.53	38.6	1.50

- A large sample is analyzed by the model. As a result, the errors should tend to be compensating.
- Results generated by the model are based on relative differences rather than absolute values. If T_m is too high when only ground suppression is considered, for example, it will also be too high when air tankers are added. The error should have only a slight effect on the difference between the two outcomes.

For the preceding reasons, it was decided that additional work with respect to the mop-up component of the model would not be undertaken. Any further analysis would have required the initiation of a significant research effort which was considered outside the scope of the project.

A final note on the mop-up equations is required. As is normally the case when regression equations are employed, unusual combinations of data can generate results which are grossly erroneous. For this reason, limits were placed on two input variables: $I_a \leq 100$ and $I_d \leq 500$. In addition, limits were placed on the range of T_m such that:

- if $T_m < 1$; $T_m = 1$ and
- if $T_m \geq 48$ and $T_m > 3 A/M$; $T_m = 3 A/M$.

C. Economics

We have modeled a fire and can thus generate a demand for activity from the fire suppression system. We have also simulated the control of that fire and can therefore study the work performed by the system. Although much has been accomplished, it is not enough to solve the problem at hand. We must be able to compare one outcome with another, to evaluate the relative merits of various suppression strategies. To do this, we must consider the goals of the system, for it is in the system goals that we will find appropriate measures of effectiveness.

One obvious goal of fire management is the reduction of area burned. This is a convenient goal in that it is readily measurable, and requires little interpretation. From a modeling standpoint, it provides a serendipitous benefit in that we have already calculated area burned. Unfortunately, the objective has a serious weakness - it is unconstrained. The system could continue to reduce area burned indefinitely by simply increasing suppression expenditures. Clearly, the reduction in area burned has to be related to the costs of obtaining the reduction as well as the resulting benefits. These considerations can be grouped

under the heading of fire economics, which is the subject of this section.

A fire management organization will be efficient, in an economic sense, if it maximizes V_p , where:

$$(174) \quad V_p = B_p - C_p - D_p$$

where: V_p = net present value of a fire,
 B_p = net present benefit,
 C_p = present value of suppression cost, and
 D_p = net present damage.

In the current application, some simplifications to Eq. 174 can be made with negligible effect on the results. First, the types of fires which generate significant benefits are most likely to be small, have low intensity, and involve little damage. They are, therefore, not likely to require air tanker activity. Conversely, those fires on which air tanker activity tends to be justified (large size, high intensity, high damage) normally involve negligible benefits. Thus, the benefit term B_p can be eliminated from Eq. 174 without introducing significant error.

Another simplification involves the present value of suppression costs. In the case of long-term decisions such as the establishment of air bases or the purchase of air tankers, the present value of C as defined in Eq. 174 would have to be used. Since the model emphasizes the suppression of individual fires, decisions should be based on short-term or viable costs only.

Fire management agencies do not consider present value when damage is recorded. They generally do not discount damage whose impact will be felt in the future nor do they consider the depreciated value of equipment and capital improvements which are destroyed by fire. They also do not generally consider the effect of substitution, nor do they include losses to noneconomic amenities provided by the wildlands over which a fire burned.

Having noted the weaknesses of the available data, we now state that the determination of theoretically correct economic damage is outside the intended scope of the model. Further, it should be mentioned that in this respect, we are interested in what is, more than what should be. Since fire management agencies have traditionally made their decisions on the basis of the recorded damage, it is appropriate that the model does so also. As a result, a simple damage variable, representing the damage recorded on the individual forest fire report form, is

used in the model instead of the present value of damage. Thus, the objective of the model has been reduced to the simple minimization of C + D.

In this section we will consider the three aspects of fire economics suggested by the preceding objective: suppression cost, damage, and savings (the process of minimization).

1) Suppression Cost

Every fire has a recorded suppression cost associated with it, which reflects what actually occurred in the field. This cost cannot be used directly in the model for two reasons. First, the simulated outcome will likely differ from the actual outcome in some respects. Second, the model is simulating "what would have happened if" and a procedure is needed to measure changes in suppression costs resulting from changes in suppression tactics. Therefore, the recorded suppression cost was used to derive a set of regression equations which are, in turn, used to estimate the ground suppression cost of each fire. Cost data for those fires where air tankers were used in the field (1% of all fires) were eliminated from the sample.

In general, within a fuel type (Fnb), suppression cost is related to the quantity of resources employed (estimated by Lc and M) and the duration of the operation (estimated by Tt, Tc, and Tm). In addition, indirect information can be obtained by estimating the amount of work accomplished (related to A and Iw).

From a large set of variables and variable combinations, the following six variables were selected for the regression procedure, based on correlation with suppression cost (Cs).

A = fire area (ac.)
Iw = fire weather index
Lc = rate of line construction (ft./hr.)
M = rate of mop-up (ac./hr.)
Tc = time required to control the fire (hr.)
Tm = time required to mop-up the fire (hr.)

Using the same procedures as for mop-up, the following equations were derived for suppression cost.

$$Fnb = 0$$

$$(175) \quad Cs = - 32.41 + 12.34 Tm + 0.3151 (Tc Lc) - 0.1947 (Tc + Tt) Lc$$

$$Fnb = 1$$

(176) $C_s = - 89.63 + 219.7 T_t + 16.05 \sqrt{T_m} + 3.366 I_w$

$F_{nb} = 2$

(177) $C_s = - 47.88 + 0.627 (T_c L_c) + 0.114 T_m^2 + 88.96 T_c - 2.46 (T_c + T_t)^2$

$F_{nb} = 3$

(178) $C_s = - 28.41 + 22.78 (T_c + T_t) + 4.290 T_m + 0.0280 (T_c L_c)$

$F_{nb} = 4$

(179) $C_s = - 37.29 + 86.85 T_c - 1.992 (T_c + T_t)^2 + 0.0094 T_m^2$

$F_{nb} = 5$

(180) $C_s = - 37.42 + 9.04 T_m + 0.0614 (T_c L_c)$

$F_{nb} = 6$

(181) $C_s = 25.77 + 4.297 T_m + 19.37 (T_c + T_t)$

$F_{nb} = 7, 8$

(182) $C_s = - 21.29 + 102.4 T_t + 2.084 (T_c + T_t)^2 + 4.154 I_w$

$F_{nb} = 9$

(183) $C_s = - 97.02 + 1.172 (T_m M) + 0.0659 T_m^2 - 1.245 (T_c + T_t)^2$
 $+ 137.6 T_c + 0.0802 A^2$

$F_{nb} = 10$

(184) $C_s = - 81.34 + 0.502 (T_c L_c) - 0.171 (T_c + T_t) L_c - 0.005 A^2$
 $+ 0.0114 T_m^2$

Fnb = 11

$$(185) \quad C_s = 12.57 + 0.0474 A^2 + 0.112 (T_c L_c)$$

Fnb = 12

$$(186) \quad C_s = - 2.553 + 0.0359 T_m^2 + 5.511 (T_c + T_t)^2 + 0.0113 (T_c T_t) L_c \\ + 2.412 I_w$$

All fuel types

$$(187) \quad C_s = - 145.8 + 9.259 T_m + 0.1499 (T_c L_c) - 0.0618 (T_c + T_t) L_c \\ + 3.957 I_w - 0.2675 (T_c + T_t)^2 + 30.70 T_c$$

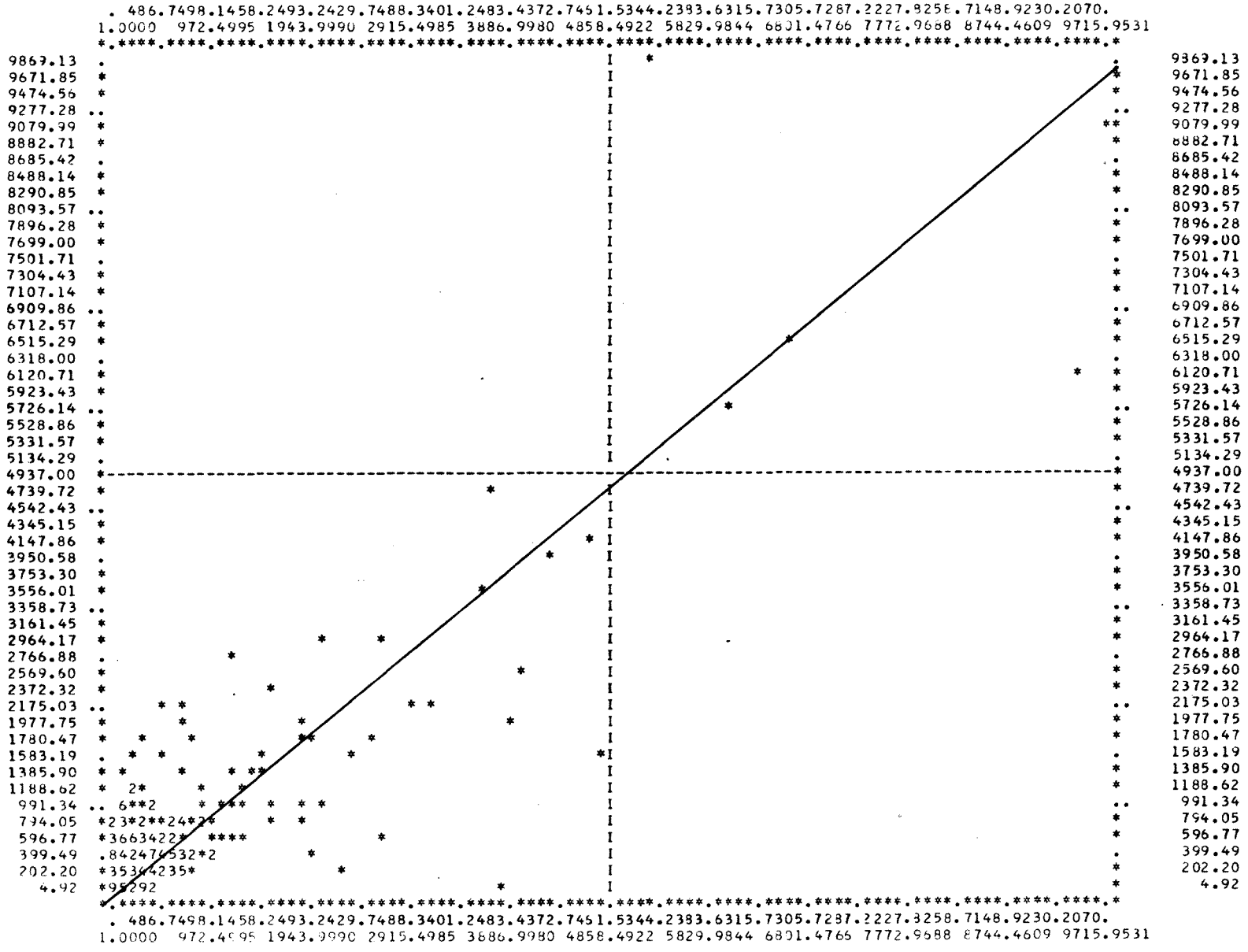
Statistics associated with Eqs. 175-187 are shown in Table 5. As was the case for the mop-up equations, the use of individual equations for each fuel type resulted in a significant reduction in the relative standard error of the estimate (40%) relative to the use of an overall equation. As a result, the individual equations were used in the model. Actual versus calculated values for C_s are plotted in Figure 15.

Due to the relative importance of the cost component, a reasonable effort was expended in an attempt to derive a good set of equations. A result of the fact that the input data are of questionable quality and the variables available for analysis are aggregations of the actual determinants of suppression cost (man-hours, equipment rental, etc.), the cost equations are less accurate than desired. It was hoped that they would have been sufficiently accurate to permit conclusions to be drawn on the basis of the outcome of individual fires. With an average relative error of approximately 120%, this is clearly not possible. As a result, it was necessary, as part of the calibration procedure (to be discussed in a subsequent report) to derive a relationship between sample size and the relative difference required for statistical significance.

Table 5 Statistics for cost regression equations

<u>Fnb</u>	<u>Sample size</u>	<u>C̄s</u>	<u>R²</u>	<u>STD. ERR.</u>	<u>SE C̄s</u>
1	122	323.	.72	452	1.40
2	25	117.	.45	107	.92
3	48	242.	.84	178	.73
4	153	155.	.55	207	1.34
5	30	130.	.84	103	.80
6	90	238.	.85	274	1.15
7,8	51	185.	.57	216	1.16
9	15	119.	.82	56	.47
10	114	388.	.78	668	1.72
11	107	322.	.80	383	1.19
12	83	301.	.73	306	1.01
13	76	131.	.96	87	.67
Weighted average	76	249.	.74	314	1.19
Overall	914	249.	.57	490	1.97

Figure 15. Actual versus calculated suppression cost



The accuracy of these results is comparable to that obtained by Capel and Tesky (1970). They used regression analysis to estimate area burned during suppression, based on a sample of 60 fires in southeastern Manitoba. Their R^2 of 0.71 is comparable with an average R^2 of 0.69 obtained with a similar analysis of 755 fires in the province of New Brunswick.*

While there are other reported uses of regression procedures for the analysis of suppression operations, researchers in the field seem to prefer other analytical techniques. The most common procedure is a simple data summary, accompanied by the use of totals or averages with respect to suppression costs (for example, see Miyagawa and Stashko 1971, Gamache 1969, and Miller 1968). This is clearly an inferior approach in that individual errors resulting from the use of simple averages would be far greater than those resulting from the use of regression equations. While over one or more seasons, the results would likely be comparable with either procedure, the intent of considering individual fires precluded the use of simple cost averages in the model.

The most accurate approach would have been to use data such as man-hours, hours of equipment rental, etc., as these are the components from which total suppression cost is derived. Unfortunately, such desirable data were not available.

Another desirable procedure which might have been considered was adapting the observed cost data directly into the model as was done with rate of line construction and rate of perimeter growth. These two variables have the dual advantage of being constant for all combinations of air tanker tactics tested as well as linearity with respect to time. The unit of measurement (ft./hr.) is independent of results generated by the model. Dollars per acre (or foot of perimeter) or dollars per hour spent in controlling the fire are specific to a particular fire size and control time. Change the size of the fire or the control time (which is the purpose of the model) and the unit cost will change also. Further, examination of the regression equations clearly indicates that no single variable dominates the first selection. This suggests that even if a nonlinear unit cost function had been developed, it would have been inferior to the regression equations. In retrospect, the unavoidable conclusion is that the results obtained herein are probably as good as is possible under the circumstances. With the use of small samples rather than individual fires, the results are adequate to permit an analysis of air tanker operations.

As was the case for mop-up, a limit ($Iw \leq 40$) is required to prevent significantly inconsistent results. In addition, a number of limits were placed on allowable values of Cs.

* Part of earlier work on perimeter growth during suppression reported by Simard et al. (1973).

- $C_s \geq 10$
- if $C_s \geq 200$ and $C_s/A > 200$; $C_s = \max (50, 200 A)$
- if $500 < A < 5,000$; $C_s \leq 50 A$
- if $A \geq 5,000$; $C_s \leq 20 A$

With the exception of $C_s \geq 10$, all the limits combined affect an estimated 1% of the fires. In the case of $C_s \geq 10$, the fires are of no consequence with respect to air tanker operations.

2) Damage

a) Forest damage

As was the case for suppression cost, a set of regression equations was developed for calculating damage to the forest resource caused by a fire. All the arguments considered under cost apply equally to damage. Since a repetition will serve no useful purpose, we will simply discuss the equations.

Forest damage, as recorded on the individual fire report forms, is basically a function of four variables:

- area burned (the total amount of resource subject to damage);
- fire intensity (the ability of a fire to cause damage);
- value-at-risk (how much is the resource worth); and
- damage potential (how well the forest resource can resist damage by fire).

Area burned (A) is available directly from the model. While intensity is available in the model, it is not available on the fire report forms. Therefore, indirect estimates using I_w , I_s , and I_a had to be made. Value-at-risk and damage potential can, to a large extent, be accounted for by stratifying the sample into various fuel types. Finally, some information of value to damage estimation can be obtained by using various suppression variables (C_s , L_c , T_c , T_m). These variables reflect the relative importance placed on the fire by management. The effort they were willing to expend in suppressing the fire should be related to the anticipated damage. In another sense, the suppression variables also reflect difficulty of control and, thus, indirectly fire intensity. Note that the sample is stratified by fuel type, which, to some extent, eliminates the effect of resistance to control. Only fires with a recorded forest damage greater than zero (25% of all fires) were included in the analysis.

The following equations were derived for estimating forest damage (Df).

$$Fnb = 0$$

$$(188) \quad Df = - 10.23 + 8.61 A + 0.0221 Tm + 2.327 Is + 0.0174 Cs$$

$$Fnb = 1$$

$$(189) \quad Df = - 4.793 + 3.016 A + 0.1034 Cs$$

$$Fnb = 2$$

$$(190) \quad Df = - 10.47 + 11.31 A - 1.679 Tc + 42.09 Is - 19.37 Iw$$

$$Fnb = 3$$

$$(191) \quad Df = 9.727 + 11.31 A - 0.1380 Lc + 9.080 Is + 20.86 Tc - 1.590 Tm$$

$$Fnb = 4$$

$$(192) \quad Df = 1.932 + 12.00 A - 0.2363 Cs + 0.4905 Tm + 1.343 Tc$$

$$Fnb = 5$$

$$(193) \quad Df = 2.276 + 0.9096 A + 0.0743 Cs - 0.0294 Lc$$

$$Fnb = 6$$

$$(194) \quad Df = 6.01 + 0.2132 Cs + 1.872 A - 6.179 Tc$$

$$Fnb = 7, 8$$

$$(195) \quad Df = - 2.489 + 9.264 A$$

Fnb = 9

(196) $Df = - 21.71 + 13.22 A + 0.0415 Cs + 2.137 Tc$

Fnb = 10

(197) $Df = 5.357 + 11.14 A - 19.90 Tc + 1.019 Tm$

Fnb = 11

(198) $Df = - 1.123 + 4.1016 A + 0.065 Cs + 4.249 Tc - 0.7986 Ia$

Fnb = 12

(199) $Df = - 1.2182 + 5.603 Iw$

All fuel types

(200) $Df = - 0.2598 + 10.78 A - 0.0412 Lc + 0.0337 Cs + 1.045 Iw$

Statistics associated with Eqs. 188-200 are shown in Table 7. As in previous cases, the fuel type equations yielded superior results relative to the overall equation, with the exception of Fnb = 13. No reason could be found for the unusually poor results for this fuel type. For the remaining fuel types, although the average and overall R² were comparable, the average relative standard error was reduced by 33% by using the set of equations for specific fuel types. The damage equations appear to be slightly more accurate than the cost equations. The average R² for damage is 15% higher than for cost, while the relating standard error for the former is a corresponding 15% less. This is likely a combination of two factors. First, there is a relatively high correlation between damage and a single variable - fire area for all fuel types but one. This, in turn, suggests that the recorded figure may simply be a constant multiplied by area burned. Second, a one-third smaller sample size no doubt partially influenced the improved R² values.

Actual versus calculated damage is plotted in Fig. 16. Again, assuming a y intercept of 0 and a slope of 1 appears to be reasonable, based on visual examination. As previously, some

limits were required with respect to the input data for damage equations: $I_w \leq 40$; $I_s \leq 25$; and $I_a \leq 100$.

Finally, limits were imposed on the range of damage values such that:

- $D_s \geq 0$, and
- if $D_s > 100$ and $A \leq 1$, $DS = \max (20, 100 A)$.

b) Nonforest damage

Nonforest damage includes such things as destruction of buildings, capital improvements, and equipment by fire. This type of damage is highly significant, in that when it is recorded on the fire report forms, it generally overshadows the forest damage associated with the same fire. On the other hand, its occurrence is stochastic, tending towards only two possible mutually exclusive outcomes - there either was or was not significant nonforest value on the fire site damaged by fire. In other words, there either was or was not a cottage, or bridge, or vehicle damaged by fire.

Table 6. Summary of Damage

	Percent of fires	Average	Total
Forest damage	25%	\$ 311.	\$ 236,400.
Equipment damage	2%	\$ 174.	\$ 11,800.
Nonforest damage	15%	\$ 3289.	\$ 1,516,400.

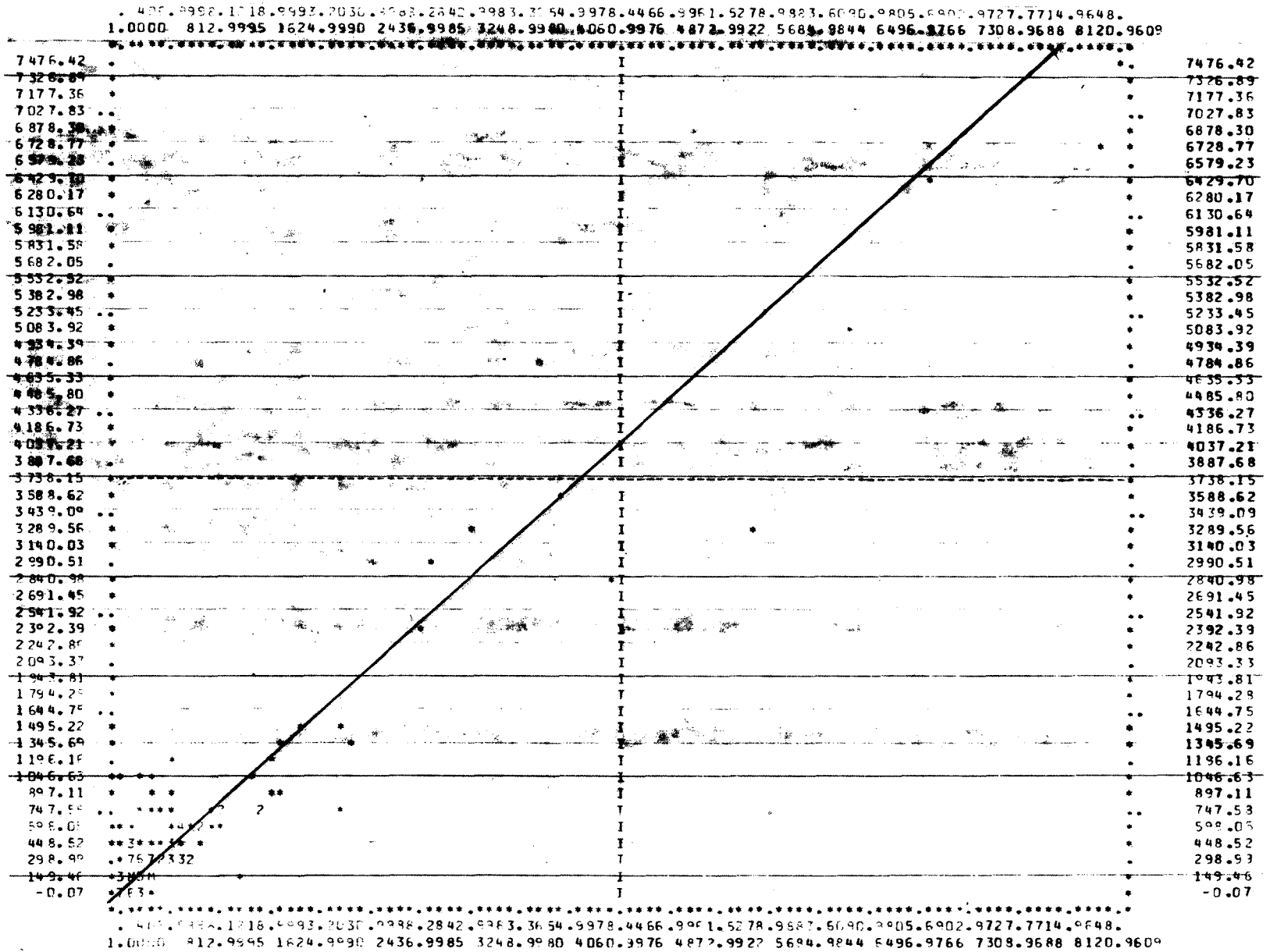
Table 6 summarizes the recorded damage data. While only 25% of all fires had recorded forest damage, the occurrence as well as the relative amount of damage was related to various fire and suppression variables as discussed in the preceding section. Conversely, only 2% of all fires resulted in equipment damage, while nonforest damage was recorded on only 15% of all fires. In neither of these cases was it possible to relate the occurrence or the amount of damage to any of the available fire or suppression variables. Equipment damage was relatively small (0.7% of the total damage) and could have been ignored. The nonforest damage (86% of the total damage) could hardly be ignored.

The only solution available was to use the recorded damage and equipment lost information as input to the model. While this precludes use of the model for predictive purposes, with respect to nonforest damage, it does permit the analysis of historical data.

Table 7 Statistics for forest damage regression equations

<u>Fnb</u>	<u>Sample size</u>	<u>Df</u>	<u>R²</u>	<u>STD. ERR.</u>	<u>SF Df</u>
1	106	95.	.89	78.	.82
2	13	31.	.84	21.	.68
3	44	101.	.86	121.	1.19
4	112	175.	.95	196.	1.12
5	16	86.	.99	11.	.13
6	77	81.	.98	42.	.52
7,8	24	51.	.65	79.	1.55
9	11	131.	.99	26.	.20
10	99	152.	.87	177.	1.17
11	86	119.	.98	113.	.95
12	53	71.	.82	73.	1.03
13	36	67.	.23	171.	2.57
Weighted average	56	112.	.87	116.	1.03
Overall	677	112.	.88	173.	1.54

Figure 16. Actual versus calculated forest damage



To conclude, total ground suppression cost (Cg) is:

$$(201) \quad C_g = C_s + D_e$$

where: D_e = equipment damage.

Total damage (D) is:

$$(202) \quad D = D_f + D_n$$

where: D_n = nonforest damage.

Cost-plus-loss for ground suppression only (Clg) is:

$$(203) \quad C_{lg} = C_g + D.$$

3) Savings

Relative cost-plus-loss savings is the basic criteria used to measure and evaluate air tanker system output. Almost all decisions with respect to selecting various combinations of air tanker resources and tactics are based on cost-plus-loss savings. While savings of area burned as well as suppression and mop-up time are also accumulated, they are used only to provide supplementary information. The model was developed in such a way, however, that with minimal programing changes, it would be possible to substitute either area or time for dollar savings, as long as a constraint was included.

There are two categories of savings calculated by the model: the maximum possible and the actual.

a) Maximum possible savings

If the model processed 2,185 air tanker resource and tactic combinations for each fire, it obviously could not be run on more than a very limited set of data. Further, the vast majority of trials would provide no useful information. Therefore, the model must be able to separate, on the basis of nominal calculations, those fires warranting a detailed examination from those on which the use of air tankers is clearly not justified. The use of maximum possible savings provides the necessary information to permit such a stratification.

The maximum possible savings for air tankers is the difference between the simulated cost-plus-loss for unaided ground forces and the cost-plus-loss that would be associated with immediately stopping fire growth at the time of detection. Calculating the potential minimum cost-plus-loss is relatively straightforward. First, the potential minimum time to control (T_{cp}) is calculated by dividing the perimeter, at the time of detection, by the observed rate of line construction:

$$(204) \quad T_{cp} = \frac{P_d}{L_c}$$

The potential minimum fire area is actually the area at detection (A_d), which is substituted for A in Eqs. 161-173 to estimate the potential minimum mop-up time (T_{mp}). Then, A, T_{cp}, and T_{mp} are appropriately substituted in Eqs. 175-187 and the potential minimum cost (C_{sp}) is determined. Finally, all four variables are used in Eqs. 188-200 to obtain the potential minimum forest damage (D_{fp}).

An additional step is required to determine the potential cost-plus-loss. The potential reduction in equipment lost and nonforest damage has to be determined. This is accomplished by first assuming that the nonforest value-at-risk is located entirely within a very small portion of the fire area. This assumption will be correct for most nonforest values of interest (cottages, vehicles, bridges, etc.). The area containing the value was assumed to be 0.03 acres, or about 1,300 square feet, a reasonable size for a cottage including the immediate surrounding area.

Another assumption was made - that the high value area was equally likely to be located anywhere within the fire area. It was further assumed that the value would be totally destroyed if the fire reached the high-value area, and undamaged if the fire was prevented from reaching the high-value area. The expected maximum relative saving (S_e) was therefore simply the ratio of the area at detection to the total area:

$$(205) \quad S_e = \frac{A_d + 0.03}{A} \quad ; \quad S_e \leq 1.$$

In other words if the area at detection was 75% of the total area, it is assumed that there was a 25% probability that nonforest damage did not occur. The use of 0.03 in the numerator prevents a reduction in damage when the total area burned is less than an assumed minimum size of a typical high-value area.

The potential minimum cost-plus-loss (C_{lp}) is therefore:

(206) $Clp = Csp + Dfp + Se (De + Dn).$

The maximum possible dollar saving (Sp) is:

(207) $Sp = Clg - Clp.$

The use of Sp will be discussed under the air tanker component. Similarly, the maximum possible area saving (Sap) is:

(208) $Sap = A - Ad.$

The maximum possible control and mop-up time saving (Stp) is:

(209) $Stp = Tc - Tcp + Tm - Tmp.$

b) Actual savings

Determining the actual⁹ saving achieved with air tankers is relatively straightforward. Similarly to the maximum possible savings, the area burned (Aa) and time to control (Tca) resulting from the use of air tankers to augment ground forces are substituted in Eqs. 161-200 to obtain mop-up time with air tankers (Tma), ground cost with air tankers (Csa), and forest damage with air tankers (Dfa). Aa is substituted for A in Eq. 205 to obtain Se. The total cost-plus-loss with air tankers (Cla) is therefore:

(210) $Cla = Csa + Dfa + Se (De + Dn) + Ca$

where: Ca = air tanker cost (to be discussed under the air tanker component).

(211) $S = Clg - Cla.$

Area burned saving (Sa) is:

(212) $Sa = A - Aa.$

⁹ As determined by the simulation model.

Finally, the saving in the time to control and mop-up the fire (St) is:

$$(213) \quad St = Tc - Tca.$$

Since the use of air tankers augments ground forces, Sa and St will always be positive, unless a fire is controlled before the first drop. S, on the other hand, may be either positive or negative, depending on whether Cla is less than or greater than Clg. Clearly, negative savings represent an increased cost-plus-loss and any air tanker combination which generates such a net loss should not be employed.

The description of the ground suppression component of the model is now complete. Although we have considered a total of 79 equations, only 42 are used for a particular fire, making this component comparable in magnitude to the fire component. Again, taken individually, the equations are relatively simple. Even collectively, they represent a significant simplification of a real-world ground suppression system.

All suppression activities (men, bulldozers, ground tankers, etc.) have been grouped into a single variable - Lc. In retrospect, it is perhaps a blessing that the available data did not permit a more detailed breakdown of the ground suppression operation. In the initial stages of model development, a finer scale was considered for ground suppression. As the complexity of the task became apparent, the amount of ground suppression detail required to analyze an air tanker system was considered. It was concluded that aggregating all ground activity under a single variable was adequate. Had that decision not been made, it is likely that an additional 12-18 months would have been spent in developing a larger more complex model than is described here. While such development may be undertaken in the future, as the current research effort expands its horizons, we will content ourselves with solving one problem at a time. To this end, the discussion now proceeds to the final component of the model, in which the core of the original problem is considered - simulation of the use of air tankers in wildland fire suppression.

6. Air Tanker Utilization

To this point, the reader has been subjected to a lengthy description of the environment within which air tankers operate. As a storyteller enriches his plot with a comprehensive background, it is hoped that the reader's understanding of a complex system will be enhanced by the approach taken here. As the last, largest, and most important piece falls into place, the rationale behind the preceding model development should become evident. No matter that the pieces may have seemed somewhat disjointed at the time; they have all been intended to serve some purpose in the analysis of the use of air tankers for fire control.

As would be expected, the air tanker component of the model is more detailed than its predecessors. While, by itself, the air tanker component constitutes only 34% of the entire model, it is considerably larger than any other single component (on the basis of the amount of programming). Of the remaining 66%, 24% is concerned with administration and tabulation, while the three technical components average about 14% each.

Air tanker utilization is divided into several subcomponents: selecting resources and tactics, delivering the retardant, dropping the retardant, air tanker suppression, and costs. Each will be discussed in this section.

A. Selecting Resources and Tactics

In the real world, when a fire is detected, the dispatcher makes an immediate decision on the mixture of initial attack forces to dispatch. His decision is based partly on knowledge, partly on intuition and experience, and partly on guesswork. While he can reduce the uncertainties by obtaining additional information, the knowledge gained could extract a very high price if a fire escapes due to the lost time. On the other hand, uncertainties can also increase costs, in that if unneeded suppression resources are dispatched, they must be paid for.

Air tankers, because of their speed, allow more flexibility in dispatch delays than ground forces. Their high cost, on the other hand, results in greater penalties when aircraft are dispatched unnecessarily. In either case, effectiveness can only be maximized when the correct dispatch decision is made immediately at the time of detection. There are about a dozen significant factors to consider when making a dispatch decision with respect to air tankers. Since the human mind normally has difficulty in coping with more than three variables simultaneously, preattack dispatch plans are often prepared to aid the decision maker. In these plans, many of the details concerning possible outcomes have already been considered so that

the dispatcher need concern himself with only one or two significant points with respect to each fire. Clearly, such an approach simplifies the dispatch procedure and reduces the potential for an erroneous decision.

Given the importance of the initial attack decision, it seemed worthwhile to examine this aspect of air tanker use in some detail. To do so required a model formulation which was not dependent on a preplanned dispatch procedure. Rather, a formulation was required that aided in developing dispatch guides. The only totally independent simulation procedure is simple enumeration. That is, dispatch all possible combinations of resources to the fire and employ all possible combinations of tactics. Then, in hindsight, select that combination which minimizes the cost-plus-loss. With a limited number of combinations to test, this is a feasible, if not an elegant technique.

In response to this requirement, the simulation model dispatches several air tanker models, from one to ten aircraft, tests three retardants, and fights each flank of the fire separately. In all, there are 2,184 possible air tanker resource and tactic combinations which could be tested on each fire, in addition to unaided ground suppression (26 models, 7 numbers of aircraft, 3 retardants, and 4 flanks). Note that missions involving 5, 7, and 9 aircraft are not tested by the model. While this set is finite, it hardly qualifies as limited. Thus, for all but small sample sizes it is not practical. In fact, 60 hours of computer time would be required to process the 6.5 million trials required with a sample of 3,000 fires. Further reductions are clearly required.

There are two approaches to reducing the number of trials: eliminate those which could not possibly improve the solution (further reduce the cost-plus-loss) and eliminate those where the improvement to the solution is likely to be insignificant. In both cases, the value of the information provided by the trial will most likely be less than the cost of computation. Both approaches are used in the selection procedure. The resource and tactic selection routine incorporate a series of preliminary tests. If a proposed trial fails any test, it indicates that one of the preceding two conditions prevails and the trial is skipped.

1) Air Tanker Model

Clearly, any resource combination, having a single drop delivery cost greater than the maximum possible savings (S_p), as calculated in Eq. 207, could not possibly reduce the cost-plus-loss for the fire. Thus, the first two preliminary tests are:

(214) if $Sp \leq Cc + Ct$ or

(215) if $Sp \leq Cf_1 + Cc + Ct$

where: Cc = circuit cost (land, load, takeoff, drop),
 Ct = initial takeoff and final landing cost,
and
 Cf_1 = round trip fire-to-base flying cost.

If either Eq. 214 or 215 holds, the model is not tested. Procedures for calculating the various delivery costs will be discussed subsequently. The sum in Eq. 215 represents the delivery cost of a single drop.

A two-step procedure is used to reduce unnecessary computation. The circuit and takeoff cost are readily determined by simple calculations. The flying cost, in contrast, requires determining the distance between the air base and the fire, a somewhat involved procedure. A significant amount of computation is eliminated for those fires which fail to pass the first test.

Each time one of the pair of tests is failed, a minimum of 84 combinations are eliminated from consideration (1 model, 7 additional air tankers, 3 retardants, and 4 flanks). The effectiveness of these tests is further increased by processing the models in a predetermined order: small, medium, and large. In this way, if a small air tanker fails the test, there is nothing to be gained by analyzing a medium or large air tanker, as the cost of a single drop will be even greater. The routine, therefore, eliminates all larger models for the same type of operation (water, land, and helicopter) from further consideration.

A third test is applied to the new air tanker model being considered to further reduce the number of superfluous trials. Each of the models is classed into one of nine types, which combine the size and mode of operation of the aircraft (small, medium, or large; and land, water, or helicopter). Within each type, the generally most effective model is chosen as primary and the rest are classed as secondary. The analysis begins with the primary model. If it fails to pass the preceding tests, or if it passes the tests, but generates a net loss, all secondary models of the same type are eliminated from further consideration. Unlike the previous two tests, this one is not absolute. On one hand, it is conceivable that a superior solution might be eliminated. On the other hand, savings generated by secondary

models, when the primary model generates a loss, are not likely to be significant.

The effectiveness of the first three tests can be demonstrated by noting that in a production run on 3,010 fires, a new model could have been chosen 78,260 times (26 models in the sample). In fact, a new model passed all three tests on only 11,405 trials or only 14.6% of the possible number of times. The 60 hours of computer time has already been reduced to 8.7 hours.

2) Number of Air Tankers

There are no tests applied to the first air tanker as the minimum costs are identical to those in the model test sequence. The minimum delivery cost for one aircraft (C1) is calculated, however, for subsequent use:

$$(216) \quad C1 = Cf_1 + Cc + Ct.$$

The first test for the number of air tankers is applied when two or more are being considered. First, the delivery cost for one drop from each air tanker (Cn) is calculated:

$$(217) \quad Cn = Na (Cf_1 + Cc + Ct) + Cbh (Bf + Tcx_{m,j})$$

where: Na = number of air tankers,
 Cbh = birddog cost per hour,
 Bf = birddog fire-to-base round trip flying
 time,
 Tcx = circuit time,
 m = air tanker model, and
 j = mode of operation.

In the model, it is assumed that one air tanker will work alone, while two or more will always be under the direction of a birddog officer. Hence, the expected minimum birddog cost is included in the calculation. It is further assumed that each air tanker dispatched will make a minimum of one drop. If this were not the case, there would be little sense in incrementing the number of aircraft.

The condition $Sp \leq Cn$ indicates that the minimum delivery cost exceeds the maximum possible savings and further analysis of this and all greater numbers of air tankers is eliminated. This test is conceptually the same as that applied in Eq. 215, except that more aircraft have been added.

A marginal test with respect to the number of air tankers dispatched is added when the third or subsequent aircraft is being considered. If, at this point, at least two number combinations have been tested previously, it is possible to determine the direction in which the sequence of results is progressing. That is, the cost-plus-loss is either increasing or decreasing, as the number of aircraft increases. If $S_n \geq S_{(n-1)}$, the results are improving and further testing continues.

If the above does not hold, a second test is made to determine if the loss is less than the birddog portion of the increased air tanker cost. If such is the case, it is possible that the marginal benefit of an additional air tanker might exceed the marginal cost by a sufficient amount that an overall reduction in the cost-plus-loss will result. The reasoning can best be explained with the aid of an example, such as three drops being made by two aircraft. Since the birddog aircraft is not employed for one air tanker, its entire cost becomes part of the marginal cost of the second air tanker. Further, the birddog has to circle the fire while one air tanker returns to the base for the third load. Adding a third air tanker decreases the final fire size, and hence ground suppression costs and losses. It also decreases the birddog cost, because the aircraft does not have to wait for the third drop.

Further, in the case of two air tankers, the entire birddog cost was offset by the increased effectiveness of only one aircraft. In the case of three air tankers, the birddog cost can be balanced against the marginal effectiveness of two aircraft. While the preceding case is the most obvious, it is possible to develop similar arguments for any combination of air tankers and number of drops. As a result, while cost-plus-loss may have increased as the result of adding one air tanker, it might decrease by adding another.

First, the birddog portion of the air tanker cost (C_b) is calculated:

$$(218) \quad k = \min(N_a - 2, 2) \text{ and}$$

$$(219) \quad C_b = C_{bh} (T_{fx_k} + T_{cx_{m,j}} - T_{lx_{m,j}})$$

where: T_{fx} = flying time,
 T_{cx} = circuit time,
 T_{lx} = loading time,
 k = flying segment (fire-to-base, fire-to-retardant),

m = air tanker model, and
j = type of operation.

Equation 219 multiplies hourly cost by the length of time flown. The significance of Eq. 218 is that when the third air tanker is being considered, the fire-to-base flying time is used to calculate the marginal birddog cost. When the fourth or subsequent air tanker is being considered, only the round trip time to the nearest retardant base is used. The marginal test thus becomes:

$$(220) \quad \text{if } S_{n-1} - S_n < C_b,$$

continue with the proposed number of air tankers. If Eq. 220 does not hold, skip to the next model.

Given the 11,405 trials where the model tests were passed, there were 79,835 possible numbers of air tankers that could have been considered (7 numbers each). Of this, only 24,900 trials or 31.2% passed the number tests. At this point, only 4.5% of the original total remains (14.6% x 31.2%) and the total computer time required would be about 2.7 hours.

3) Retardant

Since savings attributable to one retardant are not directly related to savings attributable to another retardant, each must be considered independently, as was the case for air tanker models. Therefore, only a simple absolute test is possible here. First, the minimum cost, including the retardant (C_r) is:

$$(221) \quad C_r = C_n + N_a C_{r\ell_r}$$

where: $C_{r\ell_r}$ = retardant cost per load and
 r = retardant.

If $S_p \leq C_r$, the proposed retardant is skipped. Of the 74,700 possible combinations that could have been tested at this point (24,900 additional aircraft x 3 retardants), 54,284 (73.6%) passed this test. This further reduced the overall total to 3.3% of the original or just under 2 hours of computer time.

4) Location of Attack

Since a single drop may be adequate to contain a flank, an absolute test for location of attack would have to use C_r . Thus, the only useful test at this point is a marginal one, which can

only be made after at least two flanks have been attacked. If $Sfx \geq S(f-1)x$ (the cost-plus-loss after attacking the second flank is less than after attacking the previous flank), then further testing continues.

Of 217,136 possible trials (54,284 x 4 flanks), only 93,835 passed this test (43.2%). The overall total is now only 1.4% of the maximum possible number of trials. Total computer time required at this point would be 0.8 hours.

5) Final Tests

All tests to this point have assumed one drop per aircraft. There is additional information available at the time of dispatch which will allow even finer testing.

$$(222) \quad \text{If } (Na \text{ Ph}_{n+1}) \geq P \quad ; \quad Na > 3,$$

(at least three air tankers have been tested, and the total length of line held for the number being considered (Ph) exceeds the length of perimeter (P)), skip the proposed trial. In this case, the program actually returns to test additional air tankers to cover the possibility that with the use of water, the length of line held for a greater number of aircraft may be shorter than for the current number with retardants.

$$(223) \quad \text{If: } Rhw \geq Rhr \quad ; \quad r \geq 2,$$

(either short-term or long-term retardants are being considered and the length of line held per drop for the current retardant is not greater than that for water), skip the proposed retardant. This may occur when minimum retardant depths are involved, or may be caused by rounding, as classes are used rather than actual depths.

Finally, if $Rh \leq 0$ (rate of line holding not greater than zero); or if $Rh \leq Ga$ (rate of line holding not greater than rate of arc growth), skip the proposed trial.

The preceding tests incorporate behavioral characteristics of the specific fire being analyzed. If the four tests are passed, a worthwhile combination is indicated. One last test is performed before allowing the simulation sequence to proceed. The minimum number of drops needed to control the flank (Ndm) is calculated:

$$(224) \quad Ndm = Nd + \frac{Ab}{Phd \cdot N!l} + 1$$

where: N_d = number of drops made (if any) on previous flanks,
 Ph_d = length of perimeter held per drop, and
 N_{d1} = number of drops per load.

Equation 224 essentially divides the free-burning arc length by the length of line held per drop. Note that more than one drop may be made with a single load. If the second or subsequent flank is being considered, N_d accounts for the drops made on previous flanks. N_{dm} is rounded up to the next nearest whole number by adding 1. If $N_{dm} > N_a$, the minimum delivery cost is calculated for a final test:

$$(225) \quad C_{dm} = C_r + (N_{dm} - N_a) (C_{rl} + C_{f_2} + C_c)$$

where: C_{dm} = minimum cost of delivery and
 C_{f_2} = round trip fire-to-retardant flying cost.

Essentially, Eq. 225 adds the cost of those drops needed to complete the minimum mission in excess of one drop per air tanker. Finally, if $S_p \leq C_{dm}$, the trial is skipped. This last series of tests reduced the number of trials by another 22.4% (72,859 trials processed out of 93,825 potential trials at the start of the series). The overall total number of trials has been reduced to only 1.1% of the total possible number. In terms of computer time, the requirements have been reduced from 60 hours to 0.7 hours.

Once a potential combination of resources and tactics passes all of the preliminary tests, the simulation model uses it to help suppress the fire. The manner in which this is done will be considered in subsequent sections.

B. Retardant Delivery

The first function to be performed by the air tanker system is to deliver retardants to the fire. In the model, two aspects of the delivery system are of interest: the time required and the delivery cost. In this section, we will concentrate on determining the various times of interest, while costs will be considered subsequently.

There are three times associated with retardant delivery: circuit time, flying time, and the time interval between drops.

1) Circuit Times

There is a set of activities associated with each drop that is not related to flying distances or number of air tankers.

They are a function of the individual aircraft and the mode of operation. These times only need to be calculated once at the start of a run, as they do not change regardless of the operating environment. The four components of circuit time are: takeoff time, landing time, retardant loading time, and drop time. Two different times are possible for some of these activities, depending on whether a land-based or water-based operation is used.

Loading time is the simplest of the four activities. For land-based operations, a retardant loading rate of 250 Imperial gallons per minute (15,000 Imp. Gal./hr.) is assumed. The land-based loading time is therefore:

$$(226) \quad T_{lx_{m,1}} = \frac{Q_{a_m}}{15,000}$$

where: T_{lx} = retardant loading time,
 Q_a = retardant tank capacity,
 m = air tanker model, and
 1 = landbased operation.

For water-based operations and helicopters, a loading time of 10 seconds is assumed (0.003 hr.).

The time for the remaining three activities is based on several variables which are interrelated through a complex set of processes. A mechanistic determination of the expected time for each model is well beyond the scope of this project. Ideally, empirical observations for each air tanker being tested should be obtained and incorporated into the model. Such data are, unfortunately, not available nor was it considered worthwhile to conduct extensive field testing to obtain them. Since differences of less than a minute are relatively insignificant in the model, and since the average amount of time for each activity does not exceed five minutes, an estimate of the times involved was considered sufficient.

The estimated times are based on two variables: an average for all air tankers and the variation about that average associated with each model. A set of average times is based on the field work of Maloney (1972) and personal observation by the authors. These are listed in Table 8.

The times shown in Table 8 vary from one air tanker model to another. In general, smaller, lighter, more maneuverable aircraft will be able to perform the activities more quickly than large, heavy aircraft. It was decided, therefore, that each model would be related to the overall average through the use of a maneuverability variable.

Table 8. Average times for selected air tanker activities (minutes)

	Land-based	Water-based	Helicopter
Takeoff	5.0	1.5	0.5
Landing	4.0	1.0	0.5
Drop	1.5	1.5	0.5

Although aircraft maneuverability is the end result of the complex interaction of many characteristics, a relatively simple function was considered sufficient for the present purpose. It seems reasonable that maneuverability should increase as the design load limit of the aircraft increases. It seems equally reasonable that maneuverability should decrease as the weight of the aircraft increases. More precisely, maneuverability decreases as various "loadings" increase. That is as the weight which must be supported by a unit of wing surface area (wing loading) increases, maneuverability should decrease. Similarly, the power loading (weight/horsepower) and control loading (weight/control surface area) also affect the ability to maneuver.

Using information published by Taylor (1938-70), the necessary data for computing air tanker maneuverability were obtained for most of the air tankers used in the study. A variety of other sources were used when the required information was not available from Taylor. These data are listed in Table 9.

To combine the variables listed in Table 9, it was assumed that each factor had equal influence on aircraft maneuverability. Coefficients for each variable were derived such that the sum of the three loadings would be approximately equal to the design load factor, yielding a relative maneuverability (Rm) of 1.0 for the average values. The equation for Rm is therefore:

$$(227) \quad R_m = \frac{30 G}{L_w + 2.5 L_p + 0.33 L_x}$$

where: G = design load factor,
 L_w = wing loading,
 L_p = power loading, and
 L_c = control surface loading.

Table 9 Data used to compute relative maneuverability

Aircraft	Gross Weight (lb)	Wing Loading ^{1/} (lb/ft)	Power Loading (lb/hp)	Control Loading (lb/ft) ²	Design Load Factor (G's)	Relative Maneuverability
A-26	35,000	63.5	10.7	219.1	2.8	.68
AF-2	24,800	44.5	13.9	152.6	2.5	.74
B-17	59,000	33.5	13.9	165.3	2.5	.80
B-25	34,500	55.8	13.1	242.6	2.6	.61
C-119	71,500	50.5	13.9	269.6	2.8	.64
C-130	69,300	88.8	12.8	101.6	2.8	.67
CL-215	43,500	25.4	13.6	91.2	3.25	1.38
DC-6	107,000	66.4	13.0	224.7	2.5	.56
DHC-2-II	5,100	21.5	12.3	64.2	3.5	1.59
DHC-3	8,000	21.4	17.8	40.5	3.5	1.53
DHC-6	8,400	29.8	14.4	58.3	3.5	1.52
F7F	28,000	47.5	6.9	252.5	4.2	1.15
G-164A	4,500	18.5	13.5	68.5	4.7	2.38
JRM3	162,000	42.5	25.0	139.4	2.8	.70
P2V-7	80,000	72.0	13.7	230.0	2.8	.60
PB4Y2	64,000	63.7	18.7	209.0	2.8	.60
PBY5A	30,500	24.3	18.1	119.8	2.7	.95
S2D	6,000	18.4	13.3	74.2	10.0	2.49
S2F	24,500	18.8	11.3	191.4	3.25	1.20
TBM	17,600	36.2	33.8	83.6	3.0	.74
Average	44,200	39.7	15.3	154.0	3.2	

^{1/} Main wing area only.

^{2/} Some "G" values are estimates as there is no published data available.

Values of R_m calculated with Eq. 227 are listed in Table 9. As can be seen, the highest values are for specially designed agricultural aircraft, while transport and patrol aircraft tend to congregate at the low end of the range. World War II fighter and bomber aircraft generally fall in between. Overall, the results produced by Eq. 227 appear to be consistent and in line with what would be expected.

Applying R_m in the model was relatively straightforward. Average values listed in Table 8 were simply divided by R_m . For example, takeoff time for land-based operations was calculated with the equation:

$$(228) \quad T_{ox\ m,1} = \frac{T_{ax\ 1,1}}{60 R_{m\ m}}$$

where: T_{ox} = takeoff time,
 T_{ax} = average air tanker activity time, and
 m = air tanker model.

Similarly, the remaining circuit time variables (both land-based and water-based) were calculated by dividing each average by the appropriate R_m value. The use of 60 in the denominator simply converts the input data (recorded in minutes) to hours.

No attempt was made to rate the relative maneuverability of helicopters, as differences between models were assumed to be negligible. Thus, after converting to hours, the average times listed in Table 8 were used for all helicopters.

Finally, the total circuit time is determined:

$$(229) \quad T_{cx\ m,j} = T_{lx\ m,j} + T_{ox\ m,j} + T_{dx\ m,j} + T_{ly\ m,j}$$

where: T_{dx} = drop time,
 T_{ly} = landing time,
 m = air tanker model, and
 j = type of operation.

2) Flying Time

Flying time is a function of distance and flying speed. Thus, a new set of times must be calculated each time a new model is considered. Two flying times are needed by the model: fire-to-base and fire-to-retardant. The model currently dispatches all aircraft from a single central base. This procedure is in accordance with current operating practices in the province of New Brunswick. It is a reasonable procedure for any administrative area not exceeding 200 miles across. Some

modification to the model will be required when large administrative units with more than one initial attack base are analyzed.

In the case of land-based operations, retardant is assumed to be available at the nearest usable satellite base to the fire. In the case of water-based operations, the nearest usable lake is used.

The flying time equation is:

$$(230) \quad Tfx_k = \frac{2 D_{i_k}}{Sx_m}$$

where: Tfx = round trip flying time,
 Di = distance,
 Sx = flying speed,
 k = fire-to-base ($k=1$),
fire-to-retardant ($k=2$), and
 m = air tanker model.

The birddog fire-to-base flying time (Bf) is also calculated with Eq. 230 by substituting birddog flying speed (190 mph) for Sx .

3) Time Between Drops

The time between drops is the most complex of the delivery times. It is calculated each time a drop is made, by combining various flying and circuit time variables. The form of the combination is a function of several circumstances prevailing at the time of each drop.

a) The first drop

For land-based operations, calculating the time of the first drop is fairly straightforward:

$$(231) \quad Dd = Toi + \frac{Tfx_k + Tdx_{m,l}}{2}$$

where: Dd = drop interval and
 Toi = initial takeoff time.

A constant value of 10 minutes (0.167 hr.) is used for Toi . This incorporates the time required for the pilot to receive his instructions, start and warm up the engines, perform his preflight checks, and load the aircraft (much of which is taking place simultaneously). Since Tfx is the round trip flying time,

it must be divided by two to obtain the required time to reach the drop area. Similarly, it is assumed that the actual drop occurs halfway through the drop cycle (lining up, making the drop, and pulling out).

Water-based operations are somewhat more involved:

$$(232) \quad Dd = T_{oi} + \frac{T_{fx_1} + T_{fx_2} + T_{dx_{m,2}}}{2} + T_{lx_{m,2}} + T_{ox_{m,2}}.$$

The pilot makes his preparations (T_{oi}), the aircraft takes off (T_{ox}), flies to the lake nearest the fire (T_{fx_1}) (assumed to be the same distance from the central base as the fire itself), picks up a load of water (T_{lx}), flies to the fire (T_{fx_2}), and drops the load (T_{dx}). The division by two follows the same reasoning as for Eq. 231.

A final adjustment is made whenever a birddog aircraft is used. The adjustment requires that the first drop not occur until the birddog aircraft arrives:

$$(233) \quad Dd' = \max(Dd, \frac{Bf}{2} + 0.1).$$

The addition of 0.1 hrs. allows time for takeoff and reconnoitering the fire.

b) Subsequent drops

For single aircraft:

$$(234) \quad Dd = T_{cx_{m,j}} + T_{fx_2}.$$

For multiple aircraft, where the number of previous drops is not an even multiple of the number of aircraft dispatched:

$$(235) \quad Dd = \max(T_{lx_{m,j}}, T_{dx_{m,j}}).$$

In other words, if for example, two out of three aircraft have dropped retardant, the only separation between drops is the loading or dropping time, whichever is greater. In the case where the number of previous drops is an even multiple of the number of aircraft:

$$(236) \quad Dd' = T_{cx_{m,j}} + T_{fx_2} - Dd (N_a - 1).$$

If, for example $N_a = 3$, and three (or six, or nine, etc.) drops have been made, the next drop will have to wait until the first aircraft in the group returns from loading retardant. While the second and subsequent air tankers are dropping retardant, the first is already on its way to reload, hence the subtraction in Eq. 236. The value of D_d obtained in Eq. 235 is used as input to Eq. 236.

c) Return to base

Two conditions require that all aircraft return to a base: endurance is about to be exceeded or the occurrence of sunset. The test for aircraft endurance is:

$$(237) \quad \text{if } A_{e_m} - \left(\frac{Tr}{2} + D_d\right) > D_{to}$$

where: A_e = aircraft endurance,
 Tr = round trip flying time to refueling base,
 D_{to} = time since initial takeoff, and
 m = air tanker model,

all aircraft return to base for refueling. Aircraft endurance is one of the aircraft characteristics read in by the model. Tr is equated with the nearest usable airstrip for land-based operations and the central base in the case of water-based operations. Note that the fact that water can be picked up from any lake does not imply that fuel is deliverable to the same location. The subtraction ensures that enough time is left for a complete drop cycle as well as a one-way flight to the base before allowing another drop without refueling. The drop interval then becomes:

$$(238) \quad D_d = Tr + T_{cx_{m,j}}$$

To test for the occurrence of sunset before the next drop is scheduled, the absolute time of the next drop is calculated:

$$(239) \quad E_5' = E_5 + D_d.$$

If $E_5 < E_4$, the drop is scheduled and no further calculations are necessary. If $E_5 > E_4$, the aircraft returns to base to await sunrise on the following day before further drops are made. In this case:

$$(240) \quad D_d = T_{fx_1} + T_{dx_{m,j}} \quad \text{and}$$

$$(241) \quad E_5 = E_3 + \frac{Dd}{2}$$

Note that Dd is used to compute total flying time. It must, therefore, account for the return trip as well as the trip out the next morning. The occurrence of the drop (E_5), on the other hand, will occur after a one-way trip from the base, leaving at sunrise. If no drops have been made before sunset, the first drop is scheduled to follow sunrise the next morning. In this case, Dd as calculated in Eq. 240 is divided by 2 (since the return trip does not have to be accounted for) and the division by 2 in Eq. 241 is eliminated.

We have now calculated the time interval between drops. The next step is to make the drop.

C. RETARDANT DROP

When retardant is dropped on a fire, a volume of liquid is transformed into a length of perimeter held. Relating the output of this transformation to the input is not a simple task. Although this process has been studied in considerable detail, much is still unknown. Despite the incompleteness of the available data, it was decided that field measurements and the generation of new data were outside the scope of this project. The model provides a framework within which the components of the drop subsystem are incorporated. The best currently available information was used in developing the model components. Beyond this, it will be left to others to provide more accurate and complete drop data, if such revisions are deemed necessary.

We will consider the following aspects of the drop subsystem: depth of retardant required, drop patterns, length of line held, and selection of the optimal drop tactic.

1) Depth of Retardant Required

Analysis of the drop subsystem begins with the final phase of the process - putting the fire out. We must determine retardant effectiveness in order to determine the amount required to suppress the fire. From the amount required, it is possible to determine the length of the effective drop pattern, the final objective of the drop subsystem.

The effectiveness of water in direct suppression of low intensity forest fires was determined by Stechishen and Little (1971) for three different fuel beds. The range of variation between the fuel beds was on the order of 25%. As a result of this low variation, coupled with an almost complete lack of data with respect to other fuels, an average effectiveness was used

for all fuels. The slope of the boundary between their zones of extinguishment and reignition is given by:

$$(242) \quad D_r = 0.00036 I$$

where: D_r = depth of retardant (water) applied (in.).

In further studies, they determined that short-term retardants were an average of 40% more effective than water alone.¹⁰ Grove et al. (1962) present data which indicate that with viscous water, 28% less volume is required to suppress a fire. An increased effectiveness of 30% for short-term retardants was used in the model. Thus, the appropriate coefficient in Eq. 242 for short-term retardants would be 0.00027. Stechishen and Little also determined that long-term retardants were an average of 2.4 times more effective than water. These findings indicate that for long-term retardants the appropriate coefficient would be 0.00015.

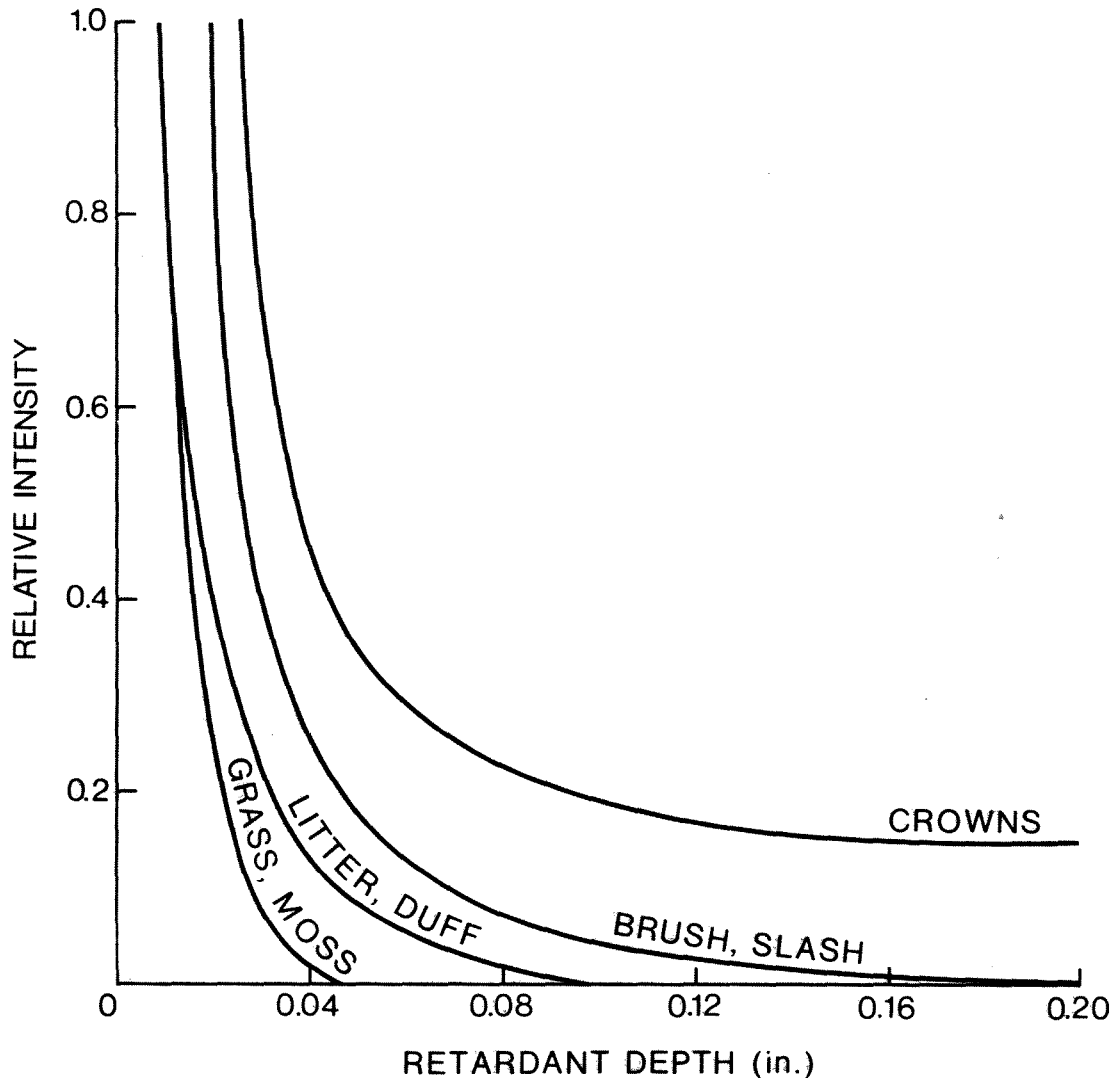
The data provided by Stechishen and Little apply to fires with intensity readings of less than 200 BTU/ft./sec. The upper end of this range is the lower end of the intensity range where air tankers are likely to be used. While they indicate that their data do not suggest any nonlinearity in the function, extrapolation to intensities of 1,000 BTU/ft./sec. would be questionable. Further, at such intensities, the depth of water required (0.36 in.) is beyond the practical capacity of any air tanker flying today.¹¹ Clearly, another approach to retardant effectiveness is required to supplement these data.

Swanson and Helvig (1973) presented the results of a theoretical study of the "cocling" effect of retardants on high intensity fires in four broad categories of fuels. From their information, it was possible to develop a set of curves relating reduced fire intensity after a drop to the predrop intensity, as a function of the quantity of retardant applied, for each of the four fuel categories. The curves for long-term retardant are shown in Fig. 17. Values of retardant effectiveness (E_r) used in the model are obtained directly from these curves. Comparable curves for water and short-term retardants were developed by using the relative values of the coefficients in Eq. 242. Admittedly, this simple relationship ignores the differential shedding of liquids of different densities by convective momentum in high intensity fires. While the phenomenon was recognized by Swanson and Helvig, it remains unquantified. It was, therefore, not incorporated in the model.

¹⁰ Information on file at the Forest Fire Research Institute.

¹¹ While spots may have greater coverage, there is no significant pattern length at such depths.

Figure 17. Percent of original intensity after a long-term retardant drop



Determining the depth of retardant required is relatively simple, given the effectiveness coefficients. Equation 242 with the appropriate coefficient, is used for direct suppression with a single drop. A few limits are imposed.

- The minimum required retardant depth for all fuels but grass is 0.02 inches.
- The required retardant depth for grass is assumed to be one-half of that for other fuels.
- Retardant depth classes rather than actual depth are used in the model. The actual depth is rounded up to the next higher class boundary. Classes are: 0.00, 0.01, 0.02, 0.04, 0.06, 0.08, 0.10, 0.13, 0.16, and 0.20 inches.

Double-drop suppression is handled somewhat differently. Starting at the minimum depth, the post-drop intensity is calculated for each depth:

$$(243) \quad I_r = I E_{r,i,j,k}$$

where: I_r = reduced intensity after a drop,
 E_r = retardant effectiveness, and
 i, j, k = retardant, fuel type (intensity class),
and depth, respectively.

Since most forest sites contain a continuum of fuels, it seemed reasonable to stratify the material likely to be consumed on the basis of the intensity potential as estimated from the FWI. There was a clear relationship between fire intensity and three of the fuel classes (litter, brush, and crowns) identified by Swanson and Helvig (1973). The three intensity classes are: 0-500, 501-2999, and 3000+ BTU/ft./sec. Grass fires are separated directly, without regard to intensity.

Starting with the lowest depth class the value of I_r after a drop is calculated. Then, the depth of retardant required to extinguish the lower intensity fire (D_r) is determined. If D_r is less than the depth class used to determine I_r , calculations stop. If not, the next higher depth is chosen and the process is repeated, starting with Eq. 243.

All limits listed under single-drop suppression also apply here. Note that the model does not limit double-drop suppression on the basis of expected time between drops. It is recognized that the retardation effect of the first drop would likely be lost after 15-20 minutes, as the fire regains its predrop intensity. The effect of the drop interval on double-drop suppression will be added before the next application.

In addition, it will be noted that regardless of whether one or two retardant drops are used in the model, the intent of dropping is fire suppression. It is recognized that there are other valid purposes for making a retardant drop. For example, the drop could be used to reduce fire intensity (as in double-drop suppression), with a ground crew providing the final suppression action equivalent to a second drop. Alternatively, the drop could represent a delaying action where the fire is held for a few minutes to provide an additional time margin for ground crews. Finally, indirect rather than direct suppression could be used whereby the drop is made well ahead of the current perimeter. All these applications are somewhat specialized, however, with their use highly dependent on the specific temporal

and spatial conditions of individual fires. To incorporate these tactics would require considerable additional programming.

In the opinion of the authors, the effort required would have greatly outweighed the additional knowledge gained. There are enough primary problems associated with analyzing simple suppression that there is no need to complicate the issue at this time by considering secondary questions.

2) Drop Patterns

Perhaps the most studied aspect of air tanker operations is the ground distribution patterns obtained from a retardant drop. Simard (1977) lists 50 references pertaining to field measurements alone. Despite the volume of data, however, there are many gaps. Not all air tankers have been tested. Of those for which data is available, it is incomplete for all but a few. Further, drop speed and altitude varied between tests. Given this state of affairs, the problem boiled down to one of filling in the information gaps and modifying the data to constant and optimal drop conditions.

Swanson et al. (1975) list several factors which affect a drop pattern in the open.

- Drop height - Examination of their "coverage footprints" indicates that maximum pattern lengths are obtained when the drops are made at between 75 feet and 125 feet above the canopy. Small loads are best at the lower end of the optimal range, while larger loads are better at the upper end. For a given quantity dropped, the altitude which resulted in a maximum pattern length did not appear to vary significantly with the retardant depth. That is, the pattern length at all coverage levels was maximized at about the same drop altitude. At drop heights of less than 75 feet, the patterns tend to be short and highly concentrated. As the drop height increases beyond 125 feet, pattern lengths begin to gradually decrease. For those air tankers evaluated by Swanson et al., the drop altitude was chosen such that the maximum pattern length resulted. For almost all of the remaining air tankers, the drop height at which the pattern was observed fell within the optimal range and no adjustment was necessary.
- Drop speed - The relationship between drop speed and pattern length is complex. As drop speed increases, peak coverage should tend to decrease and the pattern length at low coverage levels should tend to increase. After visually examining more than 100 drop patterns, it was concluded that the available data did not indicate a significant relationship between drop speed and pattern length, at the

speeds tested, particularly in the mid-coverage ranges. It was subjectively noted that as drop speed increases, the pattern breaks up to a greater extent due to increased erosion by the air stream. This could account for the lack of empirical evidence supporting a relationship between drop speed and pattern length. It might be expected that helicopters, with their significantly lower drop speeds (hence reduced erosion), would show a more pronounced speed/length interaction. There were not enough observations to test this possibility, however. As a result, the model makes no provision to vary drop speed.

- Aircraft maneuver - Diving and "tossing" the load generates effects similar to variations in drop speed. Since drop accuracy will be reduced by any drop approach other than simple horizontal flight, and since the benefits of nonstandard drop techniques are, at best, questionable, this factor is not included in the model.
- Wind - This will primarily affect the fringes of the drop pattern, displacing the lowest coverage levels downwind. Wind does not generally affect pattern length at the coverage levels of interest. Pattern displacement will be considered under drop accuracy.
- Retardant - High viscosity retardants tend to hold a pattern better than plain water. As with drop speed, the effect of thickeners on pattern length is variable depending on the coverage level desired. Pattern length at the lowest and highest coverage levels tends to be reduced whereas the length in the middle of the coverage range tends to be slightly longer. There was sufficient empirical evidence to support this effect and it was incorporated in the model.
- Sequential release - More than one retardant tank significantly increases an air tanker's flexibility. The maximum length of unbroken coverage at any desired depth can be greatly affected by the timing of the sequential release process. Lower concentrations benefit from longer intervals, whereas higher concentrations require shorter intervals. In the model, it is assumed that a pilot has an intervalometer available which is capable of timing sequential releases to within 0.1 second.
- Slope - Dropping retardant upslope should decrease the pattern length, while dropping downslope should increase it. Obviously dropping parallel to the slope should have no effect. Due to a lack of topographical data, combined with a small effect, a slope adjustment is not included in the model.

The first step in obtaining a standard drop pattern for an air tanker is to code each measured coverage level as well as its distance from the tail of the drop. A separate observation is required for every simultaneous release combination (1, 2, 4, or 8 tanks) of which the air tanker is capable. Whenever observational data were not available for a particular combination, data for a comparable tanking system of similar capacity were substituted. The observations were standardized with the equation:

$$(244) \quad dr_i' = dr_i \frac{Q}{Q_0} \frac{S_{do}}{S_d} c$$

where: dr = retardant depth,
 Q = desired drop quantity,
 Q_0 = observed quantity dropped,
 S_d = desired drop speed,
 S_{do} = observed drop speed,
 c = coefficient to convert observed units of measurement to standard units, and
 i = specific observation point in drop pattern.

While S_{do}/S_d was used in the original formulation, the lack of supporting evidence for the relationship resulted in $S_d = S_{do}$ being used in the analysis, so that the ratio always equaled 1. In some cases, the observed quantity of retardant dropped was less than tank capacity. In other cases, when a substitution was required, the observed quantity differed from the tank capacity of the air tanker being processed. Thus, the ratio Q/Q_0 was used to relate the desired quantity to the observed quantity dropped.

An iterative technique was used to calculate maximum pattern length for sequential drops. The interval between drops was varied from 0.0 to a maximum value in increments of 0.1 second. The maximum interval was based on the time it takes the aircraft to fly the distance between the start and end of the lowest useful retardant depth in a single drop. Regardless of the number of sequential releases, any longer interval would result in gaps in the drop pattern.

To find the maximum time between releases, the closest distance from the rear of the pattern to the minimum required depth (D_{cr}) must be determined:

$$(245) \quad D_{cr} = f(D_{rm}, dr, rd, N_p)$$

where: D_{rm} = minimum depth required,
 d_r = observed depth array - numbered from the tail of the drop,
 r_d = observed distances (ranges) corresponding to d_r , and
 N_p = number of data points in drop pattern.

Function f is a linear interpolation function which is embedded in an iterative search sequence. Since neither observed depths nor distances are at uniform intervals, and since the data varies with different measuring techniques, it is necessary to first find the pairs of points which are immediately higher and lower than the point at which the interpolation is to be made. Once this is accomplished, a linear interpolation function is used to determine D_{cr} :

$$(246) \quad \delta = \frac{r_{d_p} - (r_{d_{p-1}} - r_{d_p})}{(d_{r_{p-1}} - d_{r_p}) (d_{r_p} - D_{rm})} ; \quad \delta \geq 0$$

where: p = the location in data array d_r with the smallest depth which is larger than D_{rm} .

Similarly, by substituting an array of paired observations corresponding to the head of the drop (with distances still measured from the tail) the farthest distance from the tail of the drop to the minimum required depth (D_{fr}) is determined. The number of time intervals to be tested (T_{nx}) is:

$$(247) \quad T_{nx} = \frac{D_{fr} - D_{cr}}{0.1467 S_d} + 2.5.$$

The addition of 2.5 feet insures that more than enough time intervals are tested. The constant 0.1467 converts miles per hour to the distance flown in 0.1 second. The maximum distance to be covered by the distance search sequence (D_{mx}) is given by:

$$(248) \quad D_{mx} = 6 + D_{fr} + D_{dx} (N_t - 1)$$

where: D_{dx} = distance interval between drops and
 N_t = number of tanks in the air tanker.

D_{dx} is given by:

$$(249) \quad D_{dx} = 0.1467 S_d (N_i - 1)$$

where: N_i = number of time intervals to be tested.

The term N_{t-1} is used in Eq. 248 because the distance associated with the first tank is accounted for by D_{fr} . The addition of 6 feet ensures that the maximum search distance is greater than the sum of the individual intervals (5 ft.). The term N_{i-1} is used in Eq. 249 because the first interval is 0.0 second. This is necessary so that initial maximum pattern lengths can be determined.

The distance search sequence starts at the tail end of the drop and calculates total retardant depth at 5-foot intervals by adding the depth contribution for each sequential release at each point. The depth at a particular point (d_p) is given by:

$$(250) \quad d_p = \sum_{i=1}^{N_r} f(dt - (i-1) D_{dx}, rd, dr, N_p)$$

where: dt = distance from the tail of the first release and
 N_r = number of releases.

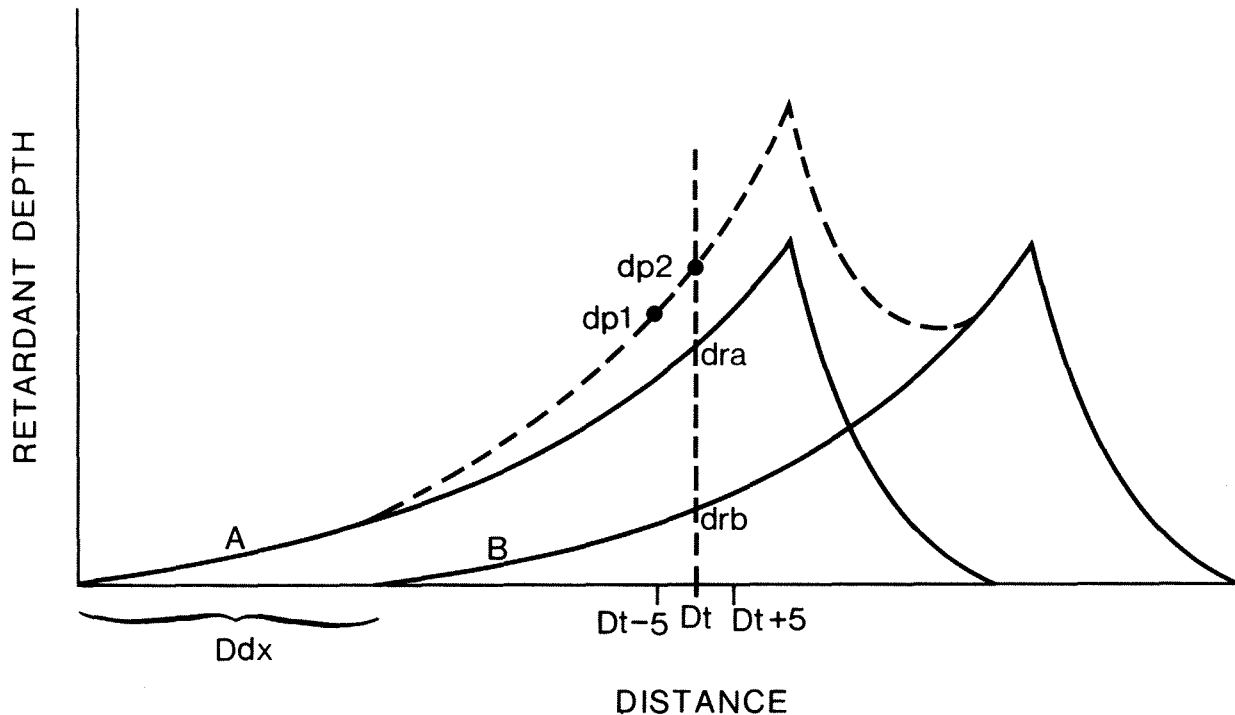
The functioning of Eq. 250 can best be described with the aid of an example such as in Fig. 18. Assume that the distance search sequence is at point dt . In the case of the first release (A), $i-1 = 0$, and the distance from the tail (dt) is used in function f . For the second release (B), the distance D_{dx} is subtracted from dt to determine the distance between dt and the tail of the second release. The total depth for both releases at point dt (dp_2) is the sum $dra + drb$ (Fig. 18). After processing dp_2 , the sequence advances to $dt + 5$, and the summation process begins again at the new distance. Note that dp_1 is the depth associated with $dt-5$ (the previously calculated dp_2).

A third iterative sequence determines whether the interval (dp_1, dp_2) contains either a starting or ending point for one of the 10 required depth classes (D_r). If the interval contains a starting point, the distance of the point from the tail of the first release (D_s) is calculated by interpolation:

$$(251) \quad D_s = dt + \frac{5(D_r - dp_2)}{(dp_2 - dp_1)}$$

If $dp_1 = dp_2$, R_s is simply equated with dt .

Figure 18. Total retardant depth for sequential releases



Similarly, if the interval contains an ending point, the distance of the point from the tail of the first release (D_{en}) is calculated with Eq. 251. If there is a break in the pattern, new start and end points are calculated as dt increases. Finally, the effective pattern length (P_{le}) at depth D_r is:

$$(252) \quad P_{le} = D_{en} - D_s$$

where: D_{en} = ending distance of effective pattern from tail of drop.

The equations described in this section can be used to obtain pattern length for any combination of release sequences (i.e., two releases, one tank at a time; four releases, two tanks at a time, etc.). A separate computer program (PATTERN)¹² was written which iteratively determines the optimum drop interval and pattern length. Since pattern lengths for four and eight releases are simply additive combinations of single and double releases, the former were not determined separately. Rather, in an effort to save storage space, they were determined within the model itself.

¹² See Simard et al. (1977).

Before leaving the drop patterns, a final note on the type of results generated by Eq. 244-252 is in order. As the interval between releases increases, greater concentrations become discontinuous while the effective pattern lengths for lower depths generally increases. This behavior can be seen in Table 10, which shows the optimum release interval versus pattern lengths for the CL-215.

Table 10. Optimum release interval versus pattern lengths for the CL-215 using two tanks

Depth required (in.)	Pattern length (ft.)	Release interval (sec.)	Distance travelled (ft.)
0.01	632	1.8	317
0.02	526	1.5	264
0.04	409	1.2	211
0.06	309	0.9	158
0.08	228	0.6	106
0.10	179	0.5	88
0.13	113	0.4	71
0.16	84	0.3	53
0.20	51	0.2	35
0.25	18	0.0	0

3) Length of Line Held

The next task of the model is to combine the required retardant depth with the drop patterns to obtain the length of line held for various drop tactics (release sequences). This is done in two steps. First, the length of line held in the open is determined. Second an adjusted length, incorporating accuracy, canopy interception, and retardant effect is calculated.

a) Pattern length in the open

The length of perimeter held for 10 required retardant depth classes is available to the model for each air tanker. There is a separate entry for each number of tanks that can be released simultaneously (1, 2, 4, or 8) for both single and sequential releases. In other words, for a single-tanked aircraft, two pattern length arrays are stored, while for two tanks, four pattern length arrays are required. Similarly, for four- and eight-tanked aircraft, six and eight pattern arrays respectively, are required. While this may appear to be a significant amount of data to store, it should be noted that for 1-, 2-, 4-, and 8-tanked aircraft, there are 2, 6, 12, and 20 possible effective pattern lengths, respectively.

An array of pattern lengths for every possible release combination is calculated twice: once for single-drop suppression and once for double-drop suppression (one drop directly on top of another). Two sets of equations for effective pattern lengths are required, depending on whether the first or a subsequent drop is being processed. In the case of the first drop, most release combinations do not require that the overlap between drops be considered. Hence, in most cases, the recorded pattern lengths may be used directly.

To calculate the pattern length for all combinations of release sequences, we begin by defining n as the number of tanks released simultaneously, k as the total number of tanks released in a drop, and $d = Dr$. For the first drop we have three possible states. For a single release ($k = n$), the equation is:

$$(253) \quad Pl_{n,k} = \frac{Ple_{d,n,1}}{Ns}$$

where: 1 = single release.

Since partial release data are stored for multi-tanked aircraft, Eq. 253 applies to all single releases. For example, a salvo drop for a two-tank aircraft does not differ from a two-tank salvo drop from a four-tank aircraft in terms of the procedures used to calculate Pl .

For a sequential release ($k = n/2$), the form of Eq. 253 is retained, with a few subscript changes:

$$(254) \quad Pl_{n,k} = \frac{Ple_{d,k,2}}{Ns}$$

where: 2 = sequential release.

The two preceding equations account for seven of the ten possible drop combinations. They account for all cases where the input data can be used directly. Four- and eight-tanked aircraft have additional flexibility in that they can generate multi-release sequences. Since multi-release data are not stored, two pattern lengths must be combined to calculate Pl when three or more releases are made. Thus, for $k > n/2$:

$$(255) \quad Pl_{n,k} = \frac{m(Ple_{d,k,2} - Ple_{d,k,1} + Ple_{d,k,1})}{Ns} ; \quad \frac{m}{k} \geq 4$$

where: $m = \frac{k}{n} - 1$.

Essentially, Eq. 255 adds one pattern length applicable to a single drop and m lengths applicable to a second drop. In other words, for eight tanks released one at a time, $m = 7$; whereas for four tanks released one at a time or eight tanks released two at a time, $m = 3$. Since the second drop overlaps the first, the effective length will be greater because retardant depths between the required amount and one-half that value will be adequate when the two patterns are combined. To obtain a pattern length with overlapping, the single-drop pattern length is subtracted from the pattern length for a double release.

All subsequent drops use a combinative form of equation to calculate Pl :

$$(256) \quad Pl_{n,k} = \frac{\frac{n}{k} (Ple_{d,k,2} - Ple_{d,k,1})}{Ns}$$

Equation 256 is used for every release combination after the first drop.

The final operation in the "line held in the open sequence" is calculating the relative effective pattern length. This variable is not required by the model, but it is useful in applying the results to field conditions. The percentage overlap, which is calculated from relative length, indicates where the aiming point should be to achieve results comparable to those generated by the computer. To compute relative length, Eqs. 253-256 are executed twice. On the first iteration, a required depth of zero is used to obtain the full pattern length (Plf). On the second pass, the required depth is used to obtain effective pattern length (Pl). Relative pattern length (Lr) is:

$$(257) \quad Lr = \frac{Pl_{n,k}}{Plf_{n,k}}$$

To this point, we have calculated an array of lengths of line held in the open for all release sequences. The model must now adjust these values for conditions on the fire site.

b) Pattern length adjustments

The model considers three factors which affect effective pattern length. Two affect the drop pattern directly: canopy interception and retardant viscosity. The remaining factor, drop accuracy, has an indirect effect, in that it causes part or all of the drop to be ineffective due to incorrect placement.

i) drop accuracy

A retardant drop which misses its intended target is not as effective as a drop which is properly located. Unless the drop lands entirely within the fire area, it can be made partially usable by modifying the location of subsequent drops to "tie it in." Such action, in fact, commonly takes place in the field. In all cases, however, unless the drop is exactly one pattern length "long," some part of the pattern will have to be duplicated by a subsequent drop.

The potential significance of drop accuracy was first noted by Vaux (1964) who concluded that placement accuracy was the most significant factor affecting the effectiveness of an air tanker drop. Quintilio and Anderson (1975) found that only 40% to 60% of all drops hit a prearranged target. They suggest, however, that field observations on fires indicate a greater degree of effectiveness than shown by their experimental data. Quintilio and Anderson (1976) use accuracy percentages of 75% to 80% for fixed-wing air tankers in a recently developed simulation model. La Mois (1961) developed a table indicating the feasibility of hitting a target as a function of pattern size. High success probabilities (90% and higher) were associated with drop errors (mean distance from target) of not more than 20% to 25% of the total pattern length. Swanson et al. (1975) list a set of "probability of hit curves" which are related to pattern length and drop height, but they do not indicate how the curves were derived. In their curves, success probabilities increase with increasing pattern length, and decrease with increasing altitude.

All of the above measure the probability of a drop either hitting or missing a target. Such a factor could be accommodated in a simulation model by the use of a random number generator to generate hits and misses. As suggested in the initial discussion on drop accuracy, however, the real world operates in a somewhat different fashion. A drop which is a "half load long" can be tied in by dropping half a load in the gap and nothing has been lost. Conversely, a drop which is short of the intended target will waste all of the unnecessary overlap with the previous drop, as will all drops which overshoot the target by a distance which is not exactly fillable by releasing some combination of the available tanks.

The actual process of tying in drops was considered too detailed and cumbersome to model. Further, it was felt that the generation of random errors would not contribute anything that could not be deduced from the use of a uniform reduction applied to all drops. It remained, therefore, to determine the average reduction in pattern length that would result from the accumulation of a series of drop errors.

Swanson et al. (1975) list 10 factors which affect drop accuracy.

- target identification
- ground speed
- altitude
- aiming error
- pilot reaction time
- true line of flight
- trajectory variability
- ballistic errors
- wind
- equipment response time

Two of the factors (trajectory variability and ballistic errors) are ignored in the model as there is little or no data available and they are felt to have only a minor effect. Further, it was decided that "cross-range" drop errors would not be included in the model because they should be significantly less than "range" errors. In addition, pattern widths are greater than necessary by a large enough amount to accommodate most lateral drop errors without leaving gaps in the sequence of patterns. Thus, the true line of flight does not have to be considered. Finally, in addition to the above, a maneuverability factor was added to reflect differences in aircraft response to pilot corrections.

The variables were recombined into five accuracy variables which, when summed and adjusted by a binominal probability (b), yield the total expected error inherent in a retardant drop:

$$(258) \quad E_t = b (E_x + E_{tr} + E_f + E_w + E_m)$$

where:

- E_t = total drop error,
- E_x = error due to target identification uncertainties,
- E_{tr} = error due to pilot and equipment reaction time,
- E_f = error due to aircraft flying errors (speed and altitude),
- E_w = error due to wind,
- E_m = error due to aircraft response time, and
- b = binominal probability.

Values for the error variables as well as for b will be discussed subsequently. Incorporating E_t into the expected length of line held in the traditional manner (a percentage of the total pattern length) is unnecessarily cumbersome. In fact, the absolute error does not change regardless of effective

pattern length. The aiming point is changed if, for example, only half the pattern is effective, but the average error associated with attempting to hit a single target remains constant. This also applies to sequential releases, in that only one target is aimed at. Thus, the model simply subtracts the expected error from the effective pattern length as each drop is made. Obviously, this technique will cause the model to favor sequential releases over separate drops, as sequential releases will minimize the loss due to drop error.

In establishing values for the drop error variables, an assumption was made that the pilot is, in fact, aware of the factors which cause drop errors and is making an effort to compensate. Thus, for example, in a case where wind would cause the drop to drift 50 feet from the target, the pilot should attempt to compensate for drift. The actual error would, therefore, be a compensation error rather than a total error. In the model it is assumed that it is possible to estimate required corrections with an accuracy on the order of $\pm 20\%$. Inexperienced pilots will not be able to achieve such accuracy, with average drop errors on the order of two or three times greater than experienced pilots. It was not the purpose of the initial study to investigate the effect of pilot experience. In future applications, air tanker system response to accuracy variations will be analyzed.

The target identification error (E_x) is likely to fall in the range of from 0 to 50 feet. An average error of 20 feet was assigned to this variable in the model. This is based primarily on field observations made by the author while observing air tanker drops from the air.

The error associated with reaction time consists of two components: human reaction to complex stimuli and the time required for the drop mechanism to open the tank doors. McCormick (1970) found that when subjects were asked to respond to a simple stimuli such as a flashing light, 80% of the reactions were completed within 0.25 second. He further found that complex stimuli required an additional 0.2 second. Since target identification certainly falls within the realm of complex stimuli (aircraft vibrations, smoke, canopy obstructions, etc.) a total human reaction time of 0.5 second is assumed in the model. Linkewich (1973) notes that the tanking system normally requires an additional 0.5 second to react to the release button being pushed by the pilot. Thus, an average reaction time of 1.0 second is used in the model. Using the previous assumption of an average error of 20% in estimating the correction required, the reaction error (E_{tr}) is given by:

(259) $E_{tr} = 0.2 S_d.$

Values of E_{tr} for each aircraft are listed in Table 11. The average reaction error is 35 feet.

Flying speed errors (E_s) are incorporated as follows. Neglecting the effect of drag for the moment, we can use a standard free-fall equation, such as given by Resnick and Halliday (1966):

$$(260) \quad y = V_0 t - \frac{1}{2} g t^2$$

where: y = free-fall distance,
 V_0 = initial velocity,
 t = free-fall time, and
 g = acceleration due to gravity,

to obtain the free-fall time by solving for t . By substituting $V_0 = 0$ at $t = 0$ and $y = -100$ feet (the average drop height or free-fall distance) we obtain $t = 2.5$ seconds. Multiplying S_d by 2.5 yields the horizontal distance travelled by the drop before reaching the ground.

Visual examination of "coverage footprints" developed by Swanson et al. (1975) suggests that when dropped from altitudes of about 100 feet, almost all of the forward momentum of small drops has been dissipated by the time the retardant reaches the ground. For larger loads (on the order of 1,000 gallons) 20% to 25% of the forward momentum is still evident after a 100-foot free-fall. Thus, the average forward velocity of a load is $(1 + 0.2)/2$ or 60% of the initial drop speed. Based on data for a series of drop tests provided by Hodgson (1967), pilots are able to keep their aircraft within $\pm 10\%$ of the intended drop speed, with an average error on the order of 5%. By combining the free-fall time (2.5 sec.), the average forward velocity percentage (60%), and the expected drop speed error (5%), we have:

$$(261) \quad E_s = 0.075 S_d.$$

Table 11 Air tanker drop errors

<u>Aircraft</u>	$\frac{S_d}{(fps)}$	$\frac{E_{tr}}{(ft)}$	$\frac{E_s}{(ft)}$	$\frac{E_h}{(ft)}$	$\frac{E_f}{(ft)}$	$\frac{E_m}{(ft)}$	$\frac{E_t^{1/}}{(ft)}$	$\frac{\bar{E}_t}{(ft)}$
A-26	205	41.0	15.4	10.2	25.6	14.7	101.3	40
AF-2	185	37.0	13.9	9.2	23.1	13.5	93.6	37
B-17	185	37.0	13.9	9.2	23.1	12.5	92.6	37
B-25	200	40.0	15.0	10.0	25.0	16.4	101.2	40
C-119	200	40.0	15.0	10.0	25.0	15.6	100.6	40
C-130	220	44.0	16.5	11.0	27.5	14.9	106.4	43
CL-215	160	32.0	12.0	8.0	20.0	7.2	79.2	32
DC-6	200	40.0	15.0	10.0	25.0	17.9	102.9	41
DHC-2-II	110	22.0	8.2	5.5	13.7	6.3	62.0	25
DHC-3	115	23.0	8.6	5.8	14.4	6.5	63.9	26
DHC-6	125	25.0	9.4	6.2	15.6	6.7	67.3	27
F7F	185	37.0	13.9	9.2	23.1	8.7	88.8	36
G-164A	115	23.0	8.6	5.8	14.4	4.2	61.6	25
JRM-3	185	37.0	13.9	9.2	23.1	14.3	94.4	38
P2V-7	200	40.0	15.0	10.0	25.0	16.7	101.7	41
PB4Y2	220	44.0	16.5	11.0	27.5	16.7	108.2	43
PBY5A	150	30.0	11.2	7.5	18.7	10.5	79.2	32
S2D	130	26.0	9.8	6.5	16.3	4.0	66.3	26
S2F	185	37.0	13.4	9.2	23.1	8.3	88.4	35
TBM	185	37.0	13.9	9.2	23.1	13.5	93.6	37
Average	173	34.6	13.0	8.6	21.6	11.4	87.6	35

1/ Without wind effect.

Altitude errors affect the duration of free-fall of the drop. From data provided by Hcdgscn (1967), pilots are consistently able to fly within ± 10 feet of the desired drop altitude under ideal conditions (an open field coupled with a helicopter to mark the altitude). Under field conditions, the range of error is likely to be on the order of ± 25 feet. At an average drop height of 100 feet, this error would alter the free-fall time by ± 0.3 second. Assuming an average drop height error of 15 feet, we have an average free-fall time error of 0.2 second. When this is multiplied by the average velocity at the time the retardant reaches the ground ($0.25 S_d$), the average drop height error is obtained:

$$(262) \quad E_h = 0.05 S_d.$$

Finally, the flying error (E_f) is the sum of the speed and altitude errors:

$$(263) \quad E_f = E_s + E_h.$$

Values of E_f are given in Table 11. The average flying error is 22 feet.

Placement errors resulting from wind stem from two variables: wind estimation errors and drift. Since winds are normally estimated with an accuracy of 5 m.p.h., the maximum possible estimation error is 2.5 m.p.h. The average estimation error is, therefore, 1.25 m.p.h. During the 2.5 seconds of free-fall, this error will result in a constant placement error of 4.5 feet. The drift error can be calculated by simply multiplying the free-fall time by the wind speed. Again, assuming that the pilot can estimate the proper correction within 20%, we have:

$$(264) \quad E_w = 4.5 + 0.75 W.$$

At a wind speed of 10 m.p.h., E_w equals 12 feet.

Finally, a maneuverability coefficient was introduced into the equation to reflect differences between aircraft in their ability to respond to last minute adjustments made by the pilot. An average error of 10 feet was associated with aircraft response. Thus:

(265)
$$E_m = \frac{10}{R_m} \cdot$$

In summing average values for the five error variables, we have a total error of 88 feet. Needless to say, pilots generally achieve greater accuracy than this value suggests. It should be obvious, however, that we are dealing with five independent variables, each of which can result in overshooting or undershooting the target. In essence, we are dealing with a binomial probability distribution with six possible outcomes: all errors are in the same direction (5,0 and 5,5); four in one direction and one in the opposite (5,1 and 5,4); or three in one direction with two in the other (5,2 and 5,3). Using an equation for binomial probability (b) given by Freund (1971):

(266)
$$b(x, n, p) = \binom{n}{x} p^x (1-p)^{n-x}$$

where: x = number of errors in one direction,
 n = total number of errors, and
 p = probability of error in one direction,

the probability of each of the preceding outcomes was determined, along with the expected value of the distribution. The calculations are summarized in Table 12.

Table 12. Expected total error using a binomial distribution for five independent errors

		$ (n - 2x)/n $	$P(n - x)/n$
$P(5, 0) = 0.03125$	$(x/2) = 0.0625$	1.0	0.0625
$P(5, 1) = 0.1562$	$(x/2) = 0.3124$	0.6	0.1875
$P(5, 2) = 0.3125$	$(x/2) = 0.6250$	0.2	0.1250
TOTAL	1.0000		0.3750

Since the binomial distribution is symmetrical, we only need to calculate the outcome for one-half of the distribution and double the result. Assuming equal values for each of the error variables, the quantity $|(n - 2x)/n|$ yields the percentage of the total error in one direction for each outcome. Note that (5,1) yields the same error in the opposite direction to (5,4). The absolute value yields the proper result, regardless of which half of the distribution is used for calculation. When this is

multiplied by the probability of the occurrence of the outcome and the results summed, the expected value of the binomial distribution is obtained. Thus, the expected distance of the center of the drop from the target will be 38% of the total error. In other words, a drop will miss its intended target by an average of 33 feet (0.38 x 88).

The pattern length (Pl) obtained from Eqs. 253-256 is adjusted for drop accuracy, yielding perimeter held per drop (Phd):

$$(267) \quad \text{Phd} = \text{Pl} - \text{Et} - 2 - 0.3 \text{ W.}$$

Values of Et (without the wind effect) listed in Table 11 are used in Eq. 267. The term (2-0.3 W) is approximately 38% of the wind effect given in Eq. 264.

In general, it can be seen in Table 11 that as wind speed or drop speed decrease, or maneuverability increases, drop accuracy will increase. Target estimation and reaction time errors are assumed to be constant for all conditions. After summing these errors, it can be seen that under no-wind conditions, the smallest aircraft (the DHC-2-II and the G-164A) have the lowest expected error - 25 feet. Conversely, the largest expected error (45 feet) is associated with large aircraft with high drop speeds (the C-130 and the PB4Y2). When the effect of wind is incorporated, the upper end of the range of expected drop errors (Et) is increased to 70 feet. Et forms a lower limit for effective pattern lengths, as any length less than Et will be reduced to zero.

ii) canopy interception

One of the most important, yet least studied aspects of dropping retardants is canopy interception. The relative importance is suggested by the limited drop tests made over a variety of forest canopies. As little as 10% of the quantity recovered in the open was recovered under a mature dense hardwood canopy, while as much as 80% was recovered under an open slash pine forest [Story et al (1959) and Johansen (1964)]. Grigel (1971) reported an average relative recovery of 45% in a lodgepole pine stand and 60% in a spruce-aspen stand. Stand recovery percentages for 200 Imp. Gal. drops averaged 50% of that in the open, while 400 Imp. Gal. drops averaged 60%. Pattern lengths in the stands ranged from a high of 95% of the pattern length in the open, at low concentration, to nil, at concentrations approaching the maximum useful depth¹³.

¹³ Maximum useful depth was arbitrarily defined for this analysis as 50 feet of pattern length to avoid anomalies created by the extreme peaks found in most patterns.

It was clear from examining the limited available data that stand and canopy characteristics were significant factors affecting interception. In addition, the quantity dropped and the depth required also had an effect. Following this reasoning, canopy interception contains two components: the stand and the drop.

The first step in developing the drop component was deciding which data or combinations of data to use. That problem was resolved by noting that Grigel plotted contours to a depth of 0.15 in., while the data of Story and Johansen stopped at a depth of about 0.04 in. Further, the stands used by Grigel were felt to be closer to a hypothetical average for all stands, while the hardwood and slash pine data were considered more representative of the limits of the range.

Development of the canopy interception component began by plotting profiles for typical drops in the open and in a stand. The results are shown in Fig. 19. Then, average pattern length in a stand, as a percentage of the length in the open, was plotted for two types of stands (lodgepole pine and spruce-aspens) for all observed depth contours (Fig. 20). These two sets of data were averaged to obtain the basic canopy interception function (heavy line in Fig. 20). To incorporate the effect of various quantities of retardant dropped, the maximum useful retardant depth for various quantities dropped was obtained by averaging all available drop pattern data. The results are plotted in Fig. 21.

Figure 19. Typical drop pattern profiles

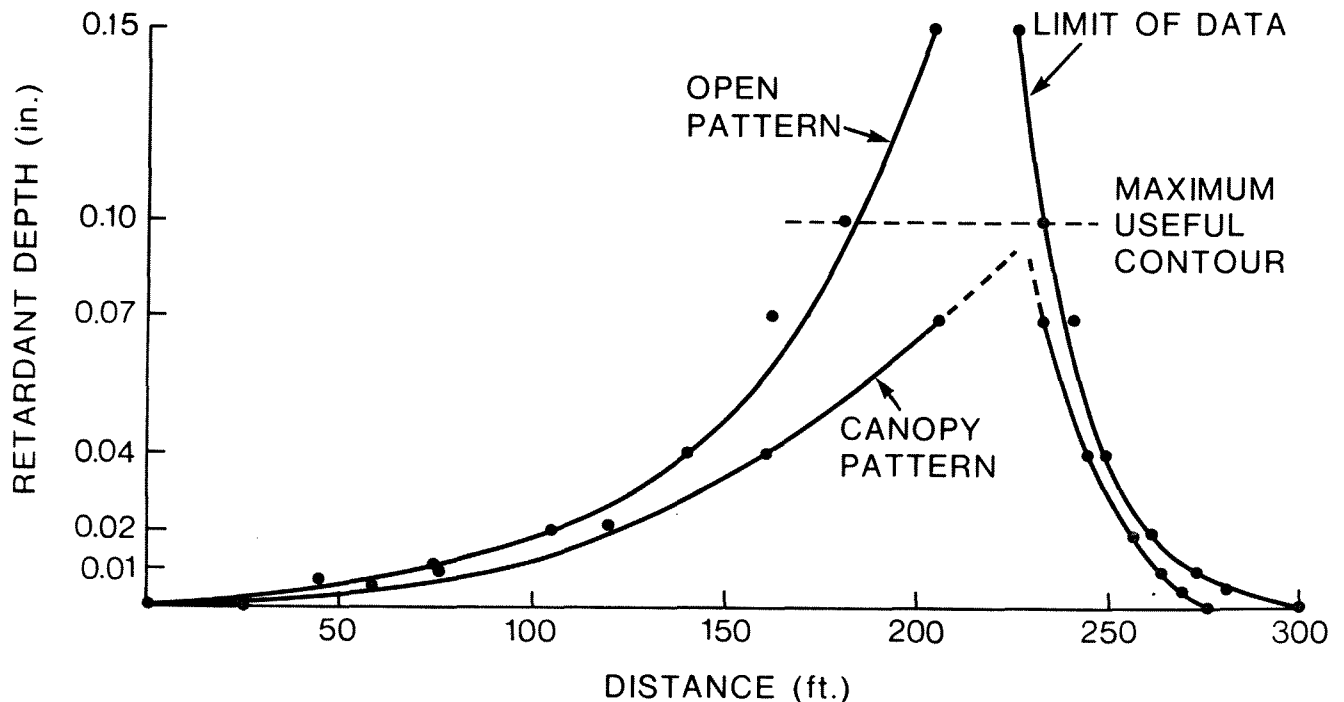
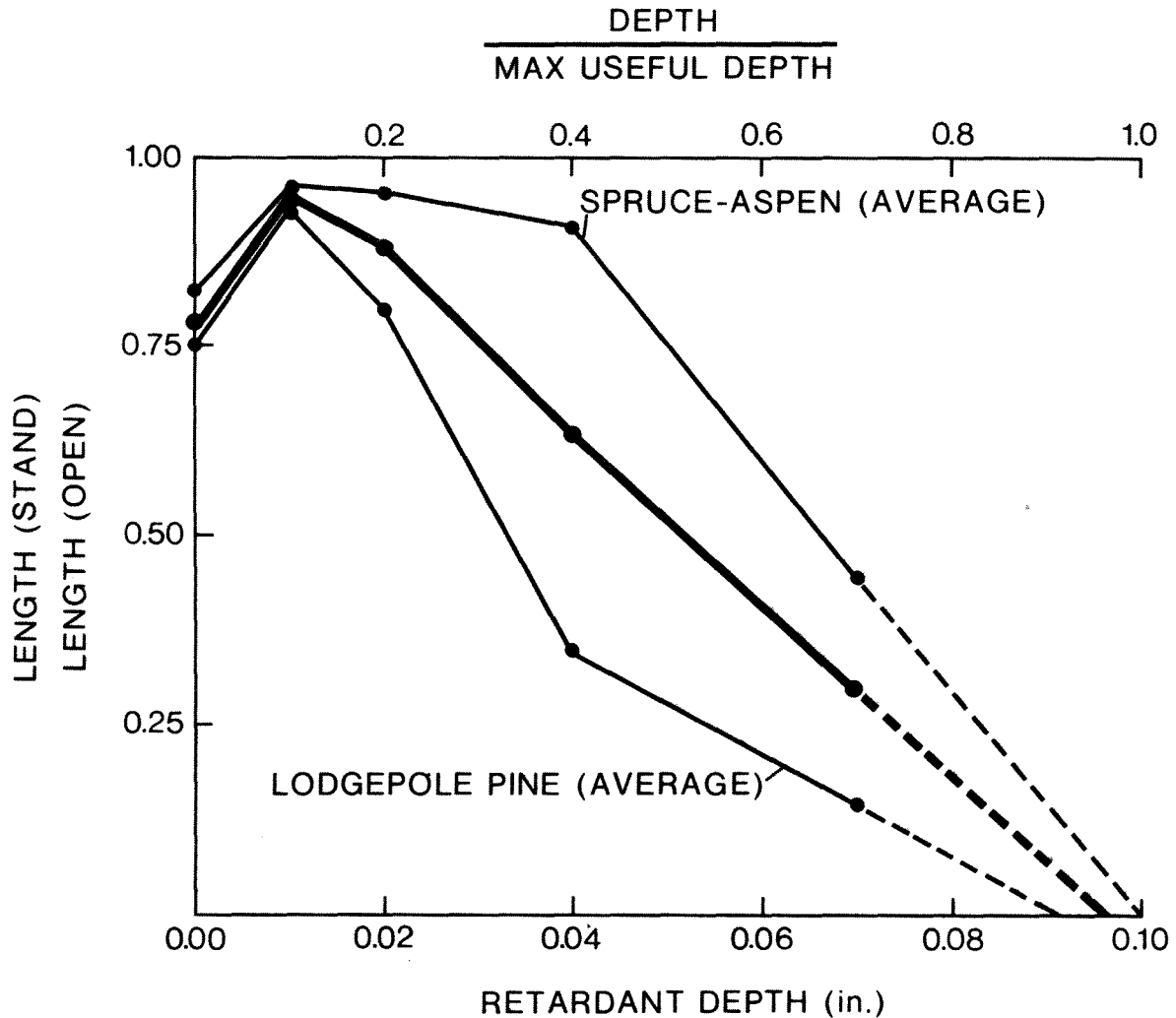


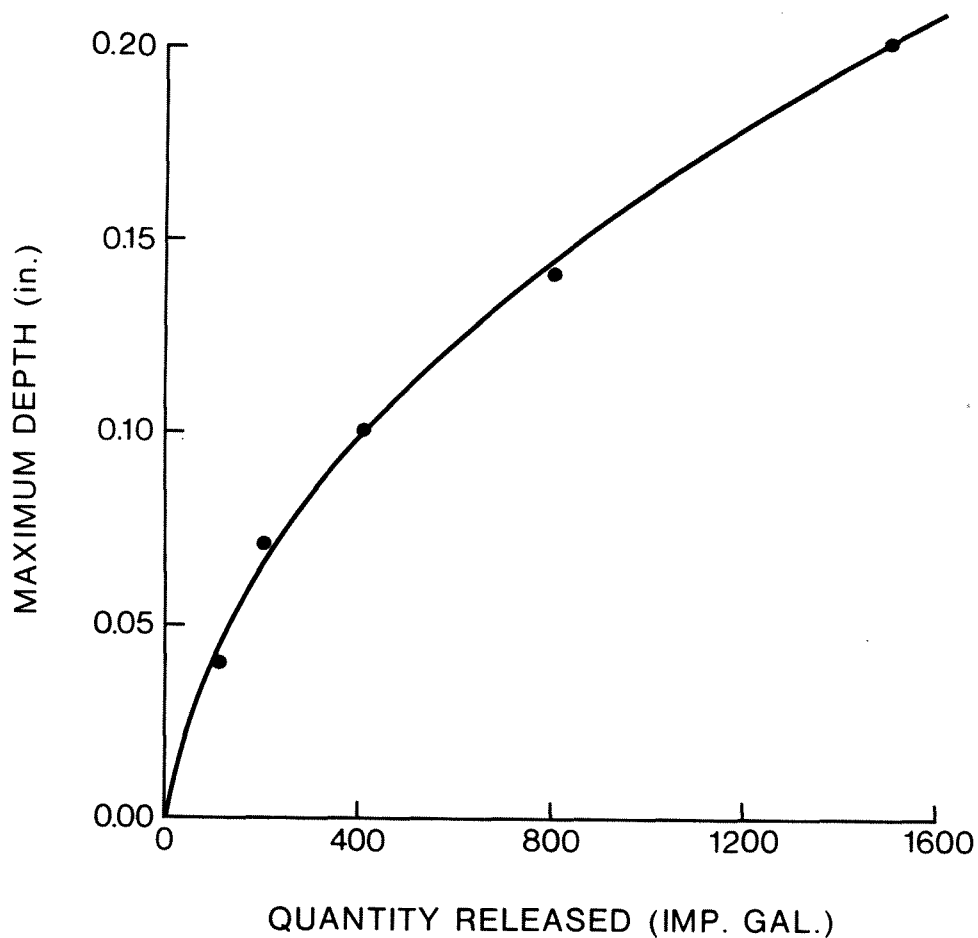
Figure 20. Average retardant pattern length under a canopy



This was followed by plotting average recovery percentage from three sets of data for 200 and 400 Imp. Gal. drops. A hypothetical curve was drawn through these two points and extrapolated in both directions (Fig. 22).

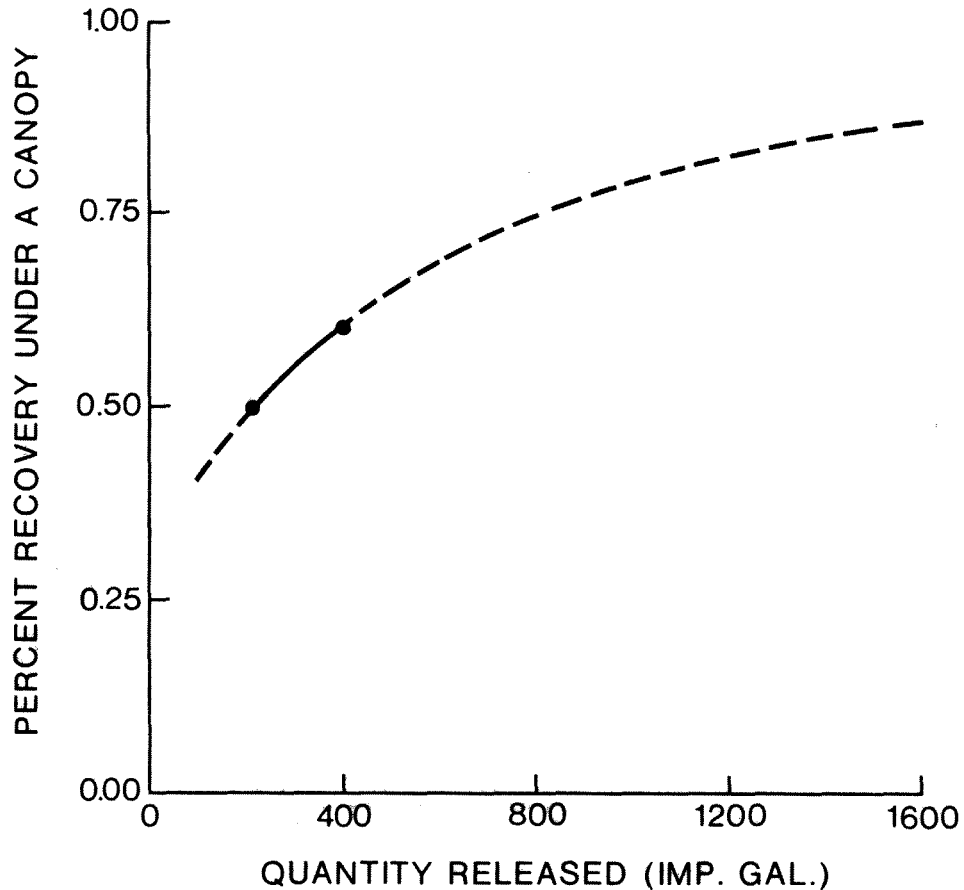
Beyond a reasonable assumption of nonlinearity, the curve itself is entirely subjective in the extrapolated regions. There is simply no data available in these regions. In fact, given the two available data points, the inherent error in Fig. 22 is not likely to be as large as might be suspected. The extrapolation to lower quantities extends for only a short distance. With respect to greater quantities dropped, the curve must be somewhere above 60% and below 100% and any reasonable extrapolation should be within $\pm 10\%$ of the true function.

Figure 21. Maximum useful retardant depth



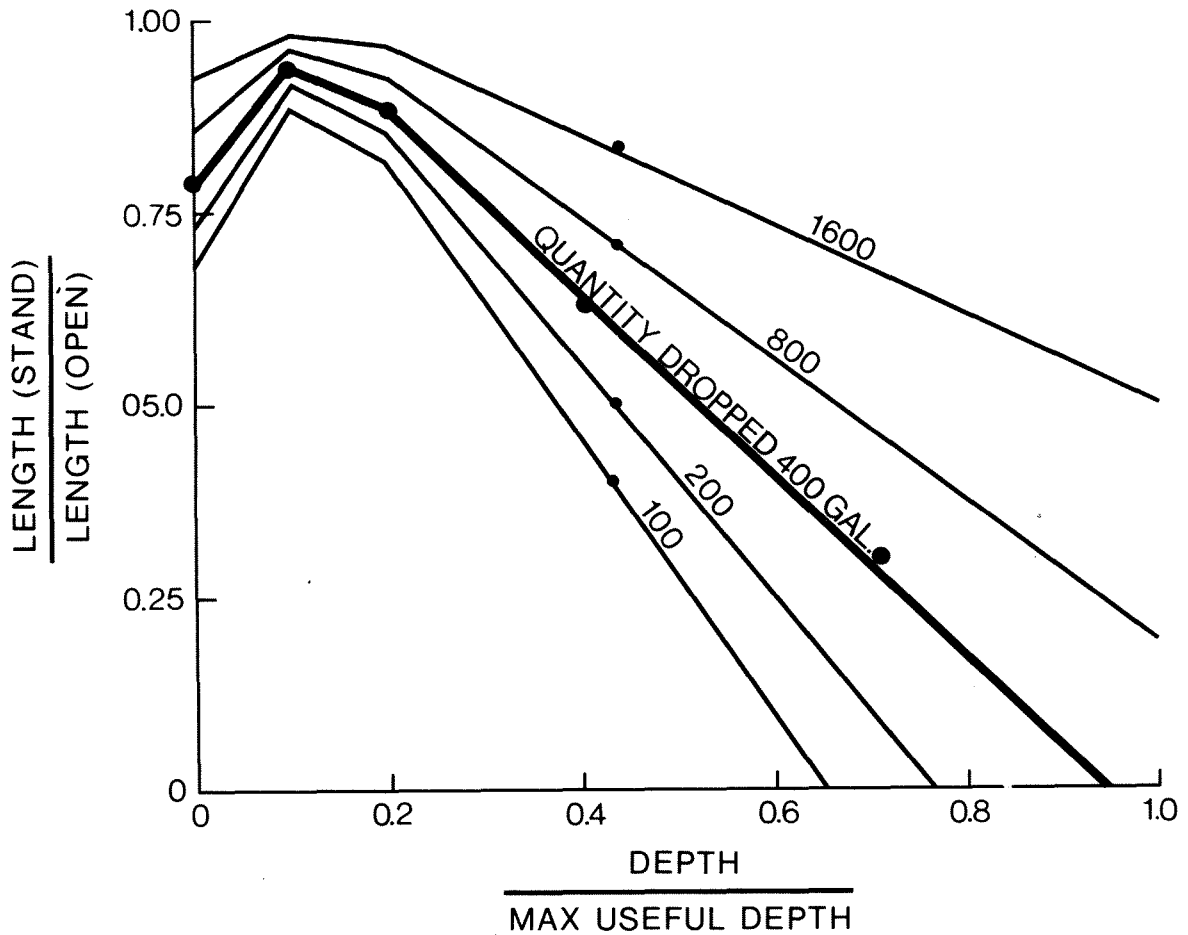
In the final step, relative pattern length under a canopy for a 400 Imp. Gal. drop (heavy line in Fig. 20) was replotted (Fig. 23) as a function of the percentage of the highest useful contour (heavy line). The percent recovery as a function of quantity dropped (Fig. 22) was applied to the 400 Imp. Gal. curve plotted in Fig. 23. It was applied at the point where the relative pattern length equaled the percentage recovery for a 400 Imp. Gal. drop (60%). This occurred at the point where depth/maximum useful depth (Fig. 23) = 0.44.

Figure 22. Percent of retardant recovery under a canopy



The series of points were used to determine the relative position for curves applicable to lesser and greater quantities of retardant released. By assuming a constant relative position, a family of curves was developed (Fig. 23) relating the length of line held under a canopy to: the length held in the open, percent of maximum useful depth, and quantity dropped. Finally, the ten required depth classes were converted to a percentage of the maximum useful contour for each quantity dropped and corresponding values for the drop component of canopy interception (C_d) were read off the appropriate curves in Fig. 23. These values are listed in Table 13.

Figure 23. Relative retardant pattern lengths under a canopy



The stand component (Cst) was divided into three subcomponents: age, stocking, and species. Age and stocking were combined into a single table. Anderson (1974) presents data for the fraction of a drop transmitted to the ground as a function of stand age in Douglas fir. Subjective stand descriptions were associated with his three age curves: 20 years = young growth, 50 years = pole timber, and 100 years = saw timber. In addition, a fourth curve (reproduction) was added to complete the spectrum. The fraction transmitted to the ground at the midpoint of the crown radius was taken as the transmission value for a fully-stocked stand. These values were then increased by 0.1 for understocked stands and decreased by 0.1 for overstocked stands. The relatively small adjustment reflects the subjective assumption that stands will naturally tend towards a fully-stocked condition. Transmission values are given in Table 14.

Table 13. Relative pattern length under a canopy (Cd)

Quantity Released (Imp. Gal.)	Retardant depth (in.)										
	0.00	0.01	0.02	0.04	0.06	0.08	0.10	0.13	0.16	0.20	
100	0.68	0.70	0.28	0.00							
200	0.73	0.88	0.72	0.30	0.00						
400	0.78	0.95	0.90	0.63	0.40	0.18	0.00				
800	0.86	0.93	0.95	0.85	0.72	0.58	0.47	0.25	0.00		
1600	0.93	0.95	0.98	0.94	0.92	0.85	0.80	0.71	0.64	0.50	

Table 14. Relative retardant transmission through a canopy

	<u>Saw timber</u>	<u>Pole</u>	<u>Young growth</u>	<u>Reproduction</u>
Understocked	0.40	0.55	0.70	0.90
Fully-stocked	0.30	0.45	0.60	0.80
Overstocked	0.25	0.35	0.50	0.70

From the stand pictures and descriptions given by Grigel, the stands from which his data were derived most nearly fall into the under- and fully-stocked categories. His recovery percentages (40-60%) suggest that either the pole or young growth category (fully-stocked) could be used as the standard. In the current version of the model, fully-stocked young growth (0.60) was chosen as the standard. In subsequent applications, the transmission percentage 0.50 will be used as the standard. The transmission data in Table 14 were converted to relative interception by dividing the standard transmission percentage by the percentage intercepted by each category. The results are shown in Table 15.

Table 15. Relative retardant interception by a canopy (Cst)

	(0.50 used as standard)			
	Saw timber	Pole	Young growth	Reproduction
Understocked	1.25	.90	0.70	0.55
Fully-stocked	1.65	1.10	0.85	0.65
Overstocked	2.00	1.45	1.00	0.70

The implication of the data presented in Table 15 is that in open stands less retardant will be intercepted, whereas denser stands will intercept a higher percentage of the drop.

The last variable to be considered is the relative difference in canopy retardant retention between species. Using data presented by Zinke (1967) (in Swanson and Helving 1973), the absolute amounts of rainfall retained in the various canopies of interest were obtained. These are listed in Table 16.

Table 16. Rainfall retention in forest canopies (Fp₅)

	<u>Amount retained</u> (in.)	<u>Relative retention</u>
Jack pine, Southern pine	0.01	0.20
White, Red, Monterey pine	0.025	0.55
Ponderosa pine	0.04	0.85
Hemlock, Balsam fir	0.03	0.65
Douglas fir	0.06	1.25
Spruce, Cedar, Fir	0.12	2.50
Birch, Poplar	0.025	0.55
Mixed wood	0.04	0.85
Maple, Oak, Beech	<u>0.075</u>	1.60
Average	0.047	

The relative rainfall retention listed in Table 16 was incorporated into the model in the form of a species parameter (Fp₅). It was used to adjust values obtained from Table 15.

Data for species not shown in Table 16 were obtained by subjective extrapolation using the most nearly comparable species.

Total canopy interception (Ci) is given by:

$$(268) \quad C_i = (1 - C_d) C_{st} F_{p_5}$$

Note that C_d is in terms of transmission through the crowns, while C_{st} and F_{p_5} are in terms of canopy retention, hence the use of $1 - C_d$. Finally, perimeter held per drop under a canopy (Phd) is given by:

$$(269) \quad Phd' = Phd (1 - C_i) \quad ; \quad C_i \leq 1.$$

iii) retardant effect

To determine the effect of thickeners on pattern lengths, data for four air tankers (CL-215, DC-6, B-17, and S2F) listed by Swanson et al. (1975) were examined. The average ratio of the pattern length for water, divided by the length for thickened retardants was tabulated for various depth classes and quantities released. Although differences in the performance of gum and clay thickeners in canopies has been noted by Vaux (1964) and Newstead¹⁴, this has not been included in the model, due to the lack of quantifiable information. The final results, after a few anomalies were smoothed are listed in Table 17.

Table 17. Relative water/thickened retardant pattern lengths

Quantity released (Imp. Gal.)	<u>Depth Class</u>									
	0.00	0.01	0.02	0.04	0.06	0.08	0.10	0.13	0.16	0.20
100	1.02	1.00	.90	.85	.80	.75	.75	.75	.75	.75
200	1.00	1.06	1.03	.90	.85	.80	.75	.75	.75	.75
400	0.99	1.00	1.07	.95	.90	.85	.80	.75	.75	.75
800	0.98	.99	1.00	1.09	1.08	.98	.85	.80	.75	.75
1600	0.97	.98	.99	1.01	1.05	1.06	1.08	1.06	.94	.90

¹⁴ R. Newstead, Northern Forest Research Centre, Canadian Forestry Service, Edmonton, Alberta, personal communication.

The value 0.75 is used in those portions of Table 17 where there is little effective pattern simply to prevent a division by zero in the model. As can be seen in Table 17, the mid-depth ranges tend to be slightly increased in length (10% or less) when water is used. Conversely, the high and low ends of the depth class range tend to have shorter pattern lengths when water is used. The effect becomes more pronounced (20%) as the maximum useful depth is approached. Due to the relatively small effect in the range of interest ($\pm 10\%$) a statistical evaluation of Table 17 was not considered worthwhile. A similar trend was noted in the data provided by Grigel (1971). Although these data were not included in this analysis, it provides subjective support for the general trends evident in Table 17.

When thickened retardants are used, the effect is included by simply dividing the pattern length per drop by the appropriate retardant adjustment (R_{ax}) from Table 17:

$$(270) \quad Phd' = \frac{Phd}{R_{ax}_{i,j}}$$

where: i = quantity dropped class and
 j = depth class.

With the calculation of the length of perimeter held per drop for all drop tactics, the model has almost completed the drop sequence. It remains only to select the appropriate drop tactic.

iv) drop tactic selection

At this point, the model has from 2 to 20 possible drop sequence options, depending on the number of tanks in the aircraft. It was initially intended that the decision criteria for selecting a specific drop tactic would be the same as for the selection of resources and suppression tactics - the minimization of cost-plus-loss. It quickly became apparent, however, that this presented a formidable logistics problem in that the number of combinations to be tested by the model would increase by a factor of about 10. Further, the usefulness of the information provided by this extra effort is certainly debatable.

For these reasons, it was decided that the drop component of the model would optimize internally. That is, drop tactic selection would be based on productivity maximization rather than cost-plus-loss minimization. Since it is highly unlikely that the lowest cost-plus-loss would result from a drop tactic that did not maximize productivity, this is felt to be a reasonable approach.

To calculate productivity (the rate at which perimeter is held), the model first calculates the number of drops that can be made with the full retardant load, given the number of tanks involved in each release sequence. This is necessary because when a partial load is sufficient to contain a flank (or one-third of the perimeter), the partial load is selected. The remaining retardant is dropped on the fire in the same manner as the initial partial load. In other words, if a two-tank sequence satisfies initial mission requirements, the entire load is dropped in a series of two-tank releases. The number of drops from a single load ($Nd1$) is given by:

$$(271) \quad Nd1 = \frac{Nt}{Ntp}$$

where: Ntp = number of tanks associated with partial load.

The average time interval between drops (Dda) is:

$$(272) \quad Dda = \frac{Tfx_2 + Tcx_{m,j} + Tdx_{m,j} (Nd1 - 1)}{Na Nd1}$$

where: m = air tanker model and
 j = operation.

When $Nd1$ is greater than 1, the extra time required for the separate dropping of each partial load must be added to the flying time. Air tanker productivity (perimeter held per hour - Phh) is, therefore:

$$(273) \quad Phh = \frac{Phd}{Dda}$$

Since each drop includes a loss for drop accuracy as well as increased flying time for dropping partial loads, the model will select that tactic or release sequence which minimizes the number of drops. In other words, full loads will be dropped unless a partial load is sufficient to complete a mission. The primary purpose of the test is to compare single- and double-drop suppression, in that at high fire intensities, two partial loads dropped on the same target might be more effective than one full load.

Having selected the drop tactic which maximizes productivity, the percentage overlap between drops (po) is calculated:

$$(274) \quad po = 10 (1 - Lr) + 1.$$

The overlap is simply that portion of the pattern which is ineffective. Multiplication by 10 stratifies the overlap into ten classes (0-9) while the addition of 1 shifts the classes to the right (1-10).

Finally, the minimum number of drops needed to complete the current mission (N_{dm}) is determined, using Eq. 224. The model now proceeds to make a drop on the fire.

D. Suppression

By the time that air tanker suppression is considered by the model, all that remains is to place the drop at the appropriate location on the fire perimeter and tabulate a few production variables.

1) Making a Drop

The first step in making a drop is to determine where to put it. The model has the built in capability of controlling any combination of flanks selected by the user. With minor modifications, it could change the order of fighting the flanks as well as the direction of attack (clockwise vs. counterclockwise). The discussion will be limited, however, to the standard attack used in the production run.

Referring to Fig. 9, air tankers begin dropping retardant on the head of the fire in a clockwise direction, at the intersection of the head and flank. After the head has been contained and if further air tanker activity is warranted, flank 2 is attacked, in the same direction. From there, the attack shifts to flank 3, in a counterclockwise direction. Finally, the rear of the fire is attacked, also in a counterclockwise direction.

A flank will be skipped if it has been controlled by ground crews before air tankers start to drop retardant. If this happens on the head of the fire, no drops are made at all, since, if the head is controlled by ground crews before a drop can be made, it is highly unlikely that dropping on a flank will provide any significant benefit. Drops are made on a flank where ground crews are working (in either direction) if there is some uncontained perimeter at the time that the drop is scheduled to occur. In such a case, the drop is placed directly in front of the ground crew if they are working in the same direction as the air tanker. The drop is tied into the previous drop if the crews are working in the opposite direction to the aircraft.

Once the flank of attack has been determined, placing the drop begins by calculating the length of free-burning flank (A_b),

using Eq. 124. Then the fire perimeter (P) is calculated, with a variant of Eq. 133. The drop length is then limited to no more than one-third of the entire perimeter:

$$(275) \quad L_d = \min(P_d, \frac{P}{3}).$$

Since a full load is always dropped, the length of line held for a partial load is multiplied by the number of partial loads contained in the aircraft:

$$(276) \quad L_d' = L_d N_d \ell \quad ; \quad L_d \leq P.$$

Note that at least a four-tank aircraft is required to completely contain a fire with partial loads, since two drops can only contain a maximum of two-thirds of the total perimeter.

The drop is then made on the flank, tagging on to the end of a previous drop or the ground crew, working in the same direction as the air tanker:

$$(277) \quad P_{ca_{f,d}}' = \max(P_{ca_{f,d}}, P_{cg_{f,d}}) + L_d$$

where: f = flank of attack and
 d = direction of attack.

The total perimeter held by aircraft (Ph) is then calculated:

$$(278) \quad P_h' = P_h + L_d.$$

Equation 278 assumes that the entire drop will be onto portions of the perimeter not previously held by air tankers or controlled by ground crews. After the drop has been placed on the flank, a check is made to determine whether any portion of the drop has spilled over onto the adjacent flank. First, the amount of spillover (Ls) is calculated:

$$(279) \quad L_s = P_{ca_{f,d}} - A \ell_f.$$

If $L_s > 0$, some spillover has occurred and it must be processed. No further drops will be made on the current flank. Before proceeding to the spillover sequence, we will consider the

case where $L_s \leq 0$ (no spillover). In this case, the amount of overlap onto line construction by either ground crews or air tankers working from the opposite direction is calculated:

$$(280) \quad Lov = L_s + \max(Pc_{g_{f,o}}, Pca_{f,o})$$

where: c = opposite to direction of attack.

Note that L_s is the distance from the opposite end of the flank and $L_s \leq 0$. Thus, if $Lov \leq 0$, no overlap has occurred, no further processing of the drop is necessary, and more drops are needed on the flank. If $Lov > 0$, the length of perimeter held is reduced by the amount of overlap:

$$(281) \quad Ph' = Ph - Lov,$$

and no further drops are made on the flank.

When $L_s > 0$, the spillover sequence begins by equating Pca with $A1$. The length of perimeter held by aircraft is then reduced by the amount of overlap (if any) on the current flank:

$$(282) \quad Ph' = Ph - \max(Pc_{g_{f,o}}, Pca_{f,o}).$$

A test is then made to determine whether the spillover will provide any useful line on the adjacent flank. Note that the adjacent flank is not necessarily the next flank of attack. For example, the rear of the fire is adjacent to flank 2 when working in a clockwise direction, but the air tanker will move on to flank 3 in a counterclockwise direction when flank 2 is contained. The spillover, however, will be placed on the rear, in a clockwise direction.

$$(283) \quad \text{If } L_s > \max(Pc_{a,d}, Pca_{a,d})$$

where: a = adjacent flank,

the spillover length exceeds any line length previously constructed on the adjacent flank, in the same direction and the spillover will provide useful line. If Eq. 283 does not hold, the spillover has no effect, and the length of perimeter held is reduced by the amount of spillover by using Eq. 282 and substituting L_s for Lov . Assuming that Eq. 283 is true, the

length of perimeter held is reduced by the length of line previously constructed in the same direction, on the adjacent flank:

$$(284) \quad Ph' = Ph - \max(Pcg_{a,d}, Pca_{a,d}).$$

The length of perimeter held on the adjacent flank is then updated by equating it with L_s .

If the length of spillover is greater than the total length of the adjacent arc, the model returns to equate Pca on the adjacent flank with A_l and reprocesses Eqs. 282-284 until all the spillover has been accounted for. In the case of a large fire (relative to the drop length) the spillover will end on the adjacent flank. In the case of a small fire coupled with two partial loads, the spillover will likely contain all of the adjacent flank and part of the subsequent flank. In the case of a small fire coupled with at least three partial releases, the spillover may well contain the entire perimeter. When the spillover ends on a flank, a final adjustment is made to Ph . Using the same logic as for Eq. 279:

$$(285) \quad L_s' = L_s - A_l a \quad \text{and}$$

$$(286) \quad Ph' = Ph - \max[0, L_s + \max(Pcg_{a,0}, Pca_{a,0})].$$

Equation 286 is similar in concept to Eqs. 280 and 281. It reduces the length of perimeter held by the amount of overlap onto line previously constructed from the opposite direction.

2) Production and Use Totals

The final sequence with respect to air tanker suppression is the tabulation of production and use totals. The number of drops is increased by 1. If an adjacent flank has been contained by the drop, the flank of attack is also increased by 1. In addition, total flying time variables are incremented. The extra time required for dropping partial loads (T_x) is calculated:

$$(287) \quad T_x = Tdx_{m,j} (Nd_l - 1)$$

where: m = air tanker model and
 j = operation.

Elapsed air tanker flying time (Ea) is given by:

$$(288) \quad E_a' = E_a + D_d + T_x.$$

Elapsed birddog flying time (Eb) is computed with:

$$(289) \quad E_b' = E_b + B_{df} + T_x$$

where: B_{df} = birddog flying time.

B_{df} is either equal to D_d (between drops) or B_{f1} (on the first drop).

Finally, the total time since initial takeoff (D_{to}) is calculated with Eq. 288 by substituting D_{to} for E_a . If the air tankers have returned to base for refueling between drops, the initial value of D_{to} is first modified:

$$(290) \quad D_{to} = \frac{-D_d}{2}.$$

In effect, this adjustment subtracts one-half of the drop interval (D_d), which is the round-trip flying time from the fire to the base.

The drop sequence is now complete. The model continues to fight the fire by processing the various events. If another drop is scheduled, the drop and air tanker suppression sequences are repeated when the drop occurs. In addition, the time of the next drop is calculated and stored in E_5 . When the fire is controlled by ground forces, the model enters the end-of-fire sequence. Part of that sequence involves the tabulation of total air tanker use and production on the fire.

The final value for elapsed air tanker flying time (E_a) is:

$$(291) \quad E_a' = E_a + 0.5 (T_{fx_1} + T_{dx_{m,j}}).$$

With Eq. 291 the last drop is completed and the air tanker returns to base. E_a reflects the total elapsed time between the initial takeoff for the first aircraft and the final landing for the last aircraft. In other words, E_a represents the time that air tankers were in the air. E_a must be known when multiple fire dispatch is being considered. E_a cannot be used to calculate

delivery cost, however, when more than one air tanker was used. Therefore, a separate flying time variable, reflecting the total flying time accumulated by all air tankers (Tfa), is calculated. It consists of three parts. The time for the first drop for all aircraft (Td1) is:

$$(292) \quad Td1 = Na (0.167 + Tfx_1 + Tcx_{m,j}).$$

The time for the second and subsequent drops for all aircraft (Td2) is:

$$(293) \quad Td2 = (Nd - Na) (Tfx_2 + Tcx_{m,j}).$$

The time for return trips to the base for all aircraft (Td3) is:

$$(294) \quad Td3 = Na Nrb Tr$$

where: Nrb = number of times that air tankers return to the base for refueling.

Finally, total air tanker flying time (Tfa) is given by:

$$(295) \quad Tfa = Td1 + Td2 + Td3.$$

The total quantity of retardant dropped (Qr) is:

$$(296) \quad Qr = Nd Qa_m.$$

The total birddog flying time (Tfb) is also calculated:

$$(297) \quad Tfb = Eb + \frac{Bf}{2} + 0.05.$$

As was the case for Tfa, the birddog aircraft returns to base and lands. We now have all the information needed to calculate air tanker costs - the final step in the air tanker component of the model.

E. Costs

Air tanker cost calculations begin with the components of delivery cost. The initial takeoff cost (Ct) is:

$$(298) \quad C_t = 0.167 C_{ah}_m$$

where: C_{ah} = air tanker cost per hour and
 m = air tanker model.

Note that C_{ah} is adjusted by a calibration coefficient (c_6) immediately after being read in by the model. The purpose of the adjustment is to standardize cost data from different time periods. Essentially, the model assumes that ten minutes are required for the initial takeoff procedure.

Circuit cost per load (Cc) is given by:

$$(299) \quad C_c = T_{cx}_{m,j} C_{ah}_m$$

Retardant cost per load (Crl) is:

$$(300) \quad C_{rl} = C_{rg} Q_{a_m}$$

where: C_{rg} = retardant cost per gallon.

Note that C_{rg} is also adjusted by c_6 .

Round trip fire-to-base flying cost per load (Cf) is:

$$(301) \quad C_{f_j} = T_{fx}_j C_{ah}_m$$

where: j = fire-to-base ($j = 1$) and
fire-to-retardant ($j = 2$).

The above component costs are used by the tactic selection routine to determine whether or not an air tanker resource and tactic combination passes the preliminary tests. At the end of a trial, mission costs are determined from the accumulated variables. Total delivery cost for the mission (Dc) is given by total flying time and hourly cost:

$$(302) \quad D_c = T_{fa} C_{ah}_m$$

In the case of land-based operations, a landing fee is added:

$$(303) \quad Dc' = Dc + (c_6 Clx Rcl_w)$$

where: Clx = average landing cost,
 Rcl = landing cost ratio, and
 w = air tanker weight class.

Rcl adjusts the landing cost on the basis of aircraft weight (three weight categories).

Retardant cost (Rct) is:

$$(304) \quad Rct = Nd Crl.$$

Equation 304 uses the number of drops and the retardant cost per drop. Rct could also be calculated by multiplying the total quantity of retardant dropped by the retardant cost per gallon.

The birddog cost is:

$$(305) \quad Bc = Tfb Cbh + (c_6 Clx).$$

Note that Cbh is multiplied by c_6 immediately after the data is read in by the model, and that Clx is for the lightest weight class of aircraft.

Finally, the model calculates total air tanker cost (Ac):

$$(306) \quad Ac = Dc + Rct + Bc.$$

With the calculation of air tanker costs, we conclude the description of the air tanker component of the model. With 93 equations (30% of the total) this is the largest component of the model. In addition to the equations, however, a significant portion of the air tanker component is based on table look-up, where the tables are derived from information in the literature. This is in contrast to most of the other components which are based almost entirely on equations. Thus, if we lump the equations and tables together, it can be said that the air tanker component constitutes over one-third of the overall model. This is the same percentage as was derived from examining relative program length.

Certain portions of the air tanker component, such as pattern lengths in the open for fixed-wing air tankers, are very well founded in empirical data. These components can be considered quite reliable. Other portions, such as canopy penetration, retardant effectiveness, and helicopter drop patterns, are supported by relatively scanty data. These aspects are the weakest links in the model. Future research will examine the model's sensitivity to these components. Still other functions, such as retardant delivery, suppression, and cost calculation, are based on the authors' interpretation of how the system operates in the real world. With respect to the last group of functions, presentations to two different fire management agencies have failed to reveal any significant discrepancies between model formulation and field operations.

In summary, all significant aspects of air tanker utilization identified in an examination of air tanker systems¹⁵ have been incorporated in the model. Those components which are poorly understood can be improved as new knowledge is gained. It is reasonable to suggest that the model is as good as possible, given the current state of knowledge in the field. It is further felt that the developmental effort expended is commensurate with the significance of the problem.

While there will no doubt be changes and improvements made to the model as it evolves from the developmental to application stages, the initial version presented here is, in the authors' opinion, the most powerful tool developed to date for the purpose of analyzing air tanker utilization. It is only through such objective, quantitative analysis that the potential effectiveness of air tankers in fire suppression will be realized. It is also only through such analysis that operational efficiency will be achieved. In contributing to these two objectives, the techniques presented here will have achieved their purpose.

¹⁵ To be described in a future report.

REFERENCES

- Albini, F.A., 1976. Estimating wildfire behavior and effects, U.S.F.S., Intermtn. For. and Range Exp. Sta., Ogden, Utah, Gen. Tech. Rpt. INT-30, 92 pp.
- Anderson, H.E., 1974. Forest fire retardant: transmission through a tree crown, U.S.F.S., Intermtn. For. and Range Exp. Sta., Ogden, Utah, Res. Pap. INT-153, 20 pp.
- Bloedsoe, L.J. and D.A. Jameson, 1969. Model structure for a grassland ecosystem, paper presented to Fifth Workshop, Int. Biol. Prog. Synthesis Proj., May 23, Buckhorn Ranch, Ft. Collins, Colo., pp. 410-437.
- Bomford G., 1962. Geodesy, Clarendon Press, Oxford, Eng., p. 105.
- Canadian Forestry Service, 1970. Canadian Forest Fire Weather Index, Dept. Fish. and For., C.F.S., Ottawa, Ont., 25 pp.
- Capel, R.E. and A.G. Teskey, 1970. Efficiency in suppressing forest fires: a study of the southeast area of Manitoba, C.F.S., For. Res. Lab., Winnipg, Man., Inf. Rpt. MS-X-24.
- Caswell, H.H., H.E. Koenig, J.A. Resa, and Q.E. Ross, 1972. An introduction to systems science for ecologists, in: Patten, B.C. ed., Systems analysis and simulation in ecology, Vol. II, Academic Press, New York, pp. 4-78.
- Clarke, A.R., 1880. Geodesy, Oxford, Eng., pp. 103, 268.
- Clymer, A.B. and L.J. Bledsoe, 1969. A guide to mathematical modelling of an ecosystem, in: Simulation and analysis of dynamics of a semi-desert grassland, Ccolorado State Univ., Range Sci. Dept., Ft. Collins, Colo, pp. 175-199.
- deNeufville, R. and J.H. Stafford, 1971. Systems analysis for engineers and managers, McGraw-Hill Book Co., New York, N.Y.
- Duncan, R.C., 1973. Techniques and guidelines for rapidly building models concerning the simulation of regional-environmental systems: an application to land-use planning on Orcas Island Washington, Univ. of Washington, Sch. Engr., Seattle, Wash., Ph.D. Thesis, 135 pp.
- Forrester, J.W., 1961. Industrial dynamics, The M.I.T. Press, Cambridge, Mass., 464 pp.
- Freund, J.E., 1971. Mathematical Statistics, Prentice-Hall Inc., Englewood Cliffs, N.J., 463 pp.

- Gamache, D.E., 1969. Development of a method for determining the optimum level of forest fire suppression manpower on a seasonal basis, Univ. of Washington, Col. For. Res., Seattle, Wash., Ph.D. Thesis, 139 pp.
- Grigel, J.E., 1971. Air drop tests with fire-trol 100 and Phos-Chek 205 fire retardants, C.F.S., Nor. For. Res. Cent., Edmonton, Alta., Inf. Rpt. NOR-X-8, 41 pp.
- Grove, C.S. Jr., S.T. Grove, and A.R. Aidun, 1962. Improving the effectiveness of water for fire fighting, Fire Res. Abs. and Revs., 4 (1 & 2), pp. 54-66.
- Hamilton, H.R., S.E. Goldstone, J.W. Milliman, A.L. Pugh IV, E.B. Roberts, and A. Zellner, 1969. Systems simulation for regional analysis, The M.I.T. Press, Cambridge, Mass., 407 pp.
- Hodgson, B.S., 1967. A procedure to evaluate ground distribution patterns for water dropping aircraft, C.F.S., For. Fire Res. Inst., Ottawa, Ont., Inf. Rpt. FF-X-9, 29 pp + app.
- Hysmans, Jan H.B.M., 1970. The implementation of operations research, Wiley-Interscience, Toronto, Ont., Oper. Res. Soc. Amer., Publ. No. 19, 234 pp.
- Johansen, R.W., 1964. Effects of overstory on ground distribution of airdropped slurries, Fire Cont. Notes, 25(2), pp. 3-4, 15.
- Kourtz, P.K. and W.G. O'Regan, 1971. A model for a small forest fire, For. Sci., 17(2), pp. 163-169.
- LaMois, L.M., 1961. Dropping accuracy - a logistics problem in air attack, Fire Cont. Notes, 22(2), pp. 27-32.
- Linkewich, A., 1972. Air attack on forest fires: history and technique, A. Linkewich, Red Deer, Alta., 321 pp.
- List, R.J., 1958. Smithsonian meteorological tables, 6th Ed., Smithsonian Inst., Washington, D.C., Pub. No. 4014, pp. 495-520.
- Maloney, J.M., 1972. Development and application of a linear model of the California Division of Forestry airtanker retardant delivery system, Univ. of Calif., Sch. For., Berkeley, Calif., Ph.D. Thesis, 434 pp.
- Mar, E.W. and W.T. Newell, 1973. Assessment of selected RANN environmental modelling efforts, Environmental Systems and

- Resource Div., Natl. Sci. Found., prepared by: Univ. of Wash., Seattle, Wash., 91 pp.
- McCormick, E.J., 1970. Human factors engineering, McGraw-Hill Book Co., Toronto, Ont., 639 pp.
- McMillan, C. and R.F. Gonzales, 1973. Systems analysis, a computer approach to decision models, Richard D. Irwin Inc., Homewood, Ill., 610 pp.
- Meier, R.C., W.T. Newell, and H. L. Dazer, 1969. Simulation in business and economics, Prentice Hall, Inc., Englewood Cliffs, N.J., 396 pp.
- Miller, C.W., 1968. A method of economic analysis and data required to determine justifiable expenditures for protection of tangible forest values from fire, Oregon St. Univ., Sch. For., MSc. Thesis, 228 pp.
- Miyagawa, R.S. and E.V. Stashko, 1971. Fire size and cost, Alta. For. Serv., For. Prct. Br., Feb., 20 pp.
- Naylor, T.H., J.I. Balintfy, D.S. Burdick, and K. Chou, 1966. Computer simulation techniques, John Wiley & Sons, New York, 352 pp.
- Newberger, A., 1966. A study into the use of aircraft in the control of forest fires, United Acft. of Can. Ltd., Longueuil, Que., Rpt. No. H-1036, 51 pp.
- Patten, B.C., ed., 1971, 1972. Systems analysis and simulation in ecology, Academic Press, N.Y., Vol. I: 607 pp., Vol. II: 592 pp.
- Peterson, A.E., 1973. Program TRAVERSE, Geodetic Survey, Can. Surveys and Mapping Br., Dept. Energy, Mines and Res., Ottawa, Ont., Aug., Unpubl. Ms., 26 pp.
- ~~Quintilio, D. and A.W. Anderson~~ ^{NEWSTEAD, R.G. and R.J. LIASKOVSKY.}, 1975. Determining airtanker accuracy, or how to make nobody happy, C.F.S., Nor. For. Res. Cent., Edmonton, Alta., Forestry Rpt., 4(4), pp. 5-6.
- Quintilio, D. and A.W. Anderson, 1976. Simulation study of initial attack fire operations in the Whitecourt Forest, Alberta, C.F.S., Nor. For. Res. Cent., Edmonton, Alta., Inf. Rpt., NOR-X-166, 35 pp.
- Resnick, R. and D. Halliday, 1968. Physics, John Wiley & Sons, Inc., New York, 649 pp. + app.

- Sanderlin, J.C. and J.M. Sunderson, 1975. A simulation for wildland fire management planning support (Fireman), Vol. II prototype models for fireman (Part II) campaign fire evaluation, Mission Res. Corp., Santa Barbara, Calif., Rpt. No. 7512-6-1075, Oct., 249 pp.
- Shubik, M. and G. Brewer, 1972. Models, simulation and games - a survey, Rand Report R-1060-ARPA/RC, May, 1972.
- Simard, A.J., 1969. Evaluation of forest fires with respect to requirements for aircraft, C.F.S., For. Fire Res. Inst., Ottawa, Ont., Int. Rpt. FF-10, 68 pp.
- Simard, A.J., 1970. Normal diurnal variation of the Canadian Forest Fire Weather Index in New Brunswick, C.F.S., For. Fire Res. Inst., Ottawa, Ont., Inf. Leaf., March, 6 pp.
- Simard, A.J., 1972. Forest Fire Weather Index data - Reference Manual and Station Catalogue, C.F.S., For. Fire Res. Inst., Ottawa, Ont., Inf. Rpt. FF-X-32, 28 pp.
- Simard, A.J., 1977. Air tankers - a bibliography, C.F.S., For. Fire Res. Inst., Ottawa, Ont., Inf. Rpt. FF-X-62, 79 pp.
- Simard, A.J., A. Young, and R. Redmond, 1977. AIRPRO - an air tanker productivity computer simulation model - the FORTRAN program (documentation), C.F.S., For. Fire Res. Inst., Ottawa, Ont., Inf. Rpt. FF-X-64, 341 pp.
- Simard, A.J., J.D. Graham, and A.S. Muir, 1973. Development of computer processing techniques for individual forest fire report data, C.F.S., For. Fire Res. Inst., Ottawa, Ont., Inf. Rpt. FF-X-40, 81 pp.
- Stade, M., 1966. Comparative cost-effectiveness of water bombers in forest fire control, Canadair Ltd., Montreal, Que., ERR-CL-RAZ-00-169, 84 pp.
- Stechishen, E. and E. C. Little, 1971. Water application depths required for extinguishment of low intensity fires in forest fuels, C.F.S., For. Fire Res. Inst., Ottawa, Ont., Inf. Rpt. FF-X-29, 64 pp.
- Storey, T.G., G.W. Wendel, and A.T. Altobellis, 1959. Testing the TBM aerial tanker in the southeast, U.S.F.S., S.E. For. Exp. Sta., Asheville, N.C., Sta. pap. No. 101, 25 pp.
- Swanson, D.H., C.W. George, and A.D. Luedeche, 1975. User guidelines for fire retardant aircraft: general instruction manual, U.S.F.S., Nor. For. Fire Lab., Missoula, Mont., Feb., Contract 26-3332, 71 pp.

- Swanson, D.H. and T.N. Helvig, 1973. Effectiveness of direct and indirect attack on wildfire with air-delivered retardants, Honeywell Inc., Hopkins, Minn., WSCI 73-14, 18 pp.
- Taylor, T.W., ed., 1938-1970. Jane's all the world's aircraft, McGraw-Hill Books, New York, (pub. every 2 years).
- Van Wagner, C.E., 1969. A simple fire-growth model, For. Chron., 45(2), 2 pp.
- Van Wagner, C.E., 1973. Rough prediction of fire spread rates by fuel type, C.F.S., Petawawa For. Exp. Sta., Chalk River, Ont., Inf. Rpt. PS-X-42, 9 pp.
- Van Wagner, C.E., 1974. Structure of the Canadian Forest Fire Weather Index, Dept. Env., C.F.S., Ottawa, Ont., Pub. No. 1333, 44 pp.
- Vaux, H., 1964. Fire retardant research and administration in the California Division of Forestry, Unpub. Ms., April 1, 114 pp.
- Zinke, P.J., 1967. Forest interception studies in the United States, in: Sopper, W.E., and H.W. Lull, ed., Forest hydrology, Pugamon Press, Oxford, Eng.

APPENDIX 1

The model contains 328 variables. These variables are used 1,381 times. To determine the number of interactions, the number of equations (306) must be subtracted from the number of variable occurrences, to eliminate double counting. Thus, the number of interactions is 1,075. To quantify the size of AIRPRO, we have the sum of the variables plus interactions (1,075 + 328) = 1,403. Based on a subjective class boundary between medium and large models of 1,000, AIRPRO would be classed as a large model.

List of Variables

<u>Name</u>	<u>Definition</u>	<u>Equations</u>
a	Intermediate variable or subscript	23-25,28,34,127,128,131,283-286
A	Fire area	107,108,161,163-173,183-185,188-198,200,205,208,212
Aa	Fire area with air tankers	161,163-173,183-185,188-198,200,212
Ab	Length of free-burning arc	124,125,127,224
Ac	Total air tanker cost	306
Ad	Fire area at detection	163-173,183-185,188-198,200,205,208
Ae	Air tanker endurance	237
Af	Relative flank arc length	93,94,113,115
Ag	Arc growth rate	75,125,127,128
Ag _i	Initial arc growth rate	122,123
Ah	Relative head arc length	90,94,112,114
ai	Average-to-initial spread adjustment	53,67,136
Aℓ	Arc length	112,113,124-127,129,133,150-153,279,285
ap	Area-to-perimeter coefficient	106-109
Az	Azimuth	29,31,35
b	Intermediate variable or subscript	23,28,34,258,266
Bc	Total birddog cost	305,306
Bdf	Birddog flying time per drop	289
Bf	Birddog round trip fire-to-base flying time	217,233,297
Bp	Present value of benefits	174
c	Constant, coefficient	1,7,60,244,303,305
C	Total cost	-
ca	Calibration coefficient	59
Ca	Air tanker cost	210
Cah	Air tanker cost per hour	298,299,301,302
Cb	Birddog portion of air tanker cost	219,220
Cbh	Birddog cost per hour	217,219,305
Cc	Circuit cost	214-217,225,299
Cd	Drop component of canopy interception	268

<u>Name</u>	<u>Definition</u>	<u>Equations</u>
Cdm	Minimum delivery cost	225
Cf ₁	Round trip fire-to-base flying cost	215-217,301
Cf ₂	Round trip fire-to-retardant flying cost	225,301
Cg	Total ground suppression cost	201,203
Ch	Horizontal component of chord growth vector	130,132
ci	Intensity calibration coefficient	65,101
Ci	Canopy interception	268,269
Cl	Chord length	126,129,132,134
Cl _a	Cost-plus-loss with air tankers	210,211
Cl _g	Cost-plus-loss for ground suppression only	203,207,211
Cl _p	Potential minimum cost-plus-loss	206,207
Cl _x	Average landing cost	303,305
Cn	Minimum delivery cost for n aircraft	217,221
Cp	Present value of suppression cost	174
Cr	Minimum delivery cost with retardants	221,225
Crg	Retardant cost per gallon	300
Cr _l	Retardant cost per load	221,225,300,304
cs	Rate of spread calibration coefficient	62
Cs	Suppression cost	175-189,192-194,196,198,200 201
Csa	Ground suppression cost with air tankers	175-189,192-194,196,198,200 210
Csp	Potential minimum suppression cost	175-189,192-194,196,198,200 206
Cst	Stand component of canopy interception	268
Ct	Takeoff and landing cost	214-217,298
Cv	Vertical component of chord growth vector	131,132
Cl	Minimum delivery cost for one aircraft	216
d	Intermediate variable or subscript	127,128,130,150,152,154,155, 253-256,277,279,283,284
D	Total damage	202,203
da	Day of month	38
Dc	Total delivery cost	302,303,306
Dcr	Closest distance from rear of pattern to minimum useful depth	245,247
Dd	Time interval between drops	231-241,288,290
Dda	Average drop interval	272,273
Ddx	Distance between sequential tank releases	248-250
De	Equipment damage	201,206,210
Den	Ending distance of effective pattern from tail of drop	252
Df	Forest damage	188-200,202
Dfa	Forest damage with air tankers	188-200,210
Dfp	Potential minimum forest damage	188-200,206
Dfr	Farthest distance from rear of pattern to minimum useful depth	247,248
Dh	Hourly component of daily index change	56,57

<u>Name</u>	<u>Definition</u>	<u>Equations</u>
Di	Distance	37,230
Dℓ	Fire-to-lake distance	22
Dℓa	Average fire-to-lake distance	22
Dℓo	Longitudinal difference	26-28,34
dm	Monthly sun declination parameter	38
Dmx	Maximum distance for pattern range search sequence	248
dn	Daily sun declination parameter	38
Dn	Nonforest damage	202,206,210
dp	Total retardant depth at point p in the pattern	250,251
Dp	Present value of damage	174
dr	Retardant depth at observed points in drop pattern	244-246,250
Dr	Depth of retardant required for extinguishment	242,251
Drf	Fire-to-retardant distance	22
Drm	Minimum required depth	245,246
ds	Sun declination	42-45
Ds	Starting distance of effective pattern from tail of drop	251,252
dt	Distance of point p from tail of first release	250,251
Dt	Time interval between calls to fire growth	19,20,149
Dte	Time interval between events	17-19
Dtn	Number of calls to fire growth between events	18,19
Dto	Time interval since initial takeoff	237,290
Dtx	Maximum interval between calls to fire growth	18
e	Eccentricity of earth	23-25,28,30,31,35
E	Time of occurrence array for all events	14
Ea	Elapsed air tanker flying time	288,291
Eb	Elapsed birddog flying time	289,297
Ef	Drop error due to flying errors	258,263
Eh	Drop error due to flying height error	262,263
Ei	Time of initial occurrence of an event	11-13
Em	Drop error due to aircraft reponse	258,265
En	Time of next event	14-16,71,72,79,239,241
Er	Retardant effectiveness	243
Es	Drop error due to flying speed error	261,263
Et	Total drop error	258,267
Etr	Drop error due to reaction time	258,259
Ew	Drop error due to wind	258,264
Ex	Drop error due to target identification uncertainty	258
f	Interpolation function	245,246,250
f	Intermediate variable or subscript	30,32,33,75,76,83,88-93,110,124-133,144-146,150-155,277,279,280,282

<u>Name</u>	<u>Definition</u>	<u>Equations</u>
F	Intermediate variable	32,37
Fc	Forward movement of center of ellipse	105,117,118
Fg	General fuel class	-
Fℓ	Flank left to control	150
Fnb	New Brunswick fuel class	-
Fp	Fuel parameter	61,268
Fs	Overstory fuel size class	-
Fsp	Overstory species class	-
Fst	Theoretical forward rate-of-spread	60-62,73,77,100
Fu	Surface fuel class	-
g	Intermediate variable	89,90,92,93,260
G	Aircraft design load factor	227
Ga	Rate-of-area growth	109,161,163-166,169
Gc	Chord growth rate	127,128,130,131
Gf	Forward chord growth rate	117,120,123
Gℓ	Lateral chord growth rate	116,122
Gm	Growth rate for semimajor axis of ellipse	104,116-119
Gr	Rear chord growth rate	118,121,123
h	Intermediate variable or subscript	31-33,40,41,46,47,51-55,57, 73-77
H	Intermediate variable	33,37,47,48,50
Hn	Hours of nighttime suppression	71,72
Hr	Hour	8-10
i	Intermediate variable or subscript	53,77,243,244,270
I	Fire intensity on a flank	76,83,101,110,144,145,242, 243
Ia	Afternoon ADMC	60,161,162,165,169-171,198
Iax	Average flank intensity	83
Id	Dc	161,162,164,166-170,173
If	Average fire intensity	110,144,145
Igd	Hourly ISI percent of afternoon (grass)	-
Im	Maximum fire intensity	83
Ir	Reduced fire intensity after a drop	243
Is	Afternoon ISI	51,60-62,188,190,191
Isa	Hourly ISI, adjusted for daily change	57
Isd	Hourly ISI percent of afternoon value	51,53,57
Ish	Hourly ISI	51,55
Isn	ISI for nth day after detection	55
Iss	Hourly ISI slope and aspect coefficient	51
It	Theoretical head fire intensity	64,65,74,101
Iw	Afternoon FWI	52,63,176,182,186,187,190, 199,200
Iwd	Hourly FWI percent of afternoon value	52
Iwh	Hourly FWI	52,54
Iwn	FWI for nth day after detection	54,56,57
Iws	Hourly FWI slope and aspect coefficient	52
ix	x coordinate of flank and head inter- section	86,88-91,114,116
iy	y coordinate of flank and head inter- section	87,88,91-93,115,117-119

<u>Name</u>	<u>Definition</u>	<u>Equations</u>
j	Intermediate variable or subscript	124,217,219,229,234-236,238, 240,243,270,272,287,291-293, 299,301
k	Intermediate variable or subscript	34-37,124,218,219,230,231, 243,253-257
ℓ	Lake length class	21,22
L	Lake length required for water pick-up	21
La	Latitude	24,25,27,28,30,31,34,35
Lac	Latitude coefficient	43-45
Lc	Rate of line construction	68-70,78,135,137-139,142,161, 164,168,169,171,172,175,177, 178,180,184-187,191,193,200, 204
Lcc	Rate of line construction per crew	139,143
Lcf	Rate of line construction on a flank	146-148
Lcn	Rate of line construction for crews on fire	142,143,146
Lcp	Percent of total rate of line construction allocated to each crew	147,148
Lcr	Relative rate of line construction	145,146
Lcs	Standard rate of line construction on a flank	147,151,152
Lcu	Rate of line construction during interval	155,156
Lcx	Augmented rate of line construction on a flank	148,153,154
Ld	Maximum drop pattern length	275-278
Lo	Longitude	26,49
Loc	Longitude of center of time zone	49
Lov	Length of pattern overlap onto perimeter previously controlled	280,281
Lp	Power loading	227
Lr	Relative pattern length	257,274
Ls	Length of pattern spillover onto adjacent flank	279,280,283,285,286
Lw	Wing loading	227
Lx	Control surface loading	227
m	Intermediate variable or subscript	21,217,219,226,228-232,234- 238,240,255,272,287,291-293, 296,298-302
M	Rate of mop-up	161-169,171-173,183
Ma	Average rate of mop-up for nearest ground station	161,163-165,170-173
n	Intermediate variable or subscript	14,54-56,141,143,220,222,253- 257,266
N	Number	4
Na	Number of air tankers	217,218,221,222,225,236,272, 292-294
Nc	Number of crew arrivals	138-140,142,143
Ncd	Number of crew divisions	158

<u>Name</u>	<u>Definition</u>	<u>Equations</u>
Nd	Number of drops	224,293,296,304
Ndℓ	Number of releases per load	224,271,272,276,287
Ndm	Minimum number of drops needed to contain one flank	224,225
Nf	Number of crews on fire	142,143
Nh	Number of hours since interval started	57
Ni	Number of time intervals to be tested	249
Np	Number of observed points in drop pattern	245,250
Nr	Number of tank releases	250
Nrb	Number of return trips to base	294
Ns	Number of drops used for suppression	253-256
Nt	Number of tanks in the air tanker	248,250,271
Ntp	Number of tanks associated with partial load	271
o	Intermediate variable or subscript	127,128,131,150,152,280,282 286
p	Intermediate variable or subscript	9-11,80,81,246,266
P	Fire perimeter	59,107-109,111,133,222,275, 276
Pc	Total perimeter controlled by ground forces	156,161,163,164,166,167,169- 171,173
Pca	Perimeter controlled by air tankers	124,152,154,277,279,280,282- 284,286
Pcg	Perimeter controlled by ground forces	124,150,152,154,155,277,280 282-284,286
Pco	Observed fire perimeter at control	70
Pd	Fire perimeter at detection	136,204
Pe	Estimated perimeter at the start of suppression	136,137
Pgf	Free-burning rate of perimeter growth	67,98,99,109
Pgs	Suppression rate of perimeter growth	58,68,78,135,136
Ph	Total perimeter held by air tankers	222,278,281,282,284,286
Phd	Perimeter held per drop	224,267,269,270,273,275
Phh	Perimeter held per hour	273
Pi	Fire growth pulse	78,79
Pℓ	Pattern length for sequential release	253-257, 267
Pℓe	Effective pattern length	252-256
Pℓf	Full pattern length	257
po	Percentage of overlapped drop pattern	274
Pr	Perimeter control rate	135,137
Ps	Fire perimeter at the start of suppression	68,69
Px	Perimeter of standard ellipse	94,97,111
q	Fire growth multiplier	79,125,130,131
Q	Quantity of retardant dropped	244
Qa	Air tanker retardant tank capacity	226,296,300
Qo	Observed quantity of retardant dropped	244
Qr	Total quantity of retardant dropped	296
r	Intermediate variable or subscript	22,35,37,221,223
R	Result	5
Ra	Average theoretical-to-observed spread ratio	81,82

<u>Name</u>	<u>Definition</u>	<u>Equations</u>
Rax	Retardant adjustment to drop pattern	270
Rc	Arc-to-chord ratio	114,115,122,123,126-129
Rcl	Landing cost ratio	303
Rct	Total retardant cost	304,306
rd	Distance from rear of pattern for each observed point	245,246,250
Re	Perimeter of fire-to-standard ellipse ratio	111-113
Rf	Free-burning theoretical-to-observed spread ratio	81,82,100,101
Rfl	Flank-to-forward rate-of-spread ratio	96,103,110
Rh	Rate of line holding	-
Rhr	Rate of line holding with retardants	223
Rhw	Rate of line holding with water	223
Ri	Current-to-initial spread ratio	77,127,128,130,131
Rl	Fire length-to-width ratio	85-87,91,106,134
Rm	Relative maneuverability	227,228,265
Ro	Old-to-new-spread and intensity ratio	73-76
Rp	Perimeter growth-to-forward rate-of-spread ratio	97-99
Rr	Rear-to-forward rate-of-spread ratio	95,96,102
Rs	Suppression theoretical-to-observed spread ratio	81
Rt	Result total	5
Rw	Fire width-to-length ratio	84
Rx	Average-to-initial spread ratio	82,83
s	Slope of ellipse at intersection of head and flank	85,86,134
S	Dollar saving with air tankers	211
Sa	Area saving with air tankers	212
Sap	Potential maximum area saving	208
Sd	Air tanker drop speed	244,247,249,259,261,262
Sdo	Observed air tanker speed	244
Se	Expected saving	205,206,210
Sf	Forward rate-of-spread	98-100,102-105
Sfx	Saving for last flank contained by air tankers	-
S ℓ	Lateral rate-of-spread	103
Sm	Saving for model m	-
Sn	Saving for n aircraft	220
Sp	Potential maximum dollar saving	207,214,215
Sr	Rear rate-of-spread	102,104,105
Srx	Saving for last retardant tested	-
St	Time saving with air tankers	213
Stp	Potential maximum time saving	209
sW	Standard deviation of wind direction	84,96
Sx	Air tanker flying speed	230
t	Free-fall time	260
T	Crew arrival time	136,141
Ta	Attack time delay	66

<u>Name</u>	<u>Definition</u>	<u>Equations</u>
Tam	Average time required for mop-up for nearest ground station	161,163,165,166,170,171,173
Tax	Average air tanker activity time	228
Tc	Time required for control with ground forces only	160-165,168-173,175,177-187,190-192,194,196-198,209,213
Tca	Time required for control with air tankers	175,177-187,190-192,194,196-198,213
Tce	Estimated time to control	68-72,79
Tco	Observed time to control	80
Tcp	Potential minimum control time	204,209
Tcx	Circuit time	217,219,229,234,236,238,272,292,293,299
Td	Time of detection (decimals)	10-13
Tdm	Time of detection (minutes)	8,9
Tds	Dispatch time	66
Tdx	Drop time	229,231,232,235,240,272,287,291
Td1	Flying time for first drop	292,295
Td2	Flying time for second and subsequent drops	293,295
Td3	Flying time for return trips to base	294,295
Te	Estimated control time	137,140
Tf	End of event interval	17,20,149,158-160
Tfa	Total air tanker flying time for all aircraft	295,302
Tfb	Total birddog flying time	297,305
Tfx	Round trip flying time	219,230-232,234,236,240,272,291-293,301
Ti	Time interval	53,66,125,130,131
Tic	Time interval between crew arrivals	140,141
Tl	Time left in interval between events	155-159
Tli	Initial time interval between events	159
Tlx	Loading time	219,226,229,232,235
Tly	Landing time	229
Tm	Time required for mop-up for ground suppression only	161-173,175-181,183,184,186-188,191,192,197,209
Tma	Time required for mop-up with air tankers	161-173,175-181,183,184,186-188,191,192,197
Tmp	Potential minimum mop-up time	161-173,175-181,183,184,186-188,191,192,197,209
Tnx	Number of time intervals to be tested	247
Tn	Time of median passage of sun	41,48,50
Toi	Initial takeoff time	231,232
Tox	Takeoff time	228,229,232
Tr	Round trip flying time to refueling base	237,238,294
Trz	Time of sunrise at center of time zone	48,49
Ts	Start of event interval	17,20,149
Tsc	Time of the start of control by ground forces	79,160
Tso	Observed time of the start of suppression	80

<u>Name</u>	<u>Definition</u>	<u>Equations</u>
Tsr	Time of sunrise	12,48
Tss	Time of sunset	13
Tsz	Time of sunset at center of time zone	50
Tt	Travel time	66,175-179,181-184,186,187
Tw	Work time until rate of line construction changes	151-154,157
Tx	Extra time required for dropping partial loads	287-289
V	General variable	1,2,3
Vi	Integer variable	6,7
Vo	Initial velocity	260
Vp	Present value	174
Vr	Read variable	6,7
Vs	Storage variable	2,3
w	Air tanker weight class	303
W	Wind speed	84,95,96,264,267
Wg	Gross air tanker weight	-
x	Intermediate variable	24,25,28,34-36,45,46,63,64,266
X	Intermediate variable	38,39,41
y	Intermediate variable	27,29,260
Y	Intermediate variable	39,40,42
z	Intermediate variable	28,29,119-121
Z	Intermediate variable	85-87

APPENDIX 2

Derivation of the Fire Growth Equations

The first step in developing the fire growth model is to determine the x and y coordinates of the intersection of the head and flank. Referring to Fig. 2-1 and starting with the basic equation for an ellipse:

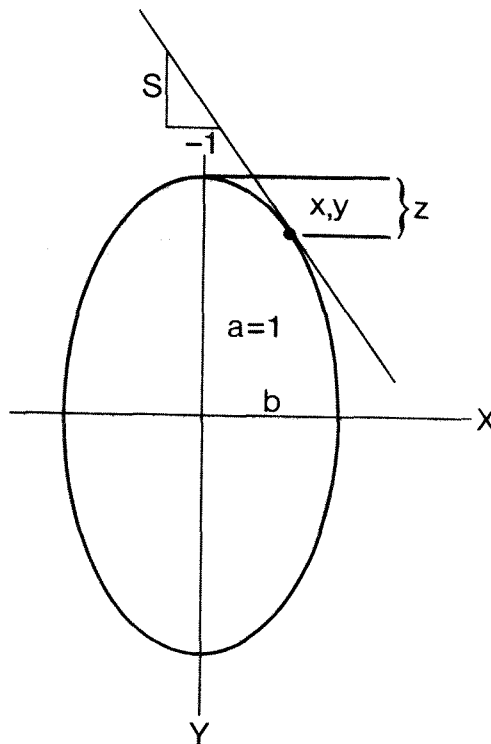
$$(1) \quad 1 = \frac{x^2}{b^2} + \frac{y^2}{a^2}$$

where: a = half-length of the major axis and
 b = half-length of the minor axis.

Taking the derivative with respect to x:

$$(2) \quad \frac{dy}{dx} = - \frac{xa^2}{yb^2}$$

Figure 2-1. The standard ellipse



Defining the slope at point (x,y) - the intersection of the head and flank - as s , we have:

$$(3) \quad s = \frac{xa^2}{yb^2}.$$

Rearranging (3) and squaring yields:

$$(4) \quad y^2 = \frac{x^2 a^4}{s^2 b^4}.$$

Substituting (4) into (1) we have:

$$(5) \quad 1 = \frac{x^2}{b^2} + \frac{x^2 a^4}{s^2 b^4 a^2}.$$

Solving for x^2 gives:

$$(6) \quad x^2 = \frac{b^4 s^2}{a^2 + s^2 b^2}.$$

Substituting (6) into (4) yields:

$$(7) \quad y^2 = \frac{a^4}{a^2 + s^2 b^2}.$$

We have now defined the intersection of the head and flank of the fire in terms of the semi-major and semi-minor axis as well as the slope at the point of intersection. While the data do not contain information on the axis, it is possible to simplify by using the ratio of a and b :

$$(8) \quad r = \frac{a}{b}.$$

Solving for b and squaring we obtain:

$$(9) \quad b^2 = \frac{a^2}{r^2}.$$

Substituting (9) into (6) and taking the square root yields x in terms of the semi-major axis, the slope, and the length-to-width ratio:

$$(10) \quad x = \frac{as}{r \sqrt{r^2 + s^2}}.$$

Similarly, substituting (9) into (7) and taking the square root yields a comparable value for y:

$$(11) \quad y = \frac{ar}{\sqrt{r^2 + s^2}}.$$

Finally, assuming a semi-major axis of 1 yields:

$$(12) \quad x = \frac{s}{r \sqrt{r^2 + s^2}} \quad \text{and}$$

$$(13) \quad y = \frac{r}{\sqrt{r^2 + s^2}}.$$

Note that Eqs. 12 and 13 are general forms and apply to all values of s. Since s was being varied during the course of model development, the general form was employed in the model. In selecting $s = r$, several convenient mathematical and behavioral properties are obtained. For example, Eq. 12 simplifies to:

$$(14) \quad x = \frac{1}{r \sqrt{2}}.$$

Similarly, Eq. 13 becomes:

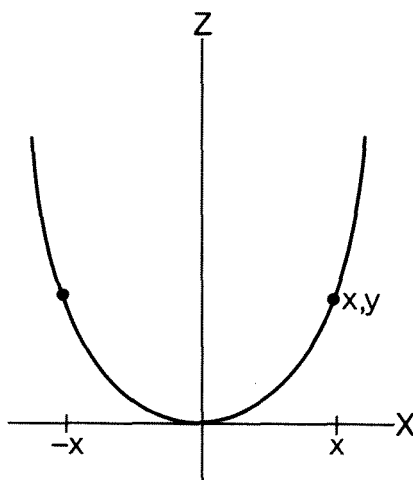
$$(15) \quad y = \frac{1}{\sqrt{2}}.$$

The second step is to determine the length of head and flank. Referring to Fig. 2-2 and using the equation for a parabola to estimate the elliptic arc length:

$$(16) \quad z = cx^2 \quad \text{and}$$

$$(17) \quad \frac{\partial z}{\partial x} = 2cx.$$

Figure 2-2. The standard parabola



The arc length (l) between $-x$ and x is given by:

$$(18) \quad l = \int_{-x}^x \sqrt{1 + (2cx)^2} \, dx.$$

Since the parabola is symmetrical about the Z-axis, we can simplify:

$$(19) \quad l = \int_0^x 2 \sqrt{1 + 4c^2 x^2} \, dx.$$

Burlington (1965) gives the integral for Eq. 19:

$$(20) \quad l = 2 \left[\frac{x}{2} \sqrt{1 + 4c^2 x^2} + \frac{1}{4c} \ln (2cx + \sqrt{1 + 4c^2 x^2}) \right]_0^x.$$

Solving for l between 0 and x yields:

$$(21) \quad l = x \sqrt{1 + 4c^2 x^2} + \frac{1}{2c} \ln (2cx + \sqrt{1 + 4c^2 x^2}).$$

Solving for c in Eq. 16 gives:

$$(22) \quad c = \frac{z}{x^2}.$$

Returning to Fig. 2-1, for an ellipse with a semi-major axis of 1, z can also be expressed as $1-y$. We can therefore redefine c :

$$(23) \quad c = \frac{1-y}{x^2}.$$

We also define g as:

$$(24) \quad g = \sqrt{1 + 4c^2 x^2}.$$

Substituting Eqs. 23 and 24 into 21, we have:

$$(25) \quad h = xg + \frac{1}{2c} \ln (2cx + g)$$

for the length of arc at the head, for an ellipse with a semi-major axis of 1. Similarly, the flank length for an ellipse with a semi-major axis of 1 can be found by substituting y for x and $(1/r)-x$ for $1-y$ in Eqs. 23-25, yielding:

$$(26) \quad c = \frac{\frac{1}{r} - x}{y^2},$$

$$(27) \quad g = \sqrt{1 + 4c^2 y^2}, \text{ and}$$

$$(28) \quad f = yg + \frac{1}{2c} \ln (2cy + g).$$

Finally, we calculate the perimeter of the standard ellipse:

$$(29) \quad p = 2(h + f).$$

We now have to relate forward rate of spread to the rate of perimeter growth. We begin by defining the perimeter to semi-major axis ratio. Since all fires will have dimensions which are proportional to the standard ellipse:

$$(30) \quad \frac{p}{a} = \frac{P}{A}$$

where: P = perimeter of the fire and
A = semi-major axis of the fire.

Substituting $a = 1$ and $A = M/2$ (one-half of the overall length) we have:

$$(31) \quad p = \frac{2P}{M}.$$

Solving for P yields:

$$(32) \quad P = p \frac{M}{2}.$$

We now substitute rate of change for the fire:

$$(33) \quad \Delta P = p \frac{\Delta M}{2}.$$

ΔM can also be defined as:

$$(34) \quad \Delta M = \Delta F + \Delta R$$

where: ΔF = forward rate of spread and
 ΔR = rear rate of spread.

Substituting Eq. (34) into (33) yields:

$$(35) \quad \Delta P = p \frac{\Delta F + \Delta R}{2}.$$

The perimeter growth-to-forward rate of spread ratio can be defined as:

$$(36) \quad \Delta PF = \frac{\Delta P}{\Delta F}.$$

Similarly, the rear-to-forward rate of spread ratio is:

$$(37) \quad \Delta RF = \frac{\Delta R}{\Delta F}.$$

Finally, by substituting (35) and (37) into (36) we have:

$$(38) \quad \Delta PF = p \left(\frac{1 + \Delta RF}{2} \right).$$

When the fire is controlled, a value of r is required for calculating the final fire area. Since r is related to x and y , we can combine Eqs. 12 and 13:

$$(39) \quad \frac{x}{y} = \frac{s}{r \sqrt{r^2 + s^2}} \cdot \frac{\sqrt{r^2 + s^2}}{r}.$$

Simplifying yields:

$$(40) \quad \frac{x}{y} = \frac{s}{r^2}.$$

We can now solve for r :

$$(41) \quad r = \sqrt{\frac{sy}{x}}.$$

While Eq. 41 is used in the model, note that in the special case where $s = r$, Eq. 41 reduces to:

$$(42) \quad r = \frac{y}{x}.$$

This concludes the discussion on the derivation of the fire growth equations.